NON-NEWTONIAN MIGRATION OF A DEFORMABLE DROP IN SHEARING FLOWS

Thesis by

Paul Chun-Ho Chan

In Partial Fulfillment of the Requirements

for the Degree of

Doctor of Philosophy

California Institute of Technology
Pasadena, California

1980

(Submitted October 24, 1979)

To my wife, Lily, and our daughter, Natalie.

ACKNOWLEDGMENTS

I would like to thank my advisor, Dr. L. G. Leal, who was most patient and generous throughout the course of this research, and was always able to provide valuable suggestions when they were needed. In addition, numerous discussions with my colleagues Dr. Bosco Ho, Dr. Phil Wood, Bill Olbricht, Seong Hee Lee and Clarke Berdan II have benefited me immensely. My Friday afternoons here at Caltech were made most pleasurable by all those who participated in the weekly bridge games.

Special thanks are due to Mr. George Griffith, who assisted in designing the Couette device, and to Mr. Seichi Nakawatase, who actually built it. Typing of this thesis was done by Ms. Kathy Lewis, who was most efficient and cooperative, despite the numerous changes and rewrites.

Most importantly, I wish to express my gratitude to my parents, without whose love, encourgagement and support this thesis would have been impossible. My work is dedicated to them.

ABSTRACT

The lateral migration of a deformable drop suspended in a unidirectional shearing flow of a slightly non-Newtonian fluid has been considered both theoretically and experimentally. Analytical expressions for the migration velocity due to the separate effects of drop deformation and fluid viscoelasticity were obtained for a two-dimensional flow, and then extended to the case of a general quadratic flow. The direction and magnitude of the migration velocity was calculated for the particular cases of Poiseuille flow in a tube and linear shear flow, and compared with experimental data.

The Couette flow problem was studied experimentally. The size of the inner rotor of the Couette device was varied systematically to assess the role of velocity profile curvature on drop migration. Both deformation and non-Newtonian effects were considered. In all cases, the agreement between experimental results and theoretical predictions was very good. Significant observations that were not reported in previous studies include the migration of a deformable Newtonian drop to an equilibrium position between the centerline and the inner rotor, and the close competition between normal stress and shape deformation contributions for the case of a Newtonian drop in a non-Newtonian fluid.

TABLE OF CONTENTS

Table of Contents (con'd) Page

CHAPTER I: INTRODUCTION

Introduction

Many problems related to multiphase flows arise in the study of fluid-like materials. Industrial processes where multiphase flows are important include: the transport of slurries in pulp processing or in sewage disposal; the extrusion of molten plastics; the motion of oil droplets in polymeric fluids during tertiary recovery; and the manufacture of magnetic tapes or films. In nature, multiphase systems are encountered in biological fluids such as blood, in porous media, and in atmospheric aerosols. Thus, an understanding of multiphase flows is very useful in scientific research as well as in industrial development.

One common objective in the study of multiphase flows is to predict the bulk properties of the multiphase, suspension-like materials. Here, two different methods are often used. In the 'phenomenological' approach, the dependent variables (e.g. the stress) are assumed to exhibit a certain functional relationship to the independent variables (e.g. the bulk strain rate in the velocity field). An obvious disadvantage of this method is that it is difficult to decide on (or guess) an appropriate constitutive form for a given flow situation. In addition, even if the "correct" choice is made, the material parameters still remain to be evaluated. In the other approach, the bulk rheological properties of the suspension are predicted statistically from a detailed knowledge of its 'microstructure' (i.e. the orientation and position of a typical particle in the suspension). Clearly, this procedure hinges on successfully solving the hydrodynamic problem of particle motion in a given flow field, which is usually difficult and simplifying assumptions must be introduced (the

most important of which is probably that of a dilute suspension according to which the particles do not interact hydrodynamically). Nevertheless, 'microrheology' is still an attractive alternative to the phenomenological approach, since it involves no unknown material parameters other than those that are already associated with the individual phases, and the bulk constitutive relationship is predicted rather than guessed. Comprehensive reviews of this research area were published in the last decade by Brenner (1970) and by Batchelor (1974).

Quite often, the theoretical analysis of the microstructure of a suspension begins with the initial assumptions of Newtonian fluid behavior, zero Reynolds number, no shape deformation, and no interaction with neighboring particles. Of course, these effects may be included later, using perturbation methods. However, the Stokes problem itself is usually quite complicated, and there may be some doubt regarding the usefulness, or even prudence, of carrying out the lengthy analysis necessary to include secondary effects. This question is especially relevant if the final objective is to determine the bulk properties of the suspension. To examine this situation in detail, let us first return to the original Stokes flow problem. Here, in general, the solution of the equations of motion may be classified into two types, one in which the predicted 'final' configuration of a suspended particle (e.g. its position and orientation for sufficiently large time) becomes independent of its initial configuration, and a second in which the configuration for all times is dependent on the initial configuration. An example of the first type, which we shall label as determinate, is the rotation of a prolate spheroid in a uniaxial extensional flow to a final orientation in which the axis

of revolution is aligned with the principle axis of the flow [Bretherton (1962)]. In this case, it is clear that small, instantaneous departures from 'Stokesian' behavior (due to non-Newtonian fluid properties or inertia, for example) will only cause small, insignificant changes in the final configuration. However, for indeterminate Stokes problems, small changes can lead to large, cumulative effects in the particle configuration, with important consequences for the rheological behavior of the suspension. Clearly, it is for this second class of problems that a perturbation analysis is most useful. Examples of flow situations of this type include the orientation of a transversely isotropic particle in sedimentation, the orbit of the same particle rotating in a simple shear flow, and the lateral position of a spherically isotropic particle relative to the bounding walls in a unidirectional shear flow [Leal (1979)]. In all of these cases, the configuration of the particle becomes determinate only when small departures in particle geometry, fluid properties or inertia are present. Thus, the orientation of a transversely isotropic particle sedimenting in a quiescent fluid remains fixed at its initial value for motion in a Newtonian fluid at zero Reynolds number [Cox (1965)], but will become either vertical or horizontal if inertia or non-Newtonian rheology [Brunn (1977)] are present. Clearly, the existence of a preferred equilibrium orientation will affect the drag on each particle and hence the overall sedimentation rate of the suspension.

In this dissertation, we consider the phenomenon of lateral migration of a neutrally buoyant drop in shearing flows, in the presence of non-Newtonian fluid properties and particle shape deformation. A theoretical analysis for the case of a two-dimensional flow is given in Chapter II. This is generalized in Chapter III to include all quadratic

flows. Finally, in Chapter IV, we report an experimental study on the migration of a deformable drop in Couette flow.

References

Batchelor, G. K. 1974 Ann. Rev. Fluid Mech. 6, 227.

Brenner, H. 1970 Ann. Rev. Fluid Mech. 2, 137.

Bretherton, F. P. 1962 J. Fluid Mech. 14, 284.

Brunn, P. 1977 J. Fluid Mech. 82, 529.

Cox, R. G. 1965 J. Fluid Mech. 23, 625.

Leal, L. G. 1979 J. non-Newt. Fluid Mech. 5, 33.

CHAPTER II: THE MOTION OF A DEFORMABLE DROP IN A SECOND-ORDER FLUID

J. Fluid Mech. (1979), *vol.* 92, *part* 1, *pp.* 131–170
Printed in Great Britain

The motion of a deformable drop in a second-order fluid

By P. C.-H. CHAN AND L. G. LEAL

Department of Chemical Engineering, California Institute of Technology, Pasadena, 91125

(Received 10 April 1978 and in revised form 20 September 1978)

The cross-stream migration of a deformable drop in a unidirectional shear flow of a second-order fluid is considered. Expressions for the particle velocity due to the separate effects of deformation and viscoelastic rheology are obtained. The direction and magnitude of migration are calculated for the particular cases of Poiseuille flow and simple shear flow and compared with experimental data.

1. Introduction

Recently, the dynamics of fluid-like materials which consist of two distinct phases has been the subject of intense investigation from both an experimental and a theoretical point of view. The present paper is concerned with one aspect of this general problem; namely, the cross-flow migration of small particles in a suspension which is undergoing a shearing flow at small Reynolds numbers. When cross-flow migration occurs, the particle concentration distribution becomes non-uniform with important consequences in the overall flow characteristics of the suspension. In addition, any effective material property whose magnitude is dependent upon the local particle concentration will also become non-uniform. One technological problem where such effects are important is the processing of two-phase (or fibre/particle filled) plastics. In this case, the particulate phase is ordinarily added to the polymer matrix in order to change one or more of the bulk properties of the composite material. However, in some cases, the particulate is simply added as a filler in order to decrease the quantity of polymer which is required per unit volume of product; for this purpose, the least expensive filler is, of course, small air bubbles. For these composite-media processing problems, the objective is usually a uniform concentration of particulate in the final product; however, in the case of added 'filler' material, one might alternatively require that the concentration of particulate at the surfaces of the finished product be small (or zero), in order to enhance its appearance. Regardless of the detailed objectives in processing applications, however, it is clearly important at the design and development stage to understand the mechanisms and dynamics of cross-flow particulate migration for rigid particles, bubbles or drops in a non-Newtonian suspending fluid. The present investigation is thus concerned with cross-flow migration for neutrally buoyant drops which are suspended in a non-Newtonian fluid that is undergoing a quadratic, unidirectional shearing flow. In this case, in the absence of external body forces, the mechanism for any particle migration must be purely hydrodynamic in origin. The focus of our present work is the development of further understanding of these hydrodynamically-induced migration mechanisms.

0022-1120/79/4196-6280 $02.00

Prior to outlining the research which is reported here, we will briefly review those previous experimental and theoretical studies which pertain directly to the problem of cross-stream migration of drops in either Newtonian or non-Newtonian fluids. The migration of drops of one Newtonian fluid in a second Newtonian fluid at zero (i.e. very small) Reynolds number was studied experimentally by Goldsmith & Mason (1962) for three-dimensional Poiseuille flows, and by Karnis & Mason (1967) for Couette flows. In both cases, migration due to drop deformation was observed to occur toward the centre-line, whereas no migration will occur if rigid spheres are used in the experiments. In an attempt to explain this phenomenon, Chaffey, Brenner & Mason (1965, 1967) considered the motion of a deformable drop in a simple shear flow near a single wall using the method of reflexions. They found that the drop would migrate away from the wall, in apparent qualitative agreement with the experimental observations. Later, Haber & Hetsroni (1971), Wohl & Rubinow (1974) and Wohl (1976) all considered the motion of a deformable drop in a unidirectional shear flow with a shear gradient, with wall effects being neglected except in the determination of the bulk velocity profile. With the exception of Haber & Hetsroni (1971) who apparently made algebraic errors, these theories also showed migration in the direction of the centre-line in Poiseuille flow, though obviously the detailed dependence on system parameters is different from the linear shear flow result of Chaffey *et al.* (1965, 1967). It may be noted that *neither* theory provides a good fit to the actual experimental trajectory data – in spite of statements to the contrary in the original papers. In addition, the results of Wohl (1976) and Wohl & Rubinow (1974) show a predicted migration velocity for three-dimensional Poiseuille flow which is approximately ten times as large as the predicted value in two-dimensional Poiseuille flow, all other conditions being exactly the same. In our opinion, this result is contrary to one's intuitive sense, and casts considerable doubt on the accuracy of both analyses. Finally, it may be reiterated that the Chaffey *et al.* (1965, 1967) theory is for a single plane boundary, whereas the available experimental work pertains primarily to circumstances where there are either two walls or a circular tube as the bounding surface. On the experimental side, it should also be remarked that the range of parameters tested so far is not extensive; for example, the ratio of internal to external fluid viscosities was always close to zero in the experiments of Mason and co-workers.

Unlike the case of two Newtonian fluids where migration occurs (at zero Reynolds number) only as a result of particle shape deformation, cross-flow migration is known to occur in non-Newtonian fluids for both rigid and deformable particles. Experimental studies of neutrally buoyant spheres and Newtonian drops in viscoelastic, as well as purely viscous, fluids have been reported by Gauthier, Goldsmith & Mason (1971*a*, *b*), following an earlier study by Karnis & Mason (1966). For a rigid sphere in a viscoelastic fluid, migration is observed to occur in the direction of decreasing absolute shear rate for both Couette and Poiseuille flows. Newtonian drops, on the other hand, migrate toward the centre-line in Poiseuille flow but at a rate greater than that for either a rigid particle in a viscoelastic fluid or a drop in a Newtonian fluid, while in a Couette flow, they migrate to an intermediate position between the 'centre-line' and the outer cylinder wall. These results were interpreted qualitatively by Mason and co-workers as resulting from a superposition of the viscoelastic migration effect for a particle of spherical shape and the deformation induced migration of a Newtonian drop in a Newtonian fluid. Unlike the Newtonian migration of a deformed drop, there

have been relatively few theoretical investigations which pertain to cross-flow migration in a non-Newtonian fluid. This is most likely a result of anticipated uncertainties in the selection of a reasonable constitutive model for non-viscometric flows, as well as the obvious difficulty in solving the equations of motion after the choice has been made. In our opinion, however, the usual constitutive equation dilemma is frequently not as serious for low Reynolds number motions involving small particles, as for non-viscometric flows in general. This is due to the fact that the creeping motion solutions for a Newtonian fluid in these cases often exhibit an 'indeterminacy' in the configuration of the particle relative either to the undisturbed bulk flow or to the container boundaries, and it is the 'resolution' of this 'indeterminacy' which is often the primary goal of the non-Newtonian analysis. For this type of problem it is sufficient, in at least a qualitative sense, to consider the influence of *small* instantaneous departures from Newtonian fluid behaviour acting over a large time (i.e. to consider particle motion for a long period of time in a nearly Newtonian fluid). Two important examples of 'configurational indeterminacies' which may be treated with an analysis of this type are the steady-state orbit of rotation of an axisymmetric particle in simple shear flow (Leal 1975) and the steady-state position of a particle relative to container boundaries in a unidirectional shearing flow. The latter is the problem which we are investigating in the present paper. It is essential to note that the appropriate constitutive model for non-viscometric flows which are nearly Newtonian is, unlike the case of a general non-viscometric flow, well-known to be the Rivlin–Ericksen fluid provided the motion is both weak and slow in a rheological sense. This model may be obtained, *via* the so-called 'retarded motion' expansion, from almost all of the currently popular nonlinear constitutive models. The case of the lateral migration of a rigid sphere in a quadratic, unidirectional undisturbed flow was considered previously by Ho & Leal (1976), who used the second-order Rivlin–Ericksen fluid model, thereby including normal stress contributions to the particle motion, but excluding shear-rate dependent viscosity. The analysis of Ho & Leal (1976) was considerably simplified, not only by use of the second-order fluid constitutive model, but also by employing the reciprocal theorem approach of Cox & Brenner (1968) and Ho & Leal (1974) to enable the migration velocity to be calculated without any need to determine the non-Newtonian contribution to the velocity and pressure fields in the suspending fluid. The result of Ho & Leal's (1976) theory predicts migration toward the outer cylinder and is therefore in apparent qualitative agreement with available experimental data.

In the present paper, we consider the related problem of the migration of a fluid drop in a unidirectional shearing flow, both with and without shear-rate gradients. Both the suspending fluid and the fluid inside the drop are assumed to be adequately modelled as second-order fluids – thus extending the domain of application somewhat beyond even the available experiments where the drop fluid was always Newtonian. The primary thrust of our present research is a systematic assessment of the co-existing roles of drop deformation and viscoelastic fluid behaviour in the migration of a drop. In effect, we investigate the relevance of Gauthier *et al.*'s (1971*a*, *b*) 'explanation' of the existing experimental observations which suggest an 'additive' effect of deformation in a Newtonian fluid and viscoelastic behaviour for a spherical drop. In so doing, we re-examine the problem of deformation-induced migration in a Newtonian fluid, as well as the more general non-Newtonian problem described above.

In the following two sections, we shall outline the formulation of the problem, and obtain, by a perturbation expansion and the reciprocal theorem, a general expression for the migration velocity. In §4, we obtain solutions for the Newtonian velocity fields that are required for evaluation of the migration velocity formula. This includes the motion of a deformable drop in a unidirectional shearing flow which is bounded by two plane walls, and the translation of a spherical drop through a quiescent fluid normal to two parallel plane walls. The migration velocity is evaluated and discussed in various limiting circumstances in §§5–7. In the case of migration in a quadratic velocity profile, we also use the method of Chan & Leal (1977) to generalize our results to a general (three-dimensional) quadratic shear flow. Finally, in §8, we compare our results with the experimental observations of Mason and his co-workers.

2. Formulation of the problem

We consider the motion of a neutrally buoyant drop freely suspended in a fluid which is undergoing a unidirectional, quadratic shearing flow. The fluid is confined between two parallel plane walls separated by a distance d; hence the undisturbed flow is assumed to be two-dimensional. The two fluids are both assumed to be Rivlin–Ericksen fluids, as discussed above, with zero shear viscosity μ_0 for the suspending phase and $\tilde{\mu}_0$ for the fluid inside the drop. The whole motion is further assumed to be dominated by viscous and pressure effects, so that the inertial terms in the equations of motion can be neglected entirely. In order to write the governing differential equations and boundary conditions in non-dimensional form, we define a characteristic length a and a characteristic velocity Ga, where a is the radius of the drop at zero deformation and G is an average shear rate for the bulk flow. The stress tensors for the two fluids are non-dimensionalized using $\mu_0 G$ and $\tilde{\mu}_0 G$ respectively. In addition, we choose a co-ordinate reference system with origin O which is fixed, for convenience, at the centroid of the drop, thus translating relative to a fixed reference frame with the velocity of the drop, which we shall denote by $\hat{\mathbf{U}}_s$. The position vector at material point R, measured relative to O, will be denoted as $\mathbf{x}$, while the complete dimensionless velocity, pressure and stress distributions, including the disturbance motion induced by the particle, are denoted in the two fluids as $(\mathbf{U}, P, \mathbf{S})$ and $(\tilde{\mathbf{U}}, \tilde{P}, \tilde{\mathbf{S}})$ respectively.

With these conventions and assumptions, the equations of motion for the suspending fluid may be written in the familiar form

$$\nabla . \mathbf{S} = 0, \quad \nabla . \mathbf{U} = 0, \tag{2.1}$$

where

$$\mathbf{S} = -P\mathbf{I} + \mathbf{D}_{(1)} + \lambda[\mathbf{D}_{(1)} . \mathbf{D}_{(1)} + \epsilon_1 \mathbf{D}_{(2)}] + \lambda^2[\epsilon_2(\mathbf{D}_{(1)} : \mathbf{D}_{(1)})\, \mathbf{D}_{(1)} + \epsilon_3 \mathbf{D}_{(3)} + \epsilon_4(\mathbf{D}_{(1)} . \mathbf{D}_{(2)} + \mathbf{D}_{(2)} . \mathbf{D}_{(1)})] + O(\lambda^3); \tag{2.2}$$

and $\mathbf{D}_{(n)}$ are Rivlin–Ericksen tensors given by

$$\left.\begin{aligned} \mathbf{D}_{(1)} &= \nabla\mathbf{U} + (\nabla\mathbf{U})^T, \\ \mathbf{D}_{(2)} &= \frac{\partial}{\partial t}\mathbf{D}_{(1)} + \mathbf{U} . \nabla\mathbf{D}_{(1)} + \mathbf{D}_{(1)} . (\nabla\mathbf{U})^T + \nabla\mathbf{U} . \mathbf{D}_{(1)}, \\ \mathbf{D}_{(3)} &= \frac{\partial}{\partial t}\mathbf{D}_{(2)} + \mathbf{U} . \nabla\mathbf{D}_{(2)} + \mathbf{D}_{(2)} . (\nabla\mathbf{U})^T + \nabla\mathbf{U} . \mathbf{D}_{(2)}. \end{aligned}\right\} \tag{2.3}$$

Here λ and ϵ_1 are dimensionless parameters, defined as $\lambda = \phi_3 G/\mu_0$ and $\epsilon_1 = \bar{\phi}_2/\phi_3$ respectively (ϕ_2 and ϕ_3 are dimensional normal stress coefficients; cf. Ho & Leal 1976). We note that λ is effectively the ratio of an intrinsic relaxation time scale for the fluid to the convective time scale of the fluid's motion. As indicated in (2.2) it will be assumed that λ is small in the present analysis so that the second-order fluid model is applicable and non-Newtonian contributions to the fluid's behaviour are automatically assumed to be small. ϵ_1, on the other hand, is of order unity (see §5.1).

Similarly for the fluid inside the drop, we obtain

$$\nabla.\tilde{\mathbf{S}} = 0, \quad \nabla.\tilde{\mathbf{U}} = 0, \tag{2.4}$$

where
$$\tilde{\mathbf{S}} = -\tilde{p}\mathbf{I} + \tilde{\mathbf{D}}_{(1)} + \tilde{\lambda}[\tilde{\mathbf{D}}_{(1)}.\tilde{\mathbf{D}}_{(1)} + \tilde{\epsilon}_1\tilde{\mathbf{D}}_{(2)}] + \tilde{\lambda}^2[\tilde{\epsilon}_2(\tilde{\mathbf{D}}_{(1)}:\tilde{\mathbf{D}}_{(1)})\tilde{\mathbf{D}}_{(1)} + \tilde{\epsilon}_3\tilde{\mathbf{D}}_{(3)} + \tilde{\epsilon}_4(\tilde{\mathbf{D}}_{(1)}.\tilde{\mathbf{D}}_{(2)} + \tilde{\mathbf{D}}_{(2)}.\tilde{\mathbf{D}}_{(1)})] + O(\tilde{\lambda}^3) \tag{2.5}$$

with $\tilde{\mathbf{D}}_{(n)}$ defined analogously to $\mathbf{D}_{(n)}$, but using $\tilde{\mathbf{U}}$ instead of $\mathbf{U}$. In this case, $\tilde{\lambda}$ and $\tilde{\epsilon}_1$ are defined using quantities relevant to the drop fluid. In this paper, we are interested in studying the case where the non-Newtonian properties of both fluids contribute to migration. The exact relationship between λ and $\tilde{\lambda}$ in this situation will be considered in §5; for now, we shall simply assume that they are of the same order of magnitude.

We next turn to the undisturbed bulk flow. It is obvious that the undisturbed velocity, pressure and stress fields, $(\mathbf{V}, Q, \mathbf{T})$, together with the corresponding Rivlin–Ericksen tensors $\mathbf{E}_{(n)}$, should also be assumed to satisfy creeping flow equations analogous to (2.1)–(2.3). These equations will not be repeated here. As indicated above, we assume that the bulk flow, when measured relative to fixed laboratory coordinates, is steady, unidirectional and two-dimensional. Since we are interested in shearing flows with a shear gradient, we may write the undisturbed flow relative to reference point O as

$$\mathbf{V} = (\alpha + \beta x_3 + \gamma x_3^2)\,\mathbf{e}_1 - \hat{\mathbf{U}}_s \tag{2.6a}$$

with

$$Q = 2\gamma x_1 + (\beta + 2\gamma x_3)^2(1 + 2\epsilon_1)\lambda + 12\gamma x_1(\beta + 2\gamma x_3)^2(\epsilon_2 + \epsilon_4)\lambda^2 + \text{constant}. \tag{2.6b}$$

Examples of flow types described by (2.6a) and (2.6b) include the simple, linear shear flow and the plane Poiseuille flow, both of which are illustrated in figure 1. For the simple shear flow, the coefficients are

$$\alpha = V_w s, \quad \beta = V_w \zeta, \quad \gamma = 0, \tag{2.7}$$

whereas for the Poiseuille flow, they are

$$\alpha = 4V_{\max} s(1-s), \quad \beta = 4V_{\max}(1-2s)\zeta, \quad \gamma = -4V_{\max}\zeta^2. \tag{2.8}$$

V_w and $V_{\max}$ are both measured relative to the fixed laboratory reference frame. In (2.7) and (2.8), s is the dimensionless distance from a wall and ζ is the drop radius to gap width ratio, given by $\zeta = a/d$. Although the assumption of a two-dimensional undisturbed flow may seem unduly restrictive, we have previously shown (Chan & Leal 1977) that the results may be extended to the corresponding three-dimensional flows, provided that hydrodynamic interactions between the particle and bounding wall are negligible. In that paper, a general method was developed by which the motion of a spherical particle in a general quadratic unidirectional flow of a second-order fluid was obtained completely from the detailed results of Ho & Leal (1976) for the

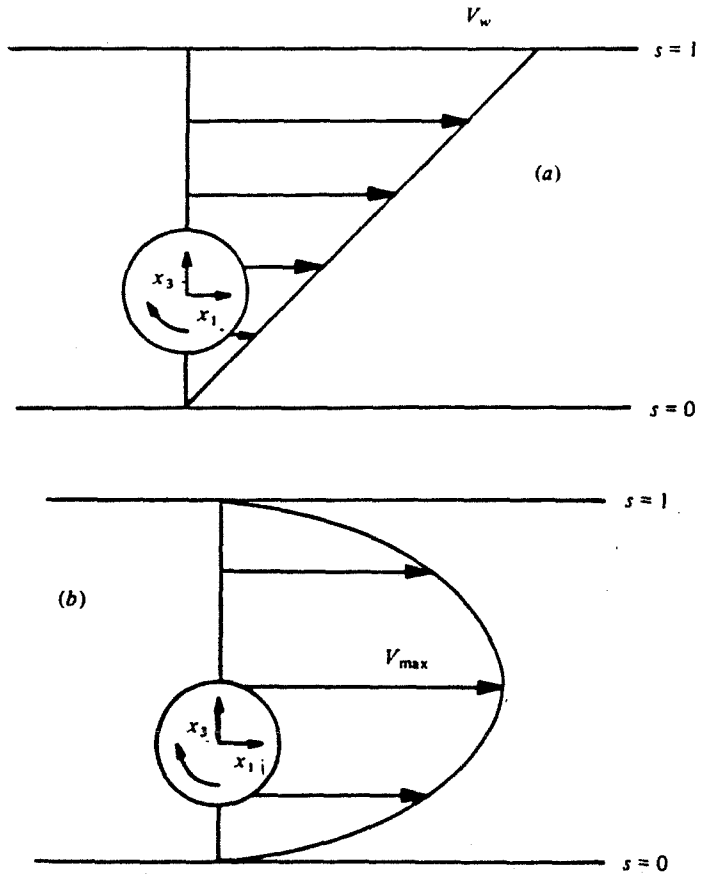

FIGURE 1. A side view of a drop in: (a) a simple shear flow; (b) a two-dimensional Poiseuille flow.

particle motion in a two-dimensional quadratic, unidirectional flow. In the present work, the method of Chan & Leal (1977) is again applied to extend our detailed results for a two-dimensional quadratic unidirectional undisturbed flow to the cases of a three-dimensional Poiseuille flow and of a Couette flow. The latter are of particular interest because most of the experimental studies of particle migration have been carried out for Poiseuille and Couette flows. The initial choice of a two-dimensional undisturbed flow geometry is made largely due to the relative simplicity of the resulting analysis.

For our present case, the boundary conditions at large distances from the drop are

$$\left.\begin{aligned} &\mathbf{U} \to \mathbf{V} && \text{as} \quad r = |\mathbf{x}| \to \infty, \\ &\mathbf{U} = V_w \mathbf{e}_1 - \hat{\mathbf{U}}_s && \text{on the walls.} \end{aligned}\right\} \tag{2.9}$$

On the surface of the *deformed* drop

$$\mathbf{U} = \tilde{\mathbf{U}}, \tag{2.10a}$$

$$\mathbf{U}.\mathbf{n} = \tilde{\mathbf{U}}.\mathbf{n} = 0, \tag{2.10b}$$

$$\mathbf{S}.\mathbf{n} = \kappa \tilde{\mathbf{S}}.\mathbf{n} + \frac{1}{\delta}\left(\frac{1}{R_1} + \frac{1}{R_2}\right)\mathbf{n}. \tag{2.10c}$$

Here κ is the viscosity ratio (i.e. $\kappa = \tilde{\mu}_0/\mu_0$) whereas R_1 and R_2 are the principal radii of curvature. δ is a comparison between viscous forces and the interfacial tension σ, and is given by $\delta = a\mu_0 G/\sigma$. In the present work, we shall restrict our attention to the case of small deformations from the spherical shape, with the spherical shape being preserved by interfacial tension. Hence, we shall assume that δ is a small parameter. Thus, in the perturbation expansion which follows, we shall adopt the procedures outlined by Taylor (1932, 1934) and Frankel & Acrivos (1970), in which the velocity, kinematic and shear stress conditions are satisfied at each order, and the deformation of the drop is then calculated using the normal stress condition, (2.10*c*).

It should be noted that a second asymptotic limit exists where the drop shape remains near to spherical; namely, the case of a very viscous drop (i.e. $\kappa \to \infty$) which was also considered by Taylor (1934) and Frankel & Acrivos (1970). There, the velocity and stress continuity conditions are satisfied on the surface of the drop at each order, and the non-zero normal velocity which results must be balanced by a deformation term. It can be easily shown in this case that the migration velocity to $O(1/\kappa)$ is identically zero, due to fore–aft symmetry of the deformed drop plus alignment of its major axis with the axis of the undisturbed velocity field. Thus no further consideration will be given to deformation-induced migration in the limit $\kappa \to \infty$ in the present paper. The migration due to deformation in the limit $\delta \ll 1$ which we shall study is restricted to $\kappa < O(1/\delta)$. On the other hand, the Newtonian velocity fields in §4, and the normal stress-induced migration calculations for a spherical drop in §5 are both valid for all values of κ.

We now proceed formally to the solution of our problem, *via* a double asymptotic expansion in λ and δ. Thus, we let

$$1 \gg \lambda,\delta \gg \lambda^2,\lambda\delta,\delta^2 \ldots$$

and write, for the particle velocity

$$\hat{\mathbf{U}}_s = \hat{\mathbf{U}}_s^{(0)} + \lambda\hat{\mathbf{U}}_s^{(\lambda)} + \delta\hat{\mathbf{U}}_s^{(\delta)} + \lambda^2\hat{\mathbf{U}}_s^{(\lambda\lambda)} + \lambda\delta\hat{\mathbf{U}}_s^{(\lambda\delta)} + \delta^2\hat{\mathbf{U}}_s^{(\delta\delta)} + \ldots, \tag{2.11}$$

$\hat{\mathbf{U}}_s^{(0)}$ is the translational velocity of a Newtonian, spherical drop in a two-dimensional, quadratic shear flow of a Newtonian fluid, whereas $\hat{\mathbf{U}}_s^{(\lambda)}$ represents the non-Newtonian (normal-stress) contribution to the translation of a spherical drop, and so on. We may also write down formal expansions for the velocity, pressure and stress fields. For the suspending phase, these are

$$\left.\begin{aligned} \mathbf{U} &= \mathbf{U}^{(0)} + \lambda\mathbf{U}^{(\lambda)} + \delta\mathbf{U}^{(\delta)} + \lambda^2\mathbf{U}^{(\lambda\lambda)} + \lambda\delta\mathbf{U}^{(\lambda\delta)} + \delta^2\mathbf{U}^{(\delta\delta)} + \ldots, \\ P &= P^{(0)} + \lambda P^{(\lambda)} + \delta P^{(\delta)} + \lambda^2 P^{(\lambda\lambda)} + \lambda\delta P^{(\lambda\delta)} + \delta^2 P^{(\delta\delta)} + \ldots, \\ \mathbf{S} &= \mathbf{S}^{(0)} + \lambda\mathbf{S}^{(\lambda)} + \delta\mathbf{S}^{(\delta)} + \lambda^2\mathbf{S}^{(\lambda\lambda)} + \lambda\delta\mathbf{S}^{(\lambda\delta)} + \delta^2\mathbf{S}^{(\delta\delta)} + \ldots, \end{aligned}\right\} \tag{2.12}$$

whereas for the fluid inside the drop, we obtain

$$\left.\begin{aligned} \tilde{\mathbf{U}} &= \tilde{\mathbf{U}}^{(0)} + \lambda\tilde{\mathbf{U}}^{(\lambda)} + \delta\tilde{\mathbf{U}}^{(\delta)} + \lambda^2\tilde{\mathbf{U}}^{(\lambda\lambda)} + \lambda\delta\tilde{\mathbf{U}}^{(\lambda\delta)} + \delta^2\tilde{\mathbf{U}}^{(\delta\delta)} + \ldots, \\ \tilde{P} &= \frac{1}{\delta}\tilde{P}^{(1/\delta)} + \tilde{P}^{(0)} + \lambda\tilde{P}^{(\lambda)} + \delta\tilde{P}^{(\delta)} + \lambda^2\tilde{P}^{(\lambda\lambda)} + \lambda\delta\tilde{P}^{(\lambda\delta)} + \delta^2\tilde{P}^{(\delta\delta)} + \ldots, \\ \tilde{\mathbf{S}} &= \frac{1}{\delta}\tilde{\mathbf{S}}^{(1/\delta)} + \tilde{\mathbf{S}}^{(0)} + \lambda\tilde{\mathbf{S}}^{(\lambda)} + \delta\tilde{\mathbf{S}}^{(\delta)} + \lambda^2\tilde{\mathbf{S}}^{(\lambda\lambda)} + \lambda\delta\tilde{\mathbf{S}}^{(\lambda\delta)} + \delta^2\tilde{\mathbf{S}}^{(\delta\delta)} + \ldots. \end{aligned}\right\} \tag{2.13}$$

Here, $\tilde{P}^{(1/\delta)}$ and $\tilde{\mathbf{S}}^{(1/\delta)}$ are needed to satisfy (2.10c) for a quiescent spherical drop, while the terms with superscripts (0) denote the Newtonian velocity, pressure and stress fields. The first non-Newtonian correction to fluid motion inside and outside the spherical drop occurs at $O(\lambda)$, which then represents the contribution from the two separate second-order fluids. Similarly, the first deformation corrections (with the fluids assumed to be Newtonian) are denoted by superscripts (δ). Inherent in the form of these asymptotic expansions is the possibility that the non-Newtonian fluid properties and the drop deformation (for Newtonian fluids) will each provide an *independent* first-order contribution to fluid motion and particle migration, with their interaction occurring only at $O(\lambda\delta)$. Obviously, the higher order non-Newtonian and deformation corrections will occur at $O(\lambda^2)$ and $O(\delta^2)$, respectively.

The shape of the drop should also be considered in the context of the expansions (2.12) and (2.13). Since the Newtonian velocity field alone is sufficient to cause deformation of a Newtonian drop at $O(\delta)$, it is obvious that the $O(\lambda)$ non-Newtonian velocity field will cause deformation at $O(\lambda\delta)$, and so on. Hence on the surface of the drop, we let

$$F = r - 1 - \delta f^{(\delta)} - \lambda\delta f^{(\lambda\delta)} - \delta^2 f^{(\delta\delta)} - \ldots = 0, \tag{2.14}$$

where $f^{(\delta)}$, $f^{(\lambda\delta)}$ and $f^{(\delta\delta)}$ denote the deformations at $O(\delta)$, $O(\lambda\delta)$ and $O(\delta^2)$ respectively. Of course, it is inherently assumed from the form of (2.14) that these shape functions $f^{(\delta)}$, $f^{(\lambda\delta)}$ and $f^{(\delta\delta)}$ at any material point on the surface will only depend on its angular position relative to the centroid O of the drop, and not on the radial position r itself. The outer normal and the principal radii of curvature are now easily expressed in terms of the shape functions as

$$\begin{aligned}\mathbf{n} &= \nabla F/|\nabla F| \\ &= \mathbf{e}_r - \delta\nabla f^{(\delta)} - \lambda\delta\nabla f^{(\lambda\delta)} - \delta^2[\nabla f^{(\delta\delta)} + \tfrac{1}{2}(\nabla f^{(\delta)}.\nabla f^{(\delta)})\,\mathbf{e}_r] - \ldots\end{aligned} \tag{2.15}$$

$$\begin{aligned}\frac{1}{R_1}+\frac{1}{R_2} = \nabla.\mathbf{n} &= 2 - \delta[2f^{(\delta)} + \nabla^2 f^{(\delta)}] - \lambda\delta[2f^{(\lambda\delta)} + \nabla^2 f^{(\lambda\delta)}] \\ &\quad - \delta^2[2f^{(\delta\delta)} - 2f^{(\delta)}f^{(\delta)} + \nabla^2 f^{(\delta\delta)}] - \ldots.\end{aligned} \tag{2.16}$$

We now substitute (2.12), (2.13), (2.15) and (2.16) into boundary conditions (2.10a)–(2.10c). Any quantities that are to be evaluated on the surface of the drop will be approximated by a Taylor's series expansion about $r = 1$ using (2.14). Hence we have, in effect, reduced the problem to that of a spherical drop. After some straightforward algebra, velocity, kinematic and stress conditions at $r = 1$ may be obtained at each order of our perturbation expansion. We shall present these equations as we need them in subsequent sections.

It should be emphasized here that a full solution of the above problem at *any* order in λ or δ will yield an expression at the *same* level in λ or δ for the cross-flow migration velocity. However, at any point beyond the initial Newtonian velocity fields for a spherical drop, the required analysis becomes exceedingly tedious and subject to uncertainty in the numerical accuracy of the many algebraic manipulations. Thus, in the next section, we describe the development of a theoretical expression for the lateral velocity of a deformed drop which can be evaluated at any order in λ or δ, using only the velocity and pressure corrections in the fluid at one order less in λ or δ (i.e. at $O(1)$ for the $O(\lambda)$ and $O(\delta)$ contributions to the migration velocity).

3. The reciprocal theorem

For problems in which perturbation expansions are used to extend results beyond the domain of zero Reynolds number for a particle of fixed shape in a Newtonian fluid, it is often possible to obtain, by use of the reciprocal theorem of Lorentz, macroscopic properties of interest (e.g. force and torque) at any order, without detailed calculations of the velocity field at that order; instead, only lower order solutions are needed for the velocity and pressure fields. This approach was outlined by Cox & Brenner (1968) in connexion with the problem of inertia-induced migration of a rigid sphere. Later, Ho & Leal (1974, 1976) also used the same method for their inertial and non-Newtonian migration calculations. So far, however, no one has applied the theorem to the case of a fluid drop. Since the derivation of the theorem is an important (and interesting) part in the development of our analysis, we shall present it in detail here, even though the rigid sphere problem has been treated thoroughly by previous authors.

To apply the reciprocal theorem to the calculation of lateral migration velocities, we must first consider the 'so-called' complementary problem of the motion of a Newtonian drop translating perpendicularly to the walls in a quiescent Newtonian fluid. The equations of motion outside the drop are simply

$$\nabla.\mathbf{t} = 0, \quad \nabla.\mathbf{u} = 0, \tag{3.1}$$

where

$$\mathbf{t} = -q\mathbf{I} + \mathbf{a} \tag{3.2}$$

$\mathbf{a}$ is, of course, the rate-of-strain tensor. Similar equations are satisfied by $(\tilde{\mathbf{u}}, \tilde{q}, \tilde{\mathbf{t}})$ inside the drop. The boundary conditions at large distances are

$$\left.\begin{aligned} \mathbf{u} &\to -\mathbf{e}_3 \quad \text{as } r \to \infty, \\ \mathbf{u} &= -\mathbf{e}_3 \quad \text{on the walls.} \end{aligned}\right\} \tag{3.3}$$

The shape of the drop and the boundary conditions on its surface remain to be discussed. In general, it is necessary to assume that the particle in the complementary problem has the same shape as the 'real' one under consideration. However, in § 2, we have effectively reduced the full problem to that of a *spherical* drop with a series of boundary conditions on the surface. Hence, we may now conveniently choose the drop for the complementary problem to be also spherical, so that the boundary conditions on $r = 1$ become

$$\mathbf{u} = \tilde{\mathbf{u}}, \tag{3.4a}$$

$$\mathbf{u}.\mathbf{e}_r = \tilde{\mathbf{u}}.\mathbf{e}_r = 0, \tag{3.4b}$$

$$(\mathbf{I} - \mathbf{e}_r\mathbf{e}_r).(\mathbf{t}.\mathbf{e}_r) = \kappa(\mathbf{I} - \mathbf{e}_r\mathbf{e}_r).(\tilde{\mathbf{t}}.\mathbf{e}_r). \tag{3.4c}$$

We see from (3.4c) that only shear stresses can be matched in our present problem of an undeformed sphere. Hence, a discontinuity in normal stress will usually exist on the sphere surface. (Equivalently, we may imagine that a force is being applied in the normal direction to prevent the sphere from deforming.) This discontinuity vanishes only for the well-known case of translation in an unbounded fluid medium, and even in this case, it is non-zero if wall reflexions are included.

We are now ready to apply the reciprocal theorem. For the fluid outside the drop,

it is desirable to use disturbance quantities which approach zero far away from the particle. Therefore, we write

$$\int_{V_f} [(\nabla . \mathbf{S} - \nabla . \mathbf{T}) . (\mathbf{u} + \mathbf{e}_3) - (\nabla . \mathbf{t}) . (\mathbf{U} - \mathbf{V})] dV = 0, \tag{3.5}$$

where V_f is the entire volume outside the drop. Rearranging, we get

$$\int_{V_f} \nabla . [(\mathbf{S} - \mathbf{T}) . (\mathbf{u} + \mathbf{e}_3) - \mathbf{t} . (\mathbf{U} - \mathbf{V})] dV = \int_{V_f} [(\mathbf{S} - \mathbf{T}) : \nabla \mathbf{u} - \mathbf{t} : \nabla (\mathbf{U} - \mathbf{V})] dV. \tag{3.6}$$

The second integral may now be easily simplified using the definitions of $\mathbf{S}$, $\mathbf{T}$ and $\mathbf{t}$, and the continuity equation. For the first integral, we apply the divergence theorem to obtain†

$$\int_{V_f} \nabla . [(\mathbf{S} - \mathbf{T}) . (\mathbf{u} + \mathbf{e}_3) - \mathbf{t} . (\mathbf{U} - \mathbf{V})] dV = - \int_{A_d} [(\mathbf{S} - \mathbf{T}) . (\mathbf{u} + \mathbf{e}_3) - \mathbf{t} . (\mathbf{U} - \mathbf{V})] . \mathbf{n} dA, \tag{3.7}$$

where A_d is the *spherical* drop interface. Hence, for a neutrally buoyant drop $\left(\text{i.e.} \int_{A_d} (\mathbf{S} - \mathbf{T}) . \mathbf{n} dA = 0\right)$,

$$\begin{aligned} - \int_{A_d} [(\mathbf{S} - \mathbf{T}) . \mathbf{u} - \mathbf{t} . (\mathbf{U} - \mathbf{V})] . \mathbf{n} dA \\ = \lambda \int_{V_f} [(\mathbf{D}_{(1)} . \mathbf{D}_{(1)} - \mathbf{E}_{(1)} . \mathbf{E}_{(1)}) + \epsilon_1 (\mathbf{D}_{(2)} - \mathbf{E}_{(2)})] : \nabla \mathbf{u} dV \\ + \lambda^2 \int_{V_f} [\epsilon_2, \epsilon_3, \epsilon_4 \text{ terms}] : \nabla \mathbf{u} dV. \end{aligned} \tag{3.8}$$

Inside the drop, similar manipulations give

$$\int_{A_d} [\tilde{\mathbf{S}} . \tilde{\mathbf{u}} - \tilde{\mathbf{t}} . \tilde{\mathbf{U}}] . \mathbf{n} dA = \tilde{\lambda} \int_{\tilde{V}_f} [\tilde{\mathbf{D}}_{(1)} . \tilde{\mathbf{D}}_{(1)} + \tilde{\epsilon}_1 \tilde{\mathbf{D}}_{(2)}] : \nabla \tilde{\mathbf{u}} dV + \tilde{\lambda}^2 \int_{\tilde{V}_f} [\tilde{\epsilon}_2, \tilde{\epsilon}_3, \tilde{\epsilon}_4 \text{ terms}] : \nabla \tilde{\mathbf{u}} dV \tag{3.9}$$

with $\tilde{V}_f$ denoting the volume of the drop. We now have two expressions (3.8) and (3.9), which both involve area integrals on the surface of the drop. To evaluate them, we need to consider the boundary conditions (2.10) at the surface of the drop, transformed to apply at $r = 1$. These conditions are of the matching type; hence, it is obvious that (3.8) and (3.9) can be combined by multiplying (3.9) by κ and adding it to (3.8). The result is

$$\begin{aligned} - \int_{A_d} [(\mathbf{S} - \kappa \tilde{\mathbf{S}}) . \mathbf{u} - (\mathbf{t} - \kappa \tilde{\mathbf{t}}) . \mathbf{U} - \kappa \tilde{\mathbf{t}} . (\mathbf{U} - \tilde{\mathbf{U}}) - \mathbf{T} . \mathbf{u} + \mathbf{t} . \mathbf{V}] . \mathbf{n} dA \\ = \lambda \left\{ \int_{V_f} [(\mathbf{D}_{(1)} . \mathbf{D}_{(1)} - \mathbf{E}_{(1)} . \mathbf{E}_{(1)}) + \epsilon_1 (\mathbf{D}_{(2)} - \mathbf{E}_{(2)})] : \nabla \mathbf{u} dV \right. \\ \left. + \kappa \frac{\tilde{\lambda}}{\lambda} \int_{\tilde{V}_f} [\tilde{\mathbf{D}}_{(1)} . \tilde{\mathbf{D}}_{(1)} + \tilde{\epsilon}_1 \tilde{\mathbf{D}}_{(2)}] : \nabla \tilde{\mathbf{u}} dV \right\} + \lambda^2 \left\{ \int_{V_f} [\epsilon_2, \epsilon_3, \epsilon_4 \text{ terms}] : \nabla \mathbf{u} dV \right. \\ \left. + \kappa (\tilde{\lambda}/\lambda)^2 \int_{\tilde{V}_f} [\tilde{\epsilon}_2, \tilde{\epsilon}_3, \tilde{\epsilon}_4 \text{ terms}] : \nabla \tilde{\mathbf{u}} dV \right\}. \end{aligned} \tag{3.10}$$

† It may be shown, for disturbance quantities which approach zero at large distances from the particle, that it is not necessary to consider the contributions at infinity. A detailed proof is provided in Chan (1979).

The advantage of combining (3.8) and (3.9) in the form (3.10) is that we can use the interface boundary conditions to evaluate the surface integral over A_d to $O(\lambda^n)$ in terms of the migration velocity contribution at $O(\lambda^n)$ and the fluid velocity and stress fields through $O(\lambda^{n-1})$. It may be noted, in this regard, that the drop shape is quasi-steady at $O(\delta^m)$ and can thus be determined via the normal stress condition at $O(\delta^m)$ from the stress fields at $O(\delta^{m-1})$. This latter fact is obviously crucial to the successful evaluation of the left-hand side of (3.10) in the manner described above. Since the right-hand side of (3.10) may obviously also be calculated at $O(\lambda^n)$ completely in terms of the velocity and stress fields at $O(\lambda^{n-1})$, the expression (3.10) can clearly be used to determine the migration velocity at $O(\lambda^n)$ completely in terms of known or calculable quantities at $O(\lambda^{n-1})$. This fact may, perhaps, be more clearly illustrated by considering the $O(\lambda)$ terms in (3.10)

$$-\int_{A_d}[(\mathbf{S}^{(\lambda)}-\kappa\tilde{\mathbf{S}}^{(\lambda)})\cdot\mathbf{u}-(\mathbf{t}-\kappa\tilde{\mathbf{t}})\cdot\mathbf{U}^{(\lambda)}-\kappa\tilde{\mathbf{t}}\cdot(\mathbf{U}^{(\lambda)}-\tilde{\mathbf{U}}^{(\lambda)})-\mathbf{T}^{(\lambda)}\cdot\mathbf{u}+\mathbf{t}\cdot\mathbf{V}^{(\lambda)}]\cdot\mathbf{e}_r\,dA$$
$$=\int_{V_f}[(\mathbf{D}^{(0)}_{(1)}\cdot\mathbf{D}^{(0)}_{(1)}-\mathbf{E}^{(0)}_{(1)}\cdot\mathbf{E}^{(0)}_{(1)})+\epsilon_1(\mathbf{D}^{(0)}_{(2)}-\mathbf{E}^{(0)}_{(2)})]:\nabla\mathbf{u}\,dV$$
$$+\kappa\frac{\tilde{\lambda}}{\lambda}\int_{\tilde{V}_f}[\tilde{\mathbf{D}}^{(0)}_{(1)}\cdot\tilde{\mathbf{D}}^{(0)}_{(1)}+\tilde{\epsilon}_1\tilde{\mathbf{D}}^{(0)}_{(2)}]:\nabla\tilde{\mathbf{u}}\,dV. \tag{3.11}$$

As we shall show in §5, the surface integral over A_d can be easily simplified using the interfacial boundary conditions so that only Newtonian velocity fields appear from $\mathbf{T}^{(\lambda)}\cdot\mathbf{u}\cdot\mathbf{e}_r$, along with the migration velocity $\hat{\mathbf{U}}^{(\lambda)}_s$ which comes from $\mathbf{t}\cdot\mathbf{V}^{(\lambda)}\cdot\mathbf{e}_r$. Obviously, expressions for $\hat{\mathbf{U}}^{(\delta)}_s$ or the higher order quadratic terms can be obtained in a similar manner, and these will be presented as needed in later sections of the paper.

4. The Newtonian solutions

We now attempt to solve, to $O(1)$, the equations of motion (2.1) and (2.4), subject to boundary conditions (2.9) and (2.10*a*)–(2.10*c*). As before, the superscript $(1/\delta)$ will denote the pressure term at quiescence, whereas the superscript (0) denotes the Newtonian contributions. Trivially, we obtain

$$\tilde{P}^{(1/\delta)}=2/\kappa. \tag{4.1}$$

It is obvious that this term represents the capillary pressure increase across the surface of a spherical drop in a quiescent fluid.

The Newtonian flow problem outside the drop is defined by

$$\nabla\cdot\mathbf{S}^{(0)}=0,\quad \nabla\cdot\mathbf{U}^{(0)}=0 \tag{4.2}$$

with boundary conditions at large distances from the drop

$$\mathbf{U}^{(0)}\to(\alpha+\beta x_3+\gamma x_3^2)\,\mathbf{e}_1-\hat{\mathbf{U}}^{(0)}_s \quad \text{as } r\to\infty, \tag{4.3a}$$

$$\mathbf{U}^{(0)}=V_w\mathbf{e}_1-\hat{\mathbf{U}}^{(0)}_s \quad \text{on the walls.} \tag{4.3b}$$

It is, of course, very difficult to obtain an exact analytic solution to the above boundary value problem. However, for a particle which is small compared to the characteristic dimension of the flow (i.e. $\zeta\ll 1$), we may utilize the well-known method of reflexions (cf. Happel & Brenner 1973), which approximates $\mathbf{U}^{(0)}$ as a series of terms alternately

satisfying the boundary conditions at the particle surface and on the walls. Inherently, it is assumed in this technique that the particle is not 'close' to either wall. For our case, we write

$$\mathbf{U}^{(0)} = {}_1\mathbf{U}^{(0)} + {}_2\mathbf{U}^{(0)} + {}_3\mathbf{U}^{(0)} + \ldots . \tag{4.4}$$

The solution of the above equations follows the method outlined by Ho & Leal (1974) for a rigid sphere. The first term in (4.4) corresponds to the velocity in an unbounded domain and is obtained using Lamb's general solution,

$$\begin{aligned}
{}_1\mathbf{U}^{(0)} = {} & (\alpha + \beta x_3 + \gamma x_3^2)\,\mathbf{e}_1 - \hat{\mathbf{U}}_s^{(0)} - \tfrac{1}{2}A_1\left(\frac{1}{r}\mathbf{e}_1 + \frac{x_1}{r^3}\mathbf{x}\right) - B_1\left(\frac{1}{r^3}\mathbf{e}_1 - \frac{3x_1}{r^5}\mathbf{x}\right) \\
& - C_1\left(\frac{x_3}{r^3}\mathbf{e}_1 - \frac{x_1}{r^3}\mathbf{e}_3\right) + \tfrac{3}{2}D_1\frac{x_1x_3}{r^5}\mathbf{x} + 3E_1\left(\frac{x_3}{r^5}\mathbf{e}_1 + \frac{x_1}{r^5}\mathbf{e}_3 - \frac{5x_1x_3}{r^7}\mathbf{x}\right) \\
& - 3F_1\left(\frac{1}{r^3}\mathbf{e}_1 - \frac{x_1}{r^5}\mathbf{x} - \frac{2x_3^2}{r^5}\mathbf{e}_1 + \frac{2x_1x_3}{r^5}\mathbf{e}_3\right) \\
& - \tfrac{1}{10}G_1\left(\frac{1}{r^3}\mathbf{e}_1 - \frac{13x_1}{r^5}\mathbf{x} - \frac{5x_3^2}{r^5}\mathbf{e}_1 - \frac{10x_1x_3}{r^5}\mathbf{e}_3 + \frac{75x_1x_3^2}{r^7}\mathbf{x}\right) \\
& + 3H_1\left(\frac{1}{r^5}\mathbf{e}_1 - \frac{5x_1}{r^7}\mathbf{x} - \frac{5x_3^2}{r^7}\mathbf{e}_1 - \frac{10x_1x_3}{r^7}\mathbf{e}_3 + \frac{35x_1x_3^2}{r^9}\mathbf{x}\right).
\end{aligned} \tag{4.5}$$

By considering (4.5), the first reflected solution ${}_2\mathbf{U}^{(0)}$ may now be expressed in terms of complicated integrals over the entire volume (i.e. Faxén's method; cf. Happel & Brenner 1973). Here, we consider only the simplified form which is relevant in the vicinity of the drop

$${}_2\mathbf{U}^{(0)} = (I_1 + \tfrac{1}{2}I_4)\,\mathbf{e}_1 - \tfrac{1}{2}\zeta(\tfrac{3}{2}I_2 + I_5)\,(x_3\mathbf{e}_1 + x_1\mathbf{e}_3) - \tfrac{1}{2}\zeta(\tfrac{1}{2}I_2 - I_7)\,(x_3\mathbf{e}_1 - x_1\mathbf{e}_3). \tag{4.6}$$

For brevity, we refer the reader to Ho & Leal (1974) for the detailed expressions for $I_1 \ldots I_7$; they do not appear in any final results of this paper. Finally, proceeding from (4.6), we obtain ${}_3\mathbf{U}^{(0)}$ in the form

$$\begin{aligned}
{}_3\mathbf{U}^{(0)} = {} & -\tfrac{1}{2}A_3\left(\frac{1}{r}\mathbf{e}_1 + \frac{x_1}{r^3}\mathbf{x}\right) - B_3\left(\frac{1}{r^3}\mathbf{e}_1 - \frac{3x_1}{r^5}\mathbf{x}\right) - C_3\left(\frac{x_3}{r^3}\mathbf{e}_1 - \frac{x_1}{r^3}\mathbf{e}_3\right) \\
& + \tfrac{3}{2}D_3\frac{x_1x_3}{r^5}\mathbf{x} + 3E_3\left(\frac{x_3}{r^5}\mathbf{e}_1 + \frac{x_1}{r^5}\mathbf{e}_3 - \frac{5x_1x_3}{r^7}\mathbf{x}\right).
\end{aligned} \tag{4.7}$$

For the fluid inside the drop, we let

$$\tilde{\mathbf{U}}^{(0)} = {}_1\tilde{\mathbf{U}}^{(0)} + {}_{2+3}\tilde{\mathbf{U}}^{(0)} + \ldots, \tag{4.8}$$

where ${}_{2+3}\tilde{\mathbf{U}}^{(0)}$ is the term needed to match ${}_2\mathbf{U}^{(0)} + {}_3\mathbf{U}^{(0)}$ at the drop surface. Again, using Lamb's general solution, we obtain

$$\begin{aligned}
{}_1\tilde{\mathbf{U}}^{(0)} = {} & -\tfrac{1}{10}\tilde{A}_1(2r^2\mathbf{e}_1 - x_1\mathbf{x}) - \tilde{B}_1\mathbf{e}_1 - \tilde{C}_1(x_3\mathbf{e}_1 - x_1\mathbf{e}_3) \\
& + \tfrac{1}{14}\tilde{D}_1(5x_3r^2\mathbf{e}_1 + 5x_1r^2\mathbf{e}_3 - 4x_1x_3\mathbf{x}) - 3\tilde{E}_1(x_3\mathbf{e}_1 + x_1\mathbf{e}_3) \\
& - 3\tilde{F}_1(r^2\mathbf{e}_1 - x_1\mathbf{x} - 2x_3^2\mathbf{e}_1 + 2x_1x_3\mathbf{e}_3) + \tfrac{1}{4}\tilde{G}_1(r^4\mathbf{e}_1 + x_1r^2\mathbf{x} - 5x_3^2r^2\mathbf{e}_1 \\
& - 10x_1x_3r^2\mathbf{e}_3 + 5x_1x_3^2\mathbf{x}) + 3\tilde{H}_1(r^2\mathbf{e}_1 + 2x_1\mathbf{x} - 5x_3^2\mathbf{e}_1 - 10x_1x_3\mathbf{e}_3).
\end{aligned} \tag{4.9}$$

The solution ${}_{2+3}\tilde{\mathbf{U}}^{(0)}$ is similar to (4.9) but with $\tilde{A}_1 \ldots \tilde{E}_1$ replaced by $\tilde{A}_3 \ldots \tilde{E}_3$, while the corresponding $\tilde{F}_3 \ldots \tilde{H}_3$ terms may be omitted at this level of approximation.

All the constants $A_1 \dots H_1$, $A_3 \dots E_3$, $\tilde{A}_1 \dots \tilde{H}_1$ and $\tilde{A}_3 \dots \tilde{E}_3$, and the unknown shape function $f^{(\delta)}$ are determined *via* application of the boundary conditions (2.10*a*)–(2.10*c*) at $r = 1$. Using (2.15) and (2.16), these conditions are

$$\mathbf{U}^{(0)} = \tilde{\mathbf{U}}^{(0)}, \tag{4.10a}$$

$$\mathbf{U}^{(0)} \cdot \mathbf{e}_r = \tilde{\mathbf{U}}^{(0)} \cdot \mathbf{e}_r = 0, \tag{4.10b}$$

$$\mathbf{S}^{(0)} \cdot \mathbf{e}_r = \kappa \tilde{\mathbf{S}}^{(0)} \cdot \mathbf{e}_r - [2f^{(\delta)} + \nabla^2 f^{(\delta)}]\, \mathbf{e}_r. \tag{4.10c}$$

After some algebra, the coefficients in (4.5), (4.7) and (4.9) are obtained from (4.10*a*), (4.10*b*), and the tangential component of (4.10*c*)

$$\left.\begin{aligned}
A_1 &= [\alpha - (\hat{U}_s^{(0)})_1]\frac{2+3\kappa}{2(1+\kappa)} + \frac{\gamma\kappa}{2(1+\kappa)}, & \tilde{A}_1 &= -[\alpha - (\hat{U}_s^{(0)})_1]\frac{5}{1+\kappa} - \frac{5\gamma}{1+\kappa}, \\
B_1 &= [\alpha - (\hat{U}_s^{(0)})_1]\frac{\kappa}{4(1+\kappa)} + \frac{\gamma(-2+3\kappa)}{20(1+\kappa)}, & \tilde{B}_1 &= [\alpha - (\hat{U}_s^{(0)})_1]\frac{1}{2(1+\kappa)} + \frac{\gamma}{2(1+\kappa)}, \\
C_1 &= 0, & \tilde{C}_1 &= -\tfrac{1}{2}\beta, \\
D_1 &= -\frac{\beta(2+5\kappa)}{3(1+\kappa)}, & \tilde{D}_1 &= \frac{7\beta}{2(1+\kappa)}, \\
E_1 &= -\frac{\beta\kappa}{6(1+\kappa)}, & \tilde{E}_1 &= -\frac{\beta}{4(1+\kappa)}, \\
F_1 &= \frac{\gamma(1-\kappa)}{9(4+\kappa)}, & \tilde{F}_1 &= \frac{5\gamma}{9(4+\kappa)}, \\
G_1 &= \frac{\gamma(2+7\kappa)}{12(1+\kappa)}, & \tilde{G}_1 &= -\frac{\gamma}{1+\kappa}, \\
H_1 &= \frac{\gamma\kappa}{24(1+\kappa)}, & \tilde{H}_1 &= \frac{\gamma}{18(1+\kappa)};
\end{aligned}\right\} \tag{4.11}$$

and

$$\left.\begin{aligned}
A_3 &= (I_1 + \tfrac{1}{2}I_4)(2+3\kappa)/2(1+\kappa), & \tilde{A}_3 &= -(I_1 + \tfrac{1}{2}I_4)\,5/(1+\kappa), \\
B_3 &= (I_1 + \tfrac{1}{2}I_4)\,\kappa/4(1+\kappa), & \tilde{B}_3 &= (I_1 + \tfrac{1}{2}I_4)\,1/2(1+\kappa), \\
C_3 &= 0, & \tilde{C}_3 &= \tfrac{1}{2}\zeta(\tfrac{1}{2}I_2 - I_7), \\
D_3 &= \zeta(\tfrac{3}{2}I_2 + I_5)(2+5\kappa)/3(1+\kappa), & \tilde{D}_3 &= -\zeta(\tfrac{3}{2}I_2 + I_5)\,7/2(1+\kappa), \\
E_3 &= \zeta(\tfrac{3}{2}I_2 + I_5)\,\kappa/6(1+\kappa), & \tilde{E}_3 &= \zeta(\tfrac{3}{2}I_2 + I_5)\,1/4(1+\kappa).
\end{aligned}\right\} \tag{4.12}$$

It is easy to see that the velocity fields (4.4) and (4.8), together with the coefficients (4.11) and (4.12), reduce to the values given by Ho & Leal (1974) for the case of a very viscous drop (i.e. $\kappa \to \infty$). In this limit the motion of the drop reduces to a rigid body rotation, as expected.

The force acting on the drop, to our present level of approximation, may be obtained by summing the Stokeslet contributions from (4.5) and (4.7), which gives

$$\mathbf{F} = 4\pi(A_1 + A_3)\,\mathbf{e}_1. \tag{4.13}$$

Obviously, for a neutrally buoyant particle, the force $\mathbf{F}$ must be zero, and it thus follows from (4.13) that

$$(\hat{U}_s^{(0)})_1 = \alpha + \kappa\gamma/(2+3\kappa) + I_1 + \tfrac{1}{2}I_4 \tag{4.14}$$

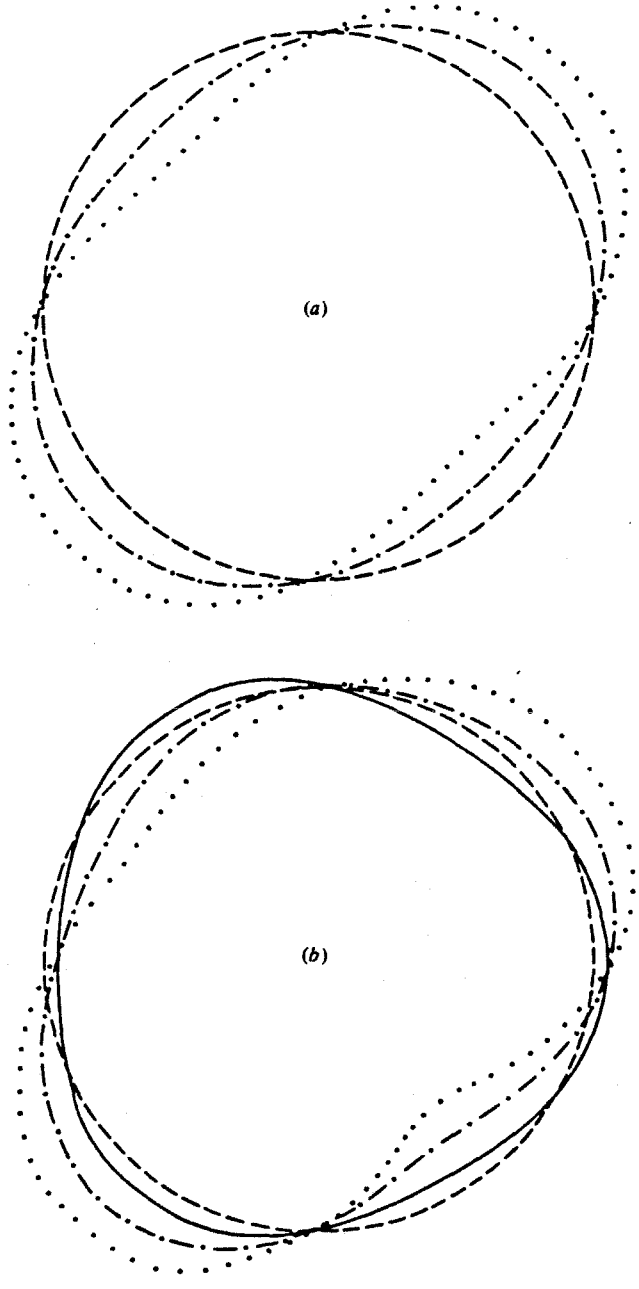

FIGURE 2. The shape of a deformed drop in: (*a*) a simple shear flow. –·–, $\chi = \delta\beta(16+19\kappa)/8(1+\kappa) = 0{\cdot}25$; ···, $\chi = 0{\cdot}50$; (*b*) a two-dimensional quadratic shearing flow ($-\delta\gamma(10+11\kappa)/40(1+\kappa) = 0{\cdot}05$). ——, $\chi = 0$ (i.e. centre-line for Poiseuille flow); –·–, $\chi = 0{\cdot}25$; ····, $\chi = 0{\cdot}50$; – – –, no deformation (i.e. $r = 1$).

in this case. For a plane Poiseuille flow, the dominant contribution to the particle velocity relative to the local undisturbed flow (i.e. $(\hat{U}_s^{(0)})_1 - \alpha$) comes from the shear gradient γ, which is negative for all values of s. Thus, the drop will always lag behind the surrounding fluid. For a simple shear flow, γ is identically zero; in this case, the slip velocity can only arise from wall reflexions. By Ho & Leal (1974), $I_1 + \frac{1}{2}I_4$ itself

depends on β and changes sign at $s = 0{\cdot}5$. As a result, in a simple shear flow, the drop leads the fluid for $s > 0{\cdot}5$ but lags behind it for $s < 0{\cdot}5$.

The shape of the drop can now be obtained, using the normal stress term of (4.10c). To this end, we assume that the volume of the drop remains constant, and that its centroid coincides with origin O of our co-ordinate system. Then, expressing $f^{(\delta)}$ in the form

$$f^{(\delta)} = {}_1f^{(\delta)} + {}_{2+3}f^{(\delta)} + \ldots, \tag{4.15}$$

we obtain

$${}_1f^{(\delta)} = \frac{\beta(16+19\kappa)}{8(1+\kappa)}\frac{x_1x_3}{r^2} - \frac{\gamma(10+11\kappa)}{40(1+\kappa)}\left(\frac{x_1}{r} - \frac{5x_1x_3^2}{r^3}\right), \tag{4.16a}$$

$${}_{2+3}f^{(\delta)} = -\zeta(\tfrac{2}{3}I_2 + I_5)\frac{16+19\kappa}{8(1+\kappa)}\frac{x_1x_3}{r^2}. \tag{4.16b}$$

It can be seen easily that (4.16a) agrees exactly with the result of Taylor (1932, 1934) for a simple, unbounded shear flow ($\gamma = 0$), and also with Haber & Hetrsoni (1971) for the case of an unbounded quadratic shearing flow. On the other hand, (4.16b) represents an additional deformation of the drop due to hydrodynamic interaction with the walls. Its form is identical to that for a drop in an unbounded linear shear flow, and its magnitude relative to the first term of (4.16a) is $-(\zeta/\beta)\times(\frac{3}{2}I_2 + I_5)$. This function is of $O(\zeta^3)$ and can be calculated numerically following Ho & Leal (1974). As expected, it is symmetric about $s = 0{\cdot}5$, and is positive for all values of s. Thus, the drop deformation is always increased by the presence of the walls. Using $\zeta = 0{\cdot}1$ and $\kappa = 0$, we calculate $-(\zeta/\beta)\times(\frac{3}{2}I_2 + I_5)$ to be 0·0057 at $s = 0{\cdot}5$ (i.e. centre-line), 0·015 at $s = 0{\cdot}3$, and 0·048 at $s = 0{\cdot}2$ (i.e. two drop radii from wall). Hence, its contribution is significant only when the drop is very near to a wall. In figure 2 (a) and (b), we plot the drop shape in the cases of a simple shear flow and a two-dimensional quadratic shearing flow.

To apply the Newtonian solution to migration calculations in the next two sections, we need also to obtain the complementary velocity fields $\mathbf{u}$ and $\tilde{\mathbf{u}}$ defined in §3. As above, they are expanded as

$$\mathbf{u} = {}_1\mathbf{u} + {}_2\mathbf{u} + {}_3\mathbf{u} + \ldots \tag{4.17}$$

and

$$\tilde{\mathbf{u}} = {}_1\tilde{\mathbf{u}} + {}_{2+3}\tilde{\mathbf{u}} + \ldots. \tag{4.18}$$

The unbounded domain solutions are

$${}_1\mathbf{u} = -\mathbf{e}_3 - \tfrac{1}{2}a_1\left(\frac{1}{r}\mathbf{e}_3 + \frac{x_3}{r^3}\mathbf{x}\right) - b_1\left(\frac{1}{r^3}\mathbf{e}_3 - \frac{3x_3}{r^5}\mathbf{x}\right), \tag{4.19a}$$

$${}_1\tilde{\mathbf{u}} = -\tfrac{1}{10}\tilde{a}_1(2r^2\mathbf{e}_3 - x_3\mathbf{x}) - \tilde{b}_1\mathbf{e}_3, \tag{4.19b}$$

where

$$a_1 = -\frac{2+3\kappa}{2(1+\kappa)}, \quad \tilde{a}_1 = \frac{5}{1+\kappa}, \quad b_1 = -\frac{\kappa}{4(1+\kappa)}, \quad \tilde{b}_1 = -\frac{1}{2(1+\kappa)}. \tag{4.20}$$

These are, of course, identical to the well-known solution of Hadamard (1911) and Rybczynski (1911) for the motion of a spherical drop in an unbounded quiescent fluid. To obtain the reflected solutions, we again follow the procedures outlined by Ho & Leal (1974). ${}_2\mathbf{u}$ is expressed in terms of complicated integrals, but simplifies near the drop to the form

$${}_2\mathbf{u} = [-(J_1 + J_4) + \tfrac{3}{2}\zeta J_2 x_3]\,\mathbf{e}_3 - \tfrac{1}{2}\zeta J_2\mathbf{x}. \tag{4.21}$$

The term J_2 will appear repeatedly in our results. Hence, we note its detailed form here

$$J_2 = \frac{\zeta}{32}\frac{2+3\kappa}{1+\kappa}\int_0^\infty \frac{\xi^3}{(1-e^{-\xi})^2-\xi^2 e^{-\xi}}\{s^2[e^{-s\xi}+e^{-(2-s)\xi}] - (1-s)^2[e^{-(1-s)\xi}+e^{-(1+s)\xi}]+2(1-2s)\,e^{-\xi}\}\,d\xi. \tag{4.22}$$

In general, this integral has to be evaluated numerically for any given value of s. However, an excellent approximation (with less than 2% error for all s) can be obtained by simply substituting the integrand with

$$\xi^3[s^2 e^{-s\xi} - (1-s)^2 e^{-(1-s)\xi} + 2(1-2s)\,e^{-\xi}],$$

and then integrating the expression analytically to obtain

$$J_2 \sim \frac{3\zeta}{16}\frac{2+3\kappa}{1+\kappa}\left[\frac{1}{s^2}-\frac{1}{(1-s)^2}+2(1-2s)\right]. \tag{4.23}$$

For convenience, we shall base all subsequent calculations upon this approximate form for J_2. Following our earlier procedures, ${}_3\mathbf{u}$ and ${}_{2+3}\tilde{\mathbf{u}}$ are now obtained from the form of ${}_2\mathbf{u}$ at the drop surface. Using Lamb's general solution, we obtain

$${}_3\mathbf{u} = -\tfrac{1}{2}a_3\left(\frac{1}{r}\mathbf{e}_3+\frac{x_3}{r^3}\mathbf{x}\right)-b_3\left(\frac{1}{r^3}\mathbf{e}_3-\frac{3x_3}{r^5}\mathbf{x}\right)-\tfrac{1}{2}d_3\left(\frac{1}{r^3}\mathbf{x}-\frac{3x_3^2}{r^5}\mathbf{x}\right) + 3e_3\left(\frac{1}{r^5}\mathbf{x}+\frac{2x_3}{r^5}\mathbf{e}_3-\frac{5x_3^2}{r^7}\mathbf{x}\right). \tag{4.24a}$$

$${}_{2+3}\tilde{\mathbf{u}} = -\tfrac{1}{10}\tilde{a}_3(2r^2\mathbf{e}_3-x_3\mathbf{x})-\tilde{b}_3\mathbf{e}_3-\tfrac{1}{7}\tilde{d}_3(r^2\mathbf{x}-5r^2\mathbf{e}_3+2x_3^2\mathbf{x})-2\tilde{e}_3(\mathbf{x}-3x_3\mathbf{e}_3). \tag{4.24b}$$

The above equations must satisfy boundary conditions (3.4a)–(3.4c) on $r=1$. The coefficients are therefore

$$\left.\begin{aligned} a_3 &= -(J_1+J_4)(2+3\kappa)/2(1+\kappa), & \tilde{a}_3 &= (J_1+J_4)\,5/(1+\kappa),\\ b_3 &= -(J_1+J_4)\,\kappa/4(1+\kappa), & \tilde{b}_3 &= -(J_1+J_4)/2(1+\kappa),\\ d_3 &= -\zeta J_2(2+5\kappa)/2(1+\kappa), & \tilde{d}_3 &= \zeta J_2\,21/4(1+\kappa),\\ e_3 &= -\zeta J_2\kappa/4(1+\kappa), & \tilde{e}_3 &= -\zeta J_2\,3/8(1+\kappa). \end{aligned}\right\} \tag{4.25}$$

This completes the solution for $\mathbf{u}$.

5. The $O(\lambda)$ problem

We now consider the $O(\lambda)$ problem of a non-Newtonian *spherical* drop suspended in a two-dimensional shearing flow of a second-order fluid. For the suspending phase, the equations of motion are

$$\nabla.\mathbf{S}^{(\lambda)} = 0, \quad \nabla.\mathbf{U}^{(\lambda)} = 0, \tag{5.1}$$

where

$$\mathbf{S}^{(\lambda)} = -P^{(\lambda)}\mathbf{I} + \mathbf{D}^{(\lambda)}_{(1)} + [\mathbf{D}^{(0)}_{(1)}.\mathbf{D}^{(0)}_{(1)} + \epsilon_1\mathbf{D}^{(0)}_{(2)}]. \tag{5.2}$$

The equations for the drop fluid are, of course, completely analogous to the above. At large distances from the drop, the boundary conditions are

$$\left.\begin{aligned} \mathbf{U}^{(\lambda)} &\to -\hat{\mathbf{U}}^{(\lambda)}_s \quad \text{as } r\to\infty,\\ \mathbf{U}^{(\lambda)} &= -\hat{\mathbf{U}}^{(\lambda)}_s \quad \text{on the walls,} \end{aligned}\right\} \tag{5.3}$$

whereas on $r = 1$

$$\mathbf{U}^{(\lambda)} = \tilde{\mathbf{U}}^{(\lambda)}, \tag{5.4a}$$

$$\mathbf{U}^{(\lambda)}.\mathbf{e}_r = \tilde{\mathbf{U}}^{(\lambda)}.\mathbf{e}_r = 0, \tag{5.4b}$$

$$\mathbf{S}^{(\lambda)}.\mathbf{e}_r = \kappa\tilde{\mathbf{S}}^{(\lambda)}.\mathbf{e}_r - [2f^{(\lambda\delta)} + \nabla^2 f^{(\lambda\delta)}]\,\mathbf{e}_r. \tag{5.4c}$$

It is apparent that a detailed calculation of the complete velocity fields will be extremely difficult. However, to obtain the migration velocity to $O(\lambda)$, we only need to consider (3.11) as we have noted above. From (3.4*a*)–(3.4*c*) and (5.4*a*)–(5.4*c*), it is obvious that the first three terms of the surface integral are all identically zero. The remaining terms simplify to

$$\int_{A_d} \mathbf{T}^{(\lambda)}.\mathbf{u}.\mathbf{e}_r\,dA = -[8\pi/15(1+\kappa)][\beta\gamma(1+J_1+J_4) - \tfrac{3}{4}\beta^2\zeta J_2](1+4\epsilon_1), \tag{5.5}$$

$$\int_{A_d} \mathbf{t}.\mathbf{V}^{(\lambda)}.\mathbf{e}_r\,dA = [2\pi(2+3\kappa)/(1+\kappa)](1+J_1+J_4)\,(\hat{U}_s^{(\lambda)})_3. \tag{5.6}$$

Rearranging, we thus obtain

$$(\hat{U}_s^{(\lambda)})_3 = -\frac{4}{15(2+3\kappa)}[\beta\gamma - \tfrac{3}{4}\beta^2\zeta J_2](1+4\epsilon_1) - \frac{1+\kappa}{2\pi(2+3\kappa)}\cdot\left\{\int_{V_f}[(\mathbf{D}_{(1)}^{(0)}.\mathbf{D}_{(1)}^{(0)} - \mathbf{E}_{(1)}^{(0)}.\mathbf{E}_{(1)}^{(0)}) + \epsilon_1(\mathbf{D}_{(2)}^{(0)} - \mathbf{E}_{(2)}^{(0)})]:\nabla\mathbf{u}\,dV + \kappa\frac{\tilde{\lambda}}{\lambda}\int_{\tilde{V}_f}[\tilde{\mathbf{D}}_{(1)}^{(0)}.\tilde{\mathbf{D}}_{(1)}^{(0)} + \tilde{\epsilon}_1\tilde{\mathbf{D}}_{(2)}^{(0)}]:\nabla\tilde{\mathbf{u}}\,dV\right\}. \tag{5.7}$$

Here $J_2/(1+J_1+J_4)$ is approximated as simply J_2, since J_1+J_4 is itself of $O(\zeta)$.

We note that an exact, direct calculation of the first integral in (5.7) over the entire volume V_f outside the drop is extremely complicated due to the presence of the bounding walls. Instead, we obtain an approximation to this term by dividing V_f into a 'near-field' region V_1 and a 'far-field' region V_2, in a manner asymptotically consistent with the expansion in ζ which is inherent in the reflexions procedure. V_1 thus corresponds to an unbounded domain with the drop immersed in it (i.e. $1 \leqslant r < \infty$), whereas V_2 includes the walls while seeing the drop as merely a point (i.e. $0 \leqslant \zeta r < \infty$, $-s \leqslant \zeta x_3 \leqslant 1-s$). For any particular flow at infinity, the order of magnitude of the integrands may then be obtained using the estimates for $({}_1\mathbf{u}, {}_2\mathbf{u}, {}_3\mathbf{u})$ and $({}_1\mathbf{U}^{(0)}, {}_2\mathbf{U}^{(0)}, {}_3\mathbf{U}^{(0)})$ in V_1 and V_2 that were provided by Ho & Leal (1974). Only the asymptotically dominant contribution needs to be evaluated. We now consider two specific cases of interest.

5.1. *The quadratic unidirectional shear flow*

Here, we consider the migration of a spherical drop in a two-dimensional quadratic unidirectional shear flow (e.g. plane Poiseuille flow). The calculation follows the general procedures that were outlined by Ho & Leal (1976) for a rigid sphere. For the suspending phase, it can be shown that the dominant contribution to the integral over V_f in (5.7) comes from the $\beta\gamma$ term in V_1, and is therefore of $O(\zeta^3)$. For the drop fluid, on the other hand, the volume integral over $\tilde{V}_f$ can be evaluated directly, without approximation. Hence, using ${}_1\mathbf{U}^{(0)}$, ${}_1\tilde{\mathbf{U}}^{(0)}$, ${}_1\mathbf{u}$ and ${}_1\tilde{\mathbf{u}}$, we obtain

$$\begin{aligned}(\hat{U}_s^{(\lambda)})_3 &= \frac{\beta\gamma}{315(2+3\kappa)^2(4+\kappa)(1+\kappa)^2}\{[(2560+10932\kappa+23252\kappa^2+24606\kappa^3+10995\kappa^4 \\ &\quad + 1575\kappa^5) + \epsilon_1(5920+27588\kappa+63341\kappa^2+70626\kappa^3+32940\kappa^4+4725\kappa^5)] \\ &\quad + \eta[(2186+2807\kappa+237\kappa^2) + \tilde{\epsilon}_1(6530+10598\kappa+3567\kappa^2+315\kappa^3)]\} \\ &= -\beta\gamma[M(\epsilon_1,\kappa) + \eta\tilde{M}(\tilde{\epsilon}_1,\kappa)].\end{aligned} \tag{5.8}$$

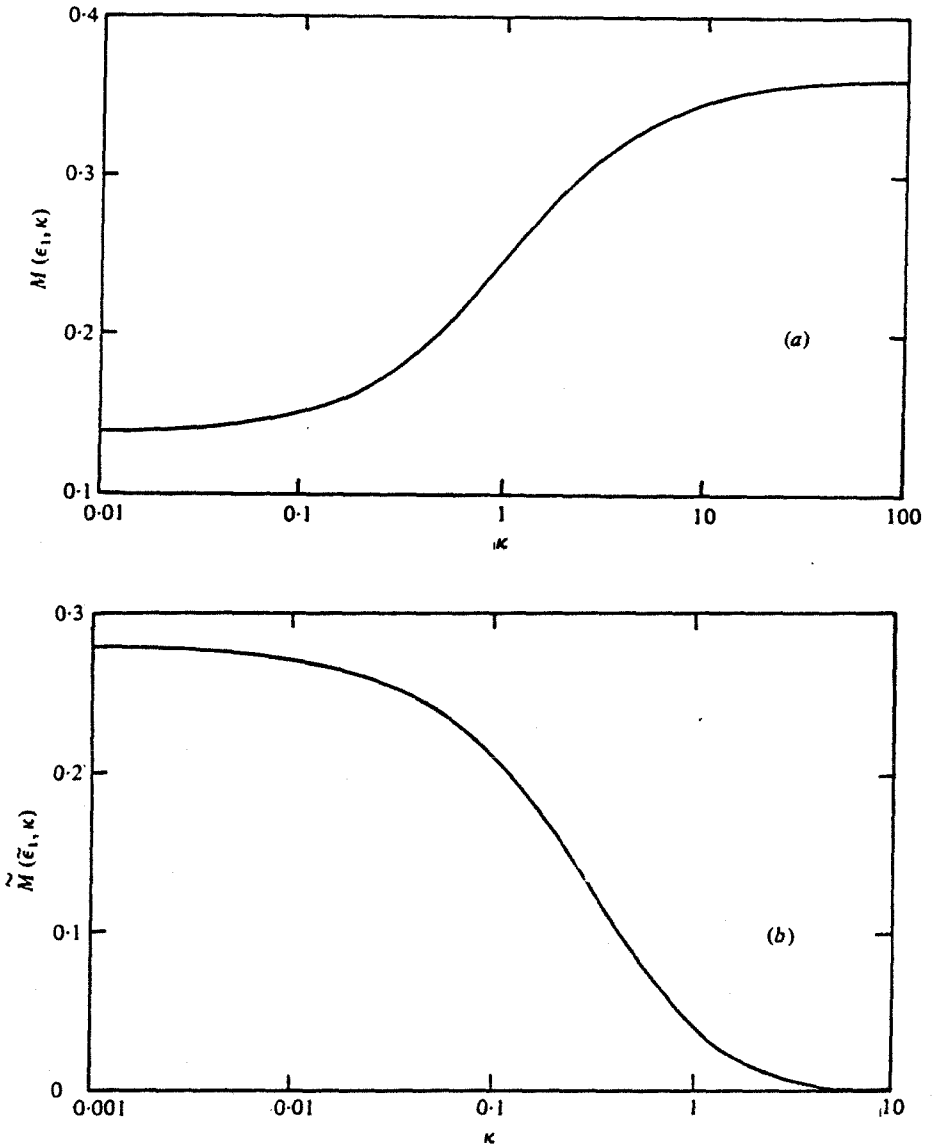

FIGURE 3. Migration velocity in a two-dimensional quadratic shearing flow due to: (*a*) a non-Newtonian suspending fluid, $\epsilon_1 = -0{\cdot}55$; (*b*) a non-Newtonian drop, $\tilde{\epsilon}_1 = -0{\cdot}55$.

We may note immediately that the migration velocity (5.8) is proportional to γ, and is thus identically zero in a linear shear flow. In this latter case, as we shall see shortly, the contributions to $(\hat{U}_s^{(\lambda)})_3$ from the inner and outer regions, V_1 and V_2, are comparable in magnitude and it is necessary to explicitly consider wall reflexions. The parameter η which appears in (5.8) represents a ratio of normal stress coefficients for the two fluids, i.e.

$$\eta \equiv (\tilde{\lambda}/\lambda)\kappa = \tilde{\phi}_3/\phi_3$$

and is thus *independent* of κ. For moderate values of κ, both fluids thus contribute to the migration velocity if η is of $O(1)$. If η approaches zero or infinity, one of the fluids may be considered Newtonian and therefore produces no direct contribution to $(\hat{U}_s)_3$ at this order.

To determine the direction of migration, we must first estimate the material parameters ϵ_1 and $\tilde{\epsilon}_1$ of the two fluids. In general, it is believed that their values should always lie between $-0{\cdot}5$ and $-0{\cdot}6$. The most significant experimental verification was obtained by Beavers & Joseph (1975) for the motor oil additive STP. Using the cone and plate device they estimated ϕ_2 to be $-2{\cdot}78$ g cm^{-1}. In addition, the parameter $3\phi_2+2\phi_3$ was measured in rod climbing experiments as approximately 0·95 g cm^{-1}. Thus $\epsilon_1 \sim -0{\cdot}60$. This value agrees exactly with that estimated by Leal (1975) for a 3 % PAA solution, based upon orbit drift experiments. For the above range of ϵ_1 and $\tilde{\epsilon}_1$, it is easily seen that M and $\tilde{M}$ are always positive, and hence migration is predicted to occur toward the region of smallest (absolute) shear rate, in agreement with the result of Ho & Leal (1976) for the case of a rigid sphere.

In figure 3 we plot the functions M and $\tilde{M}$ which represent the separate contributions from the two fluids to (5.8), as functions of κ. When κ approaches infinity, we see that the 'very viscous' drop has no direct effect on $(\hat{U}_s^{(\lambda)})_3$, whereas the contribution of the suspending phase reduces to that calculated by Ho & Leal (1976) for the rigid sphere problem. This is, of course, to be expected since the internal motion of the drop becomes that of a rotating rigid sphere for large κ. For decreasing values of κ, on the other hand, the contribution of the suspending fluid decreases whereas that of the drop fluid increases, until they reach limiting, non-zero values when κ approaches zero. Obviously, this limit means that the drop has a much lower viscosity than the suspending fluid, but it also requires comparable values for the parameters ϕ_3 and $\tilde{\phi}_3$. Thus, the limit $\kappa \to 0$ does not correspond to a gas bubble as might at first be supposed, and there is no paradox in a non-zero value for $\tilde{M}$ at $\kappa = 0$.

5.2. *The linear unidirectional shear flow*

Let us now turn to the case of a linear unidirectional shear flow, for which the shear gradient γ is zero. Here again, the calculations for the contributions of the suspending and drop fluids follow the procedures outlined previously. By dividing the entire volume V_f into 'near-field' region V_1 and 'far-field' region V_2, we obtain the leading terms in ζ in the expression for the migration velocity. For V_1, the only contribution is of $O(\zeta^4)$ and arises from the interaction of the $O(\zeta^2)$ terms in $({}_2\mathbf{u}, {}_3\mathbf{u})$ and the $O(\zeta)$ terms of ${}_1\mathbf{U}^{(0)}$. For V_2, the leading contributions are also of $O(\zeta^4)$ and may arise in principle from any combinations between $({}_1\mathbf{u}, {}_2\mathbf{u})$ and $({}_1\mathbf{U}^{(0)}, {}_2\mathbf{U}^{(0)})$, expressed in outer variables. However, most of the terms in V_2 cancel each other after integration, with the remainder coming only from ${}_1\mathbf{u}$ and ${}_1\mathbf{U}^{(0)}$. Unlike the $\beta\gamma$ contribution to the migration velocity which was shown in the previous subsection to be a 'near-field' effect, the contribution to the migration velocity in a *linear* shear flow is a result of hydrodynamic interaction between the particle and the walls. It is therefore not surprising that the integral over V_f should contain contributions both from V_1 and V_2.

Inside the drop, the calculations are straightforward with the dominant terms coming from ${}_{2+3}\tilde{\mathbf{u}}$ and ${}_1\tilde{\mathbf{U}}^{(0)}$. When the contributions from both V_f and $\tilde{V}_f$ are substituted into (5.7), we finally obtain an expression for the migration velocity (cf. Chan 1979)

$$(\hat{U}_s^{(\lambda)})_3 = -\frac{\zeta\beta^2 J_2}{420(2+3\kappa)(1+\kappa)^2}\{[(232+666\kappa+1068\kappa^2+455\kappa^3) + \epsilon_1(928+3168\kappa+4614\kappa^2+2185\kappa^3)]+12\eta[31+\tilde{\epsilon}_1(108+105\kappa)]\}. \quad (5.9)$$

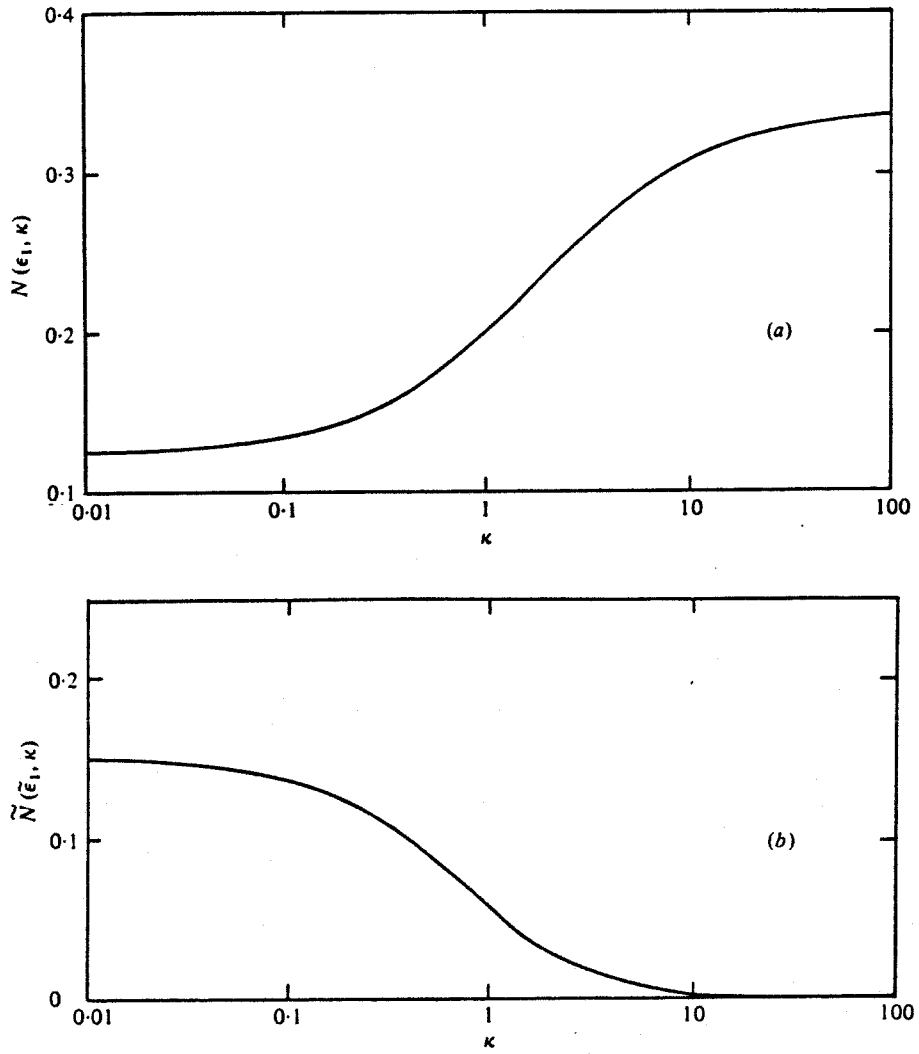

FIGURE 4. Migration velocity in a simple shear flow due to: (*a*) a non-Newtonian suspending fluid, $\epsilon_1 = -0{\cdot}55$; (*b*) a non-Newtonian drop, $\tilde{\epsilon}_1 = -0{\cdot}55$.

Using (4.23), this becomes

$$(\hat{U}_s^{(\lambda)})_3 = -\frac{\zeta^2\beta^2}{2240(1+\kappa)^3}\{[(232+666\kappa+1068\kappa^2+445\kappa^3)+\epsilon_1(928+3168\kappa + 4614\kappa^2+2185\kappa^3)]+12\eta[31+\tilde{\epsilon}_1(108+105\kappa)]\}\left[\frac{1}{s^2}-\frac{1}{(1-s)^2}+2(1-2s)\right]$$
$$= \zeta^2\beta^2[N(\epsilon_1,\kappa)+\eta\tilde{N}(\tilde{\epsilon}_1,\kappa)]\left[\frac{1}{s^2}-\frac{1}{(1-s)^2}+2(1-2s)\right]. \tag{5.10}$$

Once again, the functions $N(\epsilon_1, \kappa)$ and $\tilde{N}(\tilde{\epsilon}_1, \kappa)$ are always positive for reasonable values of ϵ_1 and $\tilde{\epsilon}_1$. Therefore the drop is predicted to migrate from the walls toward the centre-line. In figures 4(*a*) and (*b*) we plot $N(\epsilon_1, \kappa)$ and $\tilde{N}(\tilde{\epsilon}_1, \kappa)$ as functions of κ. The dependence of $(\hat{U}_s^{(\lambda)})_3$ on κ is obviously similar to that predicted for the quadratic shear flow case.

5.3. *Generalization to three-dimensional quadratic shear flows*

Although the analysis above was restricted to a two-dimensional undisturbed shearing flow, it is sometimes possible to generalize the results for the migration velocity to three-dimensional undisturbed motions of the same type, without the need to repeat the fluid dynamical calculations, by using the procedures which we have outlined in Chan & Leal (1977). The essential requirements for this type of extension is that the effect must be localized near the particle, so that hydrodynamic interactions between the particle and walls play no role. To put it another way, the dominant contribution to the integral over V_f in (5.7) must come from the inner region V_1 so that we effectively have migration in an unbounded domain with the undisturbed velocity profile, (4.3a), at infinity. Thus, the expression (5.8) for migration in a quadratic profile may be generalized using the analysis of Chan & Leal (1977), but the contribution (5.10) due to hydrodynamic interaction with the walls in a linear shear flow is specifically *excluded*.

Let us first consider the case of a non-Newtonian spherical drop in a three-dimensional Poiseuille flow of a second-order fluid. For this purpose, we consider a circular tube with radius B_0. The distance of the drop from the tube centre at any instant is denoted as D. The undisturbed flow at infinity is expressed as

$$\mathbf{V} = [\alpha + \beta x_3 + \gamma(x_3^2 + x_2^2)]\,\mathbf{e}_1 - \hat{\mathbf{U}}_s, \tag{5.11}$$

where x_3 is now in the radial direction and

$$\alpha = V_{\max}(1 - D^2/B_0^2), \quad \beta = -2V_{\max} aD/B_0^2, \quad \gamma = -V_{\max} a^2/B_0^2. \tag{5.12}$$

By substituting (5.11) into the migration velocity expression of Chan & Leal (1977), we thus obtain the result

$$\begin{aligned}(\hat{U}_s^{(\lambda)})_3 = \frac{\beta\gamma}{630(2+3\kappa)^2(1+\kappa)^2}\{&[(1520 + 5172\kappa + 10594\kappa^2 + 10560\kappa^3 + 3465\kappa^4) \\ &+ \epsilon_1(3200 + 12048\kappa + 27334\kappa^2 + 28620\kappa^3 + 9765\kappa^4)] \\ &+ 12\eta[(158 + 174\kappa) + \tilde{\epsilon}_1(425 + 564\kappa + 105\kappa^2)]\}.\end{aligned} \tag{5.13}$$

This expression should be compared with (5.8). For the same values of β and γ, we easily see that the qualitative behaviour of the two equations is very similar. Indeed, detailed numerical comparison shows that the difference in magnitude is never more than 30 %. The closest agreement occurs when $\kappa \to \infty$, in which case the discrepancy is only 10 %. In §8, we shall compare (5.13) with the experimental data of Karnis & Mason (1966) and of Gauthier *et al.* (1971a, b).

A second problem of considerable interest is the generalization of (5.8) to a Couette flow. It may be supposed that this could be approximated as a linear, unidirectional flow to which (5.10) is directly relevant. However, a small shear gradient always exists in the Couette device due to curvature and it is thus prudent, for values of ζ which are not vanishingly small, to consider both shear gradients and hydrodynamic interactions between the particle and walls in any comparison of the present theory with experimental observations. An attempt to apply (5.8) to examine the shear gradient effect in Couette flow was made by Ho & Leal (1976) for rigid spherical particles using a local (and incorrect) two-dimensional approximation to the undisturbed velocity field. We shall comment on the validity of this approach later in

this section. However, let us first apply the rigorous approach of Chan & Leal (1977) to the generalization of (5.8) for a Couette velocity field.

We follow initially the analysis of Brunn (1976) and consider the full problem of two concentric cylinders (with radii R_1, R_2; $R_2 > R_1$) rotating with angular velocities Ω_1, Ω_2, respectively. The undisturbed velocity of the flow at any material point (R, ϕ) measured from the centre of the Couette device is then given as

$$\mathbf{V}^* = (A_1 R + A_2/R)\,\mathbf{e}_\phi, \tag{5.14}$$

where $A_1 = (\Omega_2 R_2^2 - \Omega_1 R_1^2)/(R_2^2 - R_1^2)$ and $A_2 = R_1^2 R_2^2(\Omega_1 - \Omega_2)/(R_2^2 - R_1^2)$. (5.15)

We denote by (x_1, x_3) the components of a position vector, non-dimensionalized with the drop radius a, which is defined relative to a co-ordinate system with origin at the drop centre, and the x_3 axis coincident with the radial unit vector of the natural cylindrical co-ordinates for the Couette device. The sphere centre is itself a distance R_0 from the axis of the Couette device. Thus,

$$R^2 = (R_0 + a x_3)^2 + a^2 x_1^2. \tag{5.16}$$

Dividing (5.14) by the characteristic velocity Ga, we may re-express it in dimensionless form as

$$\mathbf{V}' = \left[A_1' + \frac{A_2'}{(R_0 + a x_3)^2 + a^2 x_1^2}\right][(R_0 + a x_3)\,\mathbf{e}_1 - a x_1 \mathbf{e}_3], \tag{5.17}$$

where $A_1' = A_1/Ga$ and $A_2' = A_2/Ga$. Finally, by a Taylor's series expansion about O, we may write the undisturbed velocity $\mathbf{V}$ (relative to the drop) in the quadratic form

$$\mathbf{V} = \boldsymbol{\alpha} + \boldsymbol{\beta}.\mathbf{x} + \boldsymbol{\gamma}:\mathbf{xx} - \hat{\mathbf{U}}_s, \tag{5.18}$$

where
$$\left.\begin{aligned} \boldsymbol{\alpha} &= \mathbf{V}'|_0 = (A_1' R_0 + A_2'/R_0)\,\mathbf{e}_1, \\ \boldsymbol{\beta} &= \nabla \mathbf{V}'|_0 = A_1' a(\mathbf{e}_1\mathbf{e}_3 - \mathbf{e}_3\mathbf{e}_1) - \frac{A_2' a}{R_0^2}(\mathbf{e}_1\mathbf{e}_3 + \mathbf{e}_3\mathbf{e}_1), \\ \boldsymbol{\gamma} &= \tfrac{1}{2}\nabla\nabla\mathbf{V}'|_0 = \left[\frac{A_2' a^2}{R_0^3}\right](-\mathbf{e}_1\mathbf{e}_1\mathbf{e}_1 + \mathbf{e}_1\mathbf{e}_3\mathbf{e}_3 + \mathbf{e}_3\mathbf{e}_3\mathbf{e}_1 + \mathbf{e}_3\mathbf{e}_1\mathbf{e}_3). \end{aligned}\right\} \tag{5.19}$$

Substituting (5.19) into the migration velocity expression of Chan & Leal (1977),† we obtain

$$\begin{aligned} (\hat{U}_s^{(\lambda)})_3 = -\frac{1}{63(1+\kappa)^2(2+3\kappa)}\{[(256 + 816\kappa + 1238\kappa^2 + 525\kappa^3) \\ + \epsilon_1(592 + 2112\kappa + 3254\kappa^2 + 1365\kappa^3)] + 24\eta(8 + 17\tilde{\epsilon}_1)\}\left[\frac{A_2'^2 a^3}{R_0^5}\right]. \end{aligned} \tag{5.20}$$

In the limit of a rigid sphere, this becomes

$$(\hat{U}_s^{(\lambda)})_3 = -\tfrac{5}{9}(5 + 13\epsilon_1)\left(\frac{A_2'^2 a^3}{R_0^5}\right) \tag{5.21}$$

which agrees exactly with the result of Brunn (1976).

Ho & Leal (1976) have also obtained an expression for the migration velocity of

† Ignoring temporarily the fact that Chan & Leal (1977) assumed no rotation of the particle co-ordinates, whereas the system used in (5.18) is clearly rotating. We shall see shortly, however, that for a Couette flow there is no correction to the migration velocity due to rotation.

a rigid sphere in a Couette flow of a second-order fluid. In that paper, however, the undisturbed flow was assumed to be *locally* two-dimensional, and hence represented by (2.6a) with the parameters given as (in our present notation)

$$\alpha = A_1' R_0 + A_2'/R_0, \quad \beta = A_1' a - A_2' a/R_0^2, \quad \gamma = A_2' a^2/R_0^3. \tag{5.22}$$

By this approximation, the x_3 component of V has been neglected. The migration velocity for a rigid sphere is then predicted as

$$(\hat{U}_s^{(\lambda)})_3 = \tfrac{5}{9}(1+3\epsilon_1)(A_1' - A_2'/R_0^2) A_2' a^3/R_0^3. \tag{5.23}$$

This expression, unlike the correct result (5.21), suggests a slight difference in migration rate depending upon whether the inner or outer cylinder is rotating, and this was reported in Ho & Leal (1976) as being in qualitative agreement with the observations of Karnis & Mason (1966). However, the result is incorrect† and the apparent agreement was simply fortuitous. It may be noted, in spite of this, that the direction of migration is the same as predicted by (5.21). Furthermore, for a Couette apparatus with 'small' curvature (i.e. $R_1/R_2 \sim 1$), the constant $A_1' \sim A_2'/R_0^2$ so that (5.23) differs from (5.21) simply by a numerical factor $2(1+3\epsilon_1)/(5+13\epsilon_1)$. For $\epsilon_1 \sim -0{\cdot}6$, which is a generally agreed value, this factor equals $\sim 0{\cdot}6$ and the two results differ in magnitude by about 40%.

Let us now return to the effect of rotation of the co-ordinates associated with a Couette device [see footnote immediately preceding (5.20)]. The general theory of Chan & Leal (1977) which is the basis of (5.20) has only been developed for circumstances in which the co-ordinates attached to the particle centre and parallel to the flow boundaries are non-rotating. This is appropriate, for example, for any unidirectional undisturbed flow. Generally speaking, however, these 'particle coordinates' may be expected to rotate as well as translate, and the rotation will generate non-zero contributions to the time derivatives in the Rivlin–Ericksen tensors of the second-order fluid expansion [cf. (2.3)]. We have shown (cf. Chan 1979) that this will lead to non-zero contributions dependent upon the rate of rotation, $\boldsymbol{\Omega}_f$ in the general expression for the migration velocity of the particle. Since these terms have no counterpart in the detailed unidirectional flow calculations of the present paper, it is not possible to determine their coefficients by comparison, and the results such as (5.20) are therefore incomplete if $\boldsymbol{\Omega}_f \neq 0$. As we have noted, this situation must be considered in the present calculation of particle migration in Couette flow, where it is necessary to choose a co-ordinate system whose x_3 axis always points in the radial direction with respect to the Couette device. Fortunately, however, for the velocity field (5.18) and (5.19), it can be shown (Chan 1979) by general tensorial arguments that there will be no additional contributions to the migration velocity from the rotation of the particle co-ordinates. We therefore conclude that (5.20) is valid for any Couette flow.

It is clear that the expression (5.10), representing migration in a unidirectional flow due to hydrodynamic interactions between the particle and walls, should also be modified for application to a Couette flow device. Unfortunately, no simple method exists to determine the appropriate modifications short of re-solving the complete problem with the Couette geometry and velocity field inserted from the beginning.

† We are indebted to Dr P. Brunn for this remark.

Thus, if we are to compare theoretical results with available data for this case we presently have no choice but to use (5.10) and (5.20); the comparison between (5.21) and (5.23) suggests that this may be qualitatively, or even quantitatively, correct provided we restrict our attention to a 'narrow gap' device which is the case in the existing experiments of Mason and co-workers. Although the profile curvature term is $O(\zeta^3)$ whereas the wall interaction term is $O(\zeta^4)$, the curvature in the undisturbed Couette flow is itself small in the 'narrow gap' device and so the two contributions may have numerically comparable values in practice. Since wall interactions cause migration toward the centre line [cf. (5.10)], whereas the velocity profile curvature causes migration toward the outer cylinder [cf. (5.20)], the drop in Couette flow is generally expected to attain an intermediate equilibrium position where the two contributions cancel each other. By comparing the two expressions for typical experimental conditions, we have found in fact that the wall interaction effect, corresponding to (5.10), should nearly always be dominant. Thus, the equilibrium position should be quite near the centre-line. However, this conclusion is in disagreement with existing experimental observations for rigid spheres in a viscoelastic fluid [cf. figure 8 of Karnis & Mason (1966)], which indicate migration toward the outer cylinder. This discrepancy with present theory may result from the application of (5.10) directly to the Couette flow problem. Another possibility is that the conditions for validity of the theory, e.g. $\zeta \ll 1, \lambda \ll 1$, etc. are simply not satisfied well enough in the experiments to allow a detailed correspondence between theory and experiment. In this regard, it should be noted that the 4 % PAA in water solution used by Karnis & Mason (1966) is strongly viscoelastic in the deformation-rate range of interest and is therefore not modelled well as an nth order fluid; for example, it exhibits a strong shear-thinning of the apparent viscosity. It has been found in other related problems (cf. Leal 1975) that predicted non-Newtonian contributions to particle motion in an *unbounded* fluid domain may, nevertheless, exhibit qualitative or even quantitative agreement with experiments in a strong viscoelastic fluid, provided ϕ_2 and ϕ_3 are determined from normal stress data in the shear-rate range of interest rather than at zero shear-rate as is strictly required for the nth order fluid approximation. In the present case, this is also true provided the comparison is made between data and (5.21) alone, rather than (5.21) and (5.10). Perhaps the influence of the wall effects is relatively less in a strongly viscoelastic fluid than is suggested by the comparison between (5.21) and (5.10) which we indicated above. In our opinion, it would be of considerable interest in settling these questions to perform further experiments using a fluid with 'proven' second-order fluid behaviour in the shear-rate range of interest.

5.4. *The $O(\lambda)$ velocity and pressure fields*

For the analysis of § 7, and for examining the mechanism of migration, we need also to consider the $O(\lambda)$ velocity, pressure and stress fields defined in (5.1). To this end, it will be sufficient to consider only the two-dimensional quadratic shear flow problem in an *unbounded* fluid, where wall reflexions are neglected. Furthermore, since a detailed calculation is extremely complicated, we shall only attempt to determine the *forms* of $(\mathbf{U}^{(\lambda)}, P^{(\lambda)}, \mathbf{S}^{(\lambda)})$, with identical expressions for $(\tilde{\mathbf{U}}^{(\lambda)}, \tilde{P}^{(\lambda)}, \tilde{\mathbf{S}}^{(\lambda)})$.† By keeping

† The problem of the motion of a sphere in a linear shear flow of second-order fluid was considered in the Ph.D. thesis of Peery (1966).

only the relevant β^2 and $\beta\gamma$ terms, we find

$$\mathbf{U}^{(\lambda)} = -(\hat{U}_s^{(\lambda)})_3\left[\mathbf{e}_3 - \frac{2+3\kappa}{4(1+\kappa)}\left(\frac{1}{r}\mathbf{e}_3 + \frac{x_3}{r^3}\mathbf{x}\right) - \frac{\kappa}{4(1+\kappa)}\left(\frac{1}{r^3}\mathbf{e}_3 - \frac{3x_3}{r^5}\mathbf{x}\right)\right]$$
$$+ (\beta^2\Psi_1 + \beta\gamma\theta_1)\,x_1\mathbf{e}_1 + (\beta^2\Psi_2 + \beta\gamma\theta_2)\,x_3\mathbf{e}_3 + x_1^2(\beta^2\Psi_3 + \beta\gamma\theta_3)\,x_3\mathbf{e}_3$$
$$+ (\beta^2\Psi_4 + \beta\gamma\theta_4)\,\mathbf{x} + x_1^2(\beta^2\Psi_5 + \beta\gamma\theta_5)\,\mathbf{x}; \tag{5.24}$$

$$P^{(\lambda)} = (\hat{U}_s^{(\lambda)})_3\frac{2+3\kappa}{2(1+\kappa)}\frac{x_3}{r^3} + (\beta^2\Psi_6 + \beta\gamma\theta_6) + x_1^2(\beta^2\Psi_7 + \beta\gamma\theta_7). \tag{5.25}$$

Obviously, the $(\hat{U}_s^{(\lambda)})_3$ terms of the above equations arise from (5.3). $\Psi_1 \ldots \Psi_7$ and $\theta_1 \ldots \theta_7$ are complicated functions of x_3 and r, which may be obtained by first calculating the last term of (5.2) using the Newtonian velocity, and then solving (5.1). In this problem, the Ψ's are even functions of x_3 whereas the θ's are odd.

We may now substitute (5.24) and (5.25) into (5.2) and obtain an expression for $\mathbf{S}^{(\lambda)}$. This is then dotted with the unit normal to give the stress vector acting at any point on the particle surface. In general, both $\mathbf{U}^{(\lambda)}$ and $\mathbf{S}^{(\lambda)}.\mathbf{n}$ must satisfy matching conditions (5.4*a*)–(5.4*c*) on the drop surface. However, once again it is the *form* of the stress vector which is of greatest practical interest, and we easily see that this must be analogous to (5.24). Therefore,

$$\mathbf{S}^{(\lambda)}.\mathbf{n} = -(\hat{U}_s^{(\lambda)})_3\left[\frac{3(2+3\kappa)}{2(1+\kappa)}x_3\mathbf{e}_r + \frac{3\kappa}{2(1+\kappa)}(\mathbf{e}_3 - 3x_3\mathbf{e}_r)\right] + (\beta^2\Psi_8 + \beta\gamma\theta_8)\,x_1\mathbf{e}_1$$
$$+ (\beta^2\Psi_9 + \beta\gamma\theta_9)\,x_3\mathbf{e}_3 + x_1^2(\beta^2\Psi_{10} + \beta\gamma\theta_{10})\,x_3\mathbf{e}_3$$
$$+ (\beta^2\Psi_{11} + \beta\gamma\theta_{11})\,\mathbf{e}_r + x_1^2(\beta^2\Psi_{12} + \beta\gamma\theta_{12})\,\mathbf{e}_r. \tag{5.26}$$

Let us now examine the above equation in more detail. For example, the component of the surface stress vector in the x_1 direction is obviously *odd* in x_1, regardless of the exact values of the Ψ's and the θ's. Therefore the x_1 component of the stress vector at any material point (x_1, x_2, x_3) is always balanced by its equal but opposite x_1 component at $(-x_1, x_2, x_3)$. As a result, there can be no net non-Newtonian force in the x_1 direction acting on the drop at this order, and the streamwise translational velocity of the drop will be unchanged. Similarly, if we consider the x_3 component of (5.26), we easily see that the β^2 contribution is *odd* in x_3, and hence can have no net effect on the drop motion. However, the $\beta\gamma$ contribution is *even* in x_3 and therefore has the same sign at (x_1, x_2, x_3) and at $(x_1, x_2, -x_3)$. As a result, lateral migration will occur in the x_3 direction. As noted above, these conclusions are independent of the detailed form of the Ψ's and the θ's. Of course, no definite result can be obtained from (5.26) concerning such questions as the predicted sign or magnitude of the migration velocity without these functions, and this is the purpose of the reciprocal theorem calculations.

We note that the above considerations are in fact consistent with the 'hoop' thrust arguments which were tentatively proposed by Ho & Leal (1976) as providing the mechanistic explanation of lateral migration of a rigid particle in an unbounded viscoelastic fluid. In a unidirectional shearing flow of a second-order fluid (without suspended particles), the tension along a straight streamline will obviously not result in a net force on any material point. On the other hand, if a particle is present, the streamlines are deformed and the tension along a streamline can then be partially

converted to a sideways 'hoop' thrust. However, for a linear shear flow, the streamlines are symmetric on all 'sides' of a spherical particle [as is obvious from (5.24)], and hence these 'hoop' thrusts can have no net effect. Only in the presence of a shear gradient will the streamlines be asymmetric in the lateral direction. Then, on the side with a higher undisturbed shear rate the tension along streamlines will be greater than along streamlines on the other side, and hence will have a larger net force. This means that migration will occur in the direction of decreasing shear rate.

Finally, we should remark that the assumption of a spherical drop will not be valid in general, since the normal stress condition of (5.4*c*) is not then satisfied. However, any deformation due to $\mathbf{U}^{(\lambda)}$ and $\tilde{\mathbf{U}}^{(\lambda)}$ can only occur at $O(\lambda\delta)$. Once again, it is not possible to calculate $f^{(\lambda\delta)}$ in detail; instead, we shall simply express it as

$$f^{(\lambda\delta)} = (\beta^2\Psi_{13}+\beta\gamma\theta_{13})+x_1^2(\beta^2\Psi_{14}+\beta\gamma\theta_{14}), \tag{5.27}$$

where the Ψ's and θ's have the same properties as before.

6. The $O(\delta)$ problem

In this section, we consider the motion of a Newtonian deformable drop suspended in a shearing flow of a Newtonian fluid. This problem has been examined by several previous investigators. In particular, Chaffey *et al.* (1965, 1967) have considered a simple shear flow in which the drop is near a single plane wall; in this case, wall reflexions are needed for migration to occur. In contrast, Wohl & Rubinow (1974) and Wohl (1976) considered migration in a Poiseuille flow, where the effect of the shear gradient is expected to be significant. On this basis, these authors assumed that it was sufficient to consider the drop in 'unbounded' Poiseuille flow in order to determine the migration velocity. This assumption is not justified rigorously in their analysis, but it is obviously correct since the calculated migration velocities are asymptotically larger than those obtained by Chaffey *et al.* (1965, 1967) for small ζ. However, the solution of Chaffey *et al.* (1965, 1967) is still of importance for the particular case of a simple shear flow, since the migration predicted by Wohl (1976) and Wohl & Rubinow (1974) will then reduce to zero.

We shall now reconsider the problem of drop migration in a Newtonian fluid due to flow-induced deformations of the drop shape. As noted in the introduction to this paper, the original Chaffey *et al.* (1965, 1967) analysis for a *linear* flow was limited to a fluid bounded by a single plane wall. In addition, we have noted that there are strong reasons to doubt the accuracy of the Wohl (1976) and Wohl & Rubinow (1974) results. As in the previous section, the calculations to be presented here will utilize the reciprocal theorem approach, i.e. (3.10).

The equations of motion for the *Newtonian* suspending fluid are

$$\nabla.\mathbf{S}^{(\delta)} = 0, \quad \nabla.\mathbf{U}^{(\delta)} = 0 \tag{6.1}$$

with boundary conditions at large distances from the drop

$$\left.\begin{aligned} \mathbf{U}^{(\delta)} &\to -\hat{\mathbf{U}}_g^{(\delta)} \quad \text{as } r\to\infty, \\ \mathbf{U}^{(\delta)} &= -\hat{\mathbf{U}}_g^{(\delta)} \quad \text{on the walls.} \end{aligned}\right\} \tag{6.2}$$

The equations for the drop fluid are, of course, analogous to (6.1). The matching conditions on $r = 1$, are from (2.10a)–(2.10c), (2.15) and (2.16),

$$\mathbf{U}^{(\delta)} + f^{(\delta)} \frac{\partial}{\partial r} \mathbf{U}^{(0)} = \tilde{\mathbf{U}}^{(\delta)} + f^{(\delta)} \frac{\partial}{\partial r} \tilde{\mathbf{U}}^{(0)}, \tag{6.3a}$$

$$\left[\mathbf{U}^{(\delta)} + f^{(\delta)} \frac{\partial}{\partial r} \mathbf{U}^{(0)}\right] . \mathbf{e}_r - \mathbf{U}^{(0)} . \nabla f^{(\delta)} = \left[\tilde{\mathbf{U}}^{(\delta)} + f^{(\delta)} \frac{\partial}{\partial r} \tilde{\mathbf{U}}^{(0)}\right] . \mathbf{e}_r - \tilde{\mathbf{U}}^{(0)} . \nabla f^{(\delta)} = 0, \tag{6.3b}$$

$$\left[\mathbf{S}^{(\delta)} + f^{(\delta)} \frac{\partial}{\partial r} \mathbf{S}^{(0)}\right] . \mathbf{e}_r - \mathbf{S}^{(0)} . \nabla f^{(\delta)} = \kappa \left[\left(\tilde{\mathbf{S}}^{(\delta)} + f^{(\delta)} \frac{\partial}{\partial r} \tilde{\mathbf{S}}^{(0)}\right) . \mathbf{e}_r - \tilde{\mathbf{S}}^{(0)} . \nabla f^{(\delta)}\right] + [2f^{(\delta)} + \nabla^2 f^{(\delta)}] \nabla f^{(\delta)} - [2f^{(\delta\delta)} + \nabla^2 f^{(\delta\delta)} - 2f^{(\delta)} f^{(\delta)}] \mathbf{e}_r. \tag{6.3c}$$

Here, as in the case of non-Newtonian migration, we only need to consider (3.10) to obtain $\hat{\mathbf{U}}_s^{(\delta)}$. The $O(\delta)$ expression from (3.10) is

$$-\int_{A_d} [(\mathbf{S}^{(\delta)} - \kappa \tilde{\mathbf{S}}^{(\delta)}) . \mathbf{u} - (\mathbf{t} - \kappa \tilde{\mathbf{t}}) . \mathbf{U}^{(\delta)} - \kappa \tilde{\mathbf{t}} . (\mathbf{U}^{(\delta)} - \tilde{\mathbf{U}}^{(\delta)})] . \mathbf{e}_r dA - \frac{2\pi(2+3\kappa)}{1+\kappa} (1 + J_1 + J_4) (\hat{U}_s^{(\delta)})_3 = 0. \tag{6.4}$$

The integrands may be simplified using the appropriate matching conditions from (3.4a)–(3.4c) and (6.3a)–(6.3c). These give

$$\left.\begin{aligned} (\mathbf{S}^{(\delta)} - \kappa \tilde{\mathbf{S}}^{(\delta)}) . \mathbf{u} . \mathbf{e}_r &= \left[-f^{(\delta)} \frac{\partial}{\partial r} (\mathbf{S}^{(0)} - \kappa \tilde{\mathbf{S}}^{(0)}) . \mathbf{e}_r + (\mathbf{S}^{(0)} - \kappa \tilde{\mathbf{S}}^{(0)}) . \nabla f^{(\delta)} \right. \\ &\qquad \left. + \nabla f^{(\delta)} (2f^{(\delta)} + \nabla^2 f^{(\delta)}) \right] . \mathbf{u}, \\ -(\mathbf{t} - \kappa \tilde{\mathbf{t}}) . \mathbf{U}^{(\delta)} . \mathbf{e}_r &= (\mathbf{t} - \kappa \tilde{\mathbf{t}}) : \mathbf{e}_r \mathbf{e}_r \left[f^{(\delta)} \left(\frac{\partial}{\partial r} \mathbf{U}^{(0)} \right) . \mathbf{e}_r - \mathbf{U}^{(0)} . \nabla f^{(\delta)} \right], \\ -\kappa \tilde{\mathbf{t}} . (\mathbf{U}^{(\delta)} - \tilde{\mathbf{U}}^{(\delta)}) . \mathbf{e}_r &= \kappa \tilde{\mathbf{t}} . \mathbf{e}_r \left[f^{(\delta)} \frac{\partial}{\partial r} (\mathbf{U}^{(0)} - \tilde{\mathbf{U}}^{(0)}) \right]. \end{aligned}\right\} \tag{6.5}$$

By rearranging, and neglecting the term $J_1 + J_4$, we thus obtain

$$(\hat{U}_s^{(\delta)})_3 = -\frac{1+\kappa}{2\pi(2+3\kappa)} \int_{A_d} \left\{ \left[-f^{(\delta)} \frac{\partial}{\partial r} (\mathbf{S}^{(0)} - \kappa \tilde{\mathbf{S}}^{(0)}) . \mathbf{e}_r + (\mathbf{S}^{(0)} - \kappa \tilde{\mathbf{S}}^{(0)}) . \nabla f^{(\delta)} + \nabla f^{(\delta)} (2f^{(\delta)} + \nabla^2 f^{(\delta)}) \right] . \mathbf{u} + (\mathbf{t} - \kappa \tilde{\mathbf{t}}) : \mathbf{e}_r \mathbf{e}_r \left[f^{(\delta)} \left(\frac{\partial}{\partial r} \mathbf{U}^{(0)} \right) . \mathbf{e}_r - \mathbf{U}^{(0)} . \nabla f^{(\delta)} \right] + \kappa \tilde{\mathbf{t}} . \mathbf{e}_r . \left[f^{(\delta)} \frac{\partial}{\partial r} (\mathbf{U}^{(0)} - \tilde{\mathbf{U}}^{(0)}) \right] \right\} dA. \tag{6.6}$$

We have now expressed the migration velocity at $O(\delta)$ in terms of integrals which involve only the Newtonian velocity and stress fields. In contrast to (5.7), only surface integrals on $r = 1$ are involved, and hence wall effects will arise only indirectly in the integrands. [In (5.7), the domain of integration itself is bounded by the walls.] Here we obtain the order of magnitudes of the integrands by using the estimates for $({}_1\mathbf{u}, {}_2\mathbf{u}, {}_3\mathbf{u})$ and $({}_1\mathbf{U}^{(0)}, {}_2\mathbf{U}^{(0)}, {}_3\mathbf{U}^{(0)})$ provided by Ho & Leal (1974), evaluated on the drop surface. The estimates for $\tilde{\mathbf{u}}$ and $\tilde{\mathbf{U}}^{(0)}$ are of course identical. We now calculate the dominant contributions for the two cases of quadratic and linear shear flows.

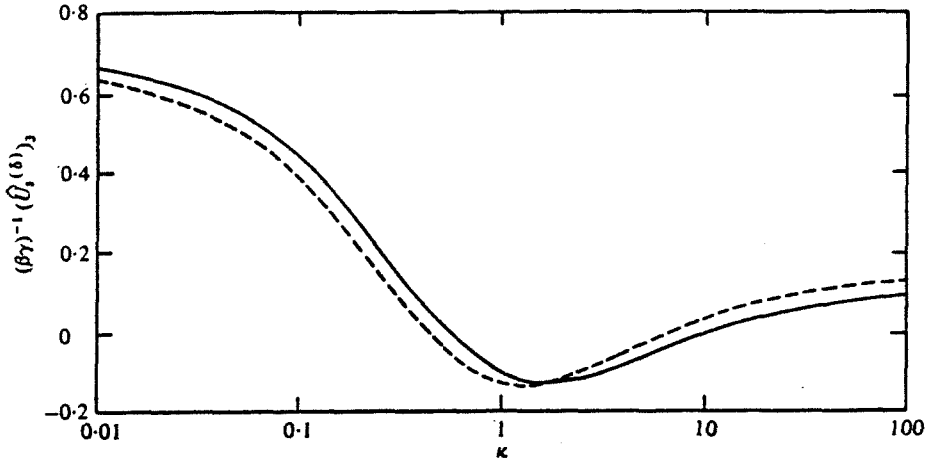

FIGURE 5. Migration velocity in a two-dimensional quadratic shearing flow due to drop deformation. ——, present theory (6.8); ---, Wohl (1976).

6.1. *The quadratic unidirectional shear flow*

For a two-dimensional quadratic unidirectional shear flow, we can express (6.6) in the form

$$\hat{U}_s^{(\delta)} \sim \int_{A_d} [O(\zeta^2) + O(\zeta^3) + O(\zeta^4)]\, dA. \tag{6.7}$$

Here, it can be shown easily that the $O(\zeta^2)$ term, which corresponds to the β^2 contribution, is odd in x_3 and hence integrates to zero. For the $O(\zeta^3)$ term, the only combination which is even in x_3 is proportional to $\beta\gamma$, and is obtained using ${}_1\mathbf{u}$, ${}_1\tilde{\mathbf{u}}$, ${}_1\mathbf{U}^{(0)}$, ${}_1\tilde{\mathbf{U}}^{(0)}$ and ${}_1f^{(\delta)}$. These terms correspond of course to the unbounded domain problem; thus Wohl's (1976) assumption that wall effects could be neglected at this order in ζ is justified. However, upon carrying out the detailed integrations for this dominant contribution, we obtain

$$(\hat{U}_s^{(\delta)})_3 = -\frac{\beta\gamma}{(1+\kappa)^2(2+3\kappa)}\left[\frac{16+19\kappa}{42(2+3\kappa)(4+\kappa)}(13-36\kappa-73\kappa^2-24\kappa^3) + \frac{10+11\kappa}{105}(8-\kappa+3\kappa^2)\right]. \tag{6.8}$$

This result is in disagreement with that of Wohl (1976), which is somewhat more complicated:

$$(\hat{U}_s^{(\delta)})_3 = -\frac{\beta\gamma}{(1+\kappa)^2(2+3\kappa)}\left[\frac{16+19\kappa}{483840(2+3\kappa)(4+\kappa)}(138672-684612\kappa-678210\kappa^2 - 214362\kappa^3+6237\kappa^4) + \frac{10+11\kappa}{940800}(71876-27898\kappa+29691\kappa^2)\right]. \tag{6.9}$$

We are sceptical of the accuracy of the complicated expression that Wohl (1976) obtained, particularly in view of the fact that Wohl used the much more complicated 'direct' approach of calculating *all* variables at $O(\delta)$ in order to determine $(\hat{U}_s^{(\delta)})_3$. However, on plotting the two migration velocities as functions of κ (see figure 5), we find that the agreement between the theories is extremely good for $0{\cdot}01 \leqslant \kappa \leqslant 100$. Interestingly, both theories predict that the direction of migration depends on the

value of κ. For κ between $\frac{1}{2}$ and 10, the drop migrates *toward* the walls, while the inverse (toward the centre) is true for all other values of κ. Migration toward the walls has not previously been observed experimentally; however, so far as we are aware no experiments have yet been reported for $\frac{1}{2} \leqslant \kappa \leqslant 10$.

The expression (6.8) is, of course, limited to two-dimensional unidirectional flow. However, this dominant contribution to $(\hat{U}_s^{(\delta)})_3$ corresponds to an unbounded domain, and it is thus possible to extend (6.8) to the important case of a three-dimensional Poiseuille flow. For this purpose, an expression for the $O(\delta)$ migration velocity of a deformable drop in a general quadratic flow of a Newtonian fluid is first needed. The coefficients in this expression are then determined by careful comparison with the two-dimensional problem. The required procedures are analogous to those of Chan & Leal (1977), and will be discussed in detail in the appendix. For the undisturbed velocity profile, (5.11), of a three-dimensional Poiseuille flow, the final expression is

$$(\hat{U}_s^{(\delta)})_3 = -\frac{\beta\gamma}{(1+\kappa)^2(2+3\kappa)}\left[\frac{3}{14}\times\frac{16+19\kappa}{2+3\kappa}(1-\kappa-2\kappa^2)+\frac{10+11\kappa}{140}(8-\kappa+3\kappa^2)\right]. \quad (6.10)$$

Unfortunately, this disagrees quite significantly with the result of Wohl & Rubinow (1974) for the same problem

$$(\hat{U}_s^{(\delta)})_3 = -\frac{\beta\gamma}{(1+\kappa)^2(2+3\kappa)}\left[\frac{16+19\kappa}{26880(2+3\kappa)}(27688+29354\kappa+3741\kappa^2-4284\kappa^3)\right.$$
$$\left.+\frac{10+11\kappa}{78400}(14364-20191\kappa+12310\kappa^2)\right]. \quad (6.11)$$

Comparing (6.11) with (6.9), the magnitude of migration for three-dimensional Poiseuille flow is predicted by Wohl (1976) and Wohl & Rubinow (1974) to be nearly ten times that for a two-dimensional Poiseuille flow when κ approaches zero, provided that β and γ both remain the same. This prediction is at odds with intuition, according to which the qualitative behaviour of the two cases should be very similar. In fact, when we examine our own expressions [i.e. (6.8) and (6.10)], we find that they never differ by more than 50 %. We are confident that our calculations are correct. In § 8, we shall compare (6.10) with previous experimental results.

6.2. *The linear unidirectional shear flow*

Let us now consider the case of simple (linear) shear flow, where the shear gradient γ is zero. All $O(\zeta^3)$ terms of (6.7) will then vanish, and the leading contribution to the migration velocity is of $O(\zeta^4)$. We have found by careful consideration of the Newtonian velocity fields that the only relevant terms are $({}_2\mathbf{u}, {}_3\mathbf{u})$ and ${}_1\mathbf{U}^{(0)}$ from the suspending fluid, and ${}_{2+3}\tilde{\mathbf{u}}$ and ${}_1\tilde{\mathbf{U}}^{(0)}$ from the drop. By substitution into (6.6), we obtain

$$(\hat{U}_s^{(\delta)})_3 = \zeta\beta^2 J_2 \frac{(16+19\kappa)(54+97\kappa+54\kappa^2)}{280(1+\kappa)^2(2+3\kappa)} \quad (6.12)$$

which is then simplified using (4.23) to give

$$(\hat{U}_s^{(\delta)})_3 = \zeta^2\beta^2 \frac{3(16+19\kappa)(54+97\kappa+54\kappa^2)}{4480(1+\kappa)^3}\left[\frac{1}{s^2}-\frac{1}{(1-s)^2}+2(1-2s)\right]. \quad (6.13)$$

By comparison, the migration velocity given by Chaffey *et al.* (1965, 1967) is

$$(\hat{U}_s^{(\delta)})_3 = 33\zeta^2\beta^2(16+19\kappa)(54+102\kappa+54\kappa^2)/4480(1+\kappa)^3 s^2. \tag{6.14}$$

Both theories predict migration toward the centre-line of the apparatus. Obviously, the difference in dependence on radial position s arises because we have considered the presence of two walls. When the drop is indeed much closer to either wall (i.e. $s \sim 0$ or $s \sim 1$), the last term in (6.13) reduces to $1/s^2$ (or $1/(1-s)^2$) as expected. Furthermore, if (6.14) is extended in an *ad hoc* manner with $1/s^2$ replaced by

$$1/s^2 - 1/(1-s^2),$$

the dependence on s will be quite similar to that of our full, two-wall analysis. It may be recalled, however, that (4.23) is itself an approximation of the full equation for J_2.

Let us examine the remaining parts of (6.13) and (6.14) more carefully. The factors $54+97\kappa+54\kappa^2$ and $54+102\kappa+54\kappa^2$ are, of course, effectively the same, hence the dependence on the viscosity ratio κ is identical. However, the migration velocity predicted by Chaffey *et al.* (1965, 1967) is still seen to be exactly 11 times greater than ours. To explain this discrepancy, we have performed some of the calculations outlined in their paper,† and have indeed found that the '33' should actually be '3' instead. With this correction the two expressions essentially agree with each other.

Once again, it is difficult, in practice, to satisfy the assumption of a simple linear shear flow, since a small curvature always exists in a Couette device. The contribution of this curvature to particle motion can be calculated by first writing the velocity field as (5.11), and then using the general method developed in the appendix. Thus, we obtain

$$(\hat{U}_s^{(\delta)})_3 = -\frac{2(4+61\kappa+85\kappa^2+25\kappa^3)}{7(2+3\kappa)(1+\kappa)^2}\frac{A_2^2 a^3}{R_0'^5}. \tag{6.15}$$

The above expression predicts that the curvature effect always causes migration toward the *inner* cylinder. [Quite surprisingly, if we use only the local two-dimensional approximation of Ho & Leal (1976) to represent the bulk undisturbed velocity, the predicted direction would be toward the *outer* cylinder.] Thus, when both wall reflexion and shear gradient contributions are included, the drop should be expected to migrate to an equilibrium position which is between the centre-line and the inner wall. In spite of the fact that (6.15) is $O(\zeta^3)$, and therefore asymptotically dominant for $\zeta \to 0$ over (6.13) which is $O(\zeta^4)$, the velocity profile curvature is itself small for a 'narrow gap' Couette device so that the two effects may be expected to be of comparable magnitude. However, under the conditions of existing Couette flow experiments, comparison of (6.13) and (6.15) suggests that the wall interaction contribution dominates *numerically* and hence that the equilibrium position should be quite near the centre-line. This conclusion agrees very well with the experimental observations of Karnis & Mason (1967). We shall present a more detailed comparison of experiment and theory in §8.

To calculate the contribution of the quadratic terms in the next section, we also need to obtain expressions for the $O(\delta)$ velocity and pressure fields. This is accomplished by following the same procedures as in the previous $O(\lambda)$ case. As expected,

† The number 33 first appears in the expression of $\tilde{u}_r$ in §5 of Chaffey *et al.* (1965, 1967), and is therefore independent of the values of $A_{-3}^{(2)}$ and A_{-3} from previous sections. Hence we only need to start from their equation (17) if we wish to check the validity of this coefficient.

the predicted *forms* will be exactly the same as (5.24) and (5.25). We shall not repeat the cumbersome equations here.

7. Higher order corrections

We have now obtained estimates for the separate normal stress and deformation contributions to the migration velocity of the drop. In the presence of a shear gradient, their magnitudes are of $O(\lambda\zeta^3)$ and $O(\delta\zeta^3)$ respectively, whereas for a simple shear flow, they are of $O(\lambda\zeta^4)$ and $O(\delta\zeta^4)$. An obvious question that arises, at this stage, is whether these two terms are necessarily dominant over the quadratic combinations in all situations. For example, it is still possible that the next non-Newtonian contribution might be of $O(\lambda^2\zeta^3)$, thereby becoming important in the simple shear case for some values of λ and ζ. In order to verify or refute these possibilities, it is necessary to carry our calculations to higher order terms, $O(\lambda^2)$, $O(\lambda\delta)$ and $O(\delta^2)$. Of course, these terms are of some intrinsic interest on their own. For example, the $O(\lambda^2)$ term in an nth order fluid expansion represents the first dependence of the viscosity on the shear rate [the $O(\lambda)$ term includes normal stresses only]. Similarly, the $O(\lambda\delta)$ contribution is of some interest because it represents the first interaction of normal stress and deformation effects.

For the $O(\lambda^2)$ problem, the equations of motion for the suspending phase are

$$\nabla.\mathbf{S}^{(\lambda\lambda)} = 0 \quad \text{and} \quad \nabla.\mathbf{U}^{(\lambda\lambda)} = 0, \tag{7.1}$$

where
$$\mathbf{S}^{(\lambda\lambda)} = -P^{(\lambda\lambda)}\mathbf{I} + \mathbf{D}^{(\lambda\lambda)}_{(1)} + [\mathbf{D}^{(0)}_{(1)}.\mathbf{D}^{(\lambda)}_{(1)} + \mathbf{D}^{(\lambda)}_{(1)}.\mathbf{D}^{(0)}_{(1)} + \epsilon_1\mathbf{D}^{(\lambda)}_{(2)}] + [\epsilon_2(\mathbf{D}^{(0)}_{(1)}:\mathbf{D}^{(0)}_{(1)})\mathbf{D}^{(0)}_{(1)} + \epsilon_3\mathbf{D}^{(0)}_{(3)} + \epsilon_4(\mathbf{D}^{(0)}_{(1)}.\mathbf{D}^{(0)}_{(2)} + \mathbf{D}^{(0)}_{(2)}.\mathbf{D}^{(0)}_{(1)})]. \tag{7.2}$$

The equations for the drop fluid are similar to (7.1) and (7.2). On the surface of the drop, the boundary conditions are

$$\left.\begin{aligned} &\mathbf{U}^{(\lambda\lambda)} = \tilde{\mathbf{U}}^{(\lambda\lambda)}, \quad \mathbf{U}^{(\lambda\lambda)}.\mathbf{e}_r = \tilde{\mathbf{U}}^{(\lambda\lambda)}.\mathbf{e}_r = 0, \\ &\mathbf{S}^{(\lambda\lambda)}.\mathbf{e}_r = \kappa\tilde{\mathbf{S}}^{(\lambda\lambda)}.\mathbf{e}_r - [2f^{(\lambda\lambda\delta)} + \nabla^2 f^{(\lambda\lambda\delta)}]\mathbf{e}_r. \end{aligned}\right\} \tag{7.3}$$

As before, we obtain an expression for the $O(\lambda^2)$ migration velocity from the reciprocal theorem. Hence, using (3.10), we get

$$\begin{aligned} &-\int_{A_d}[(\mathbf{S}^{(\lambda\lambda)} - \kappa\tilde{\mathbf{S}}^{(\lambda\lambda)}).\mathbf{u} - (\mathbf{t} - \kappa\tilde{\mathbf{t}}).\mathbf{U}^{(\lambda\lambda)} \\ &\quad - \kappa\tilde{\mathbf{t}}.(\mathbf{U}^{(\lambda\lambda)} - \tilde{\mathbf{U}}^{(\lambda\lambda)}) - \mathbf{T}^{(\lambda\lambda)}.\mathbf{u}].\mathbf{e}_r dA - 2\pi\frac{2+3\kappa}{1+\kappa}(\hat{U}^{(\lambda\lambda)}_s)_3 \\ &\quad = \int_{V_f}[(\mathbf{D}^{(0)}_{(1)}.\mathbf{D}^{(\lambda)}_{(1)} + \mathbf{D}^{(\lambda)}_{(1)}.\mathbf{D}^{(0)}_{(1)} - \mathbf{E}^{(0)}_{(1)}.\mathbf{E}^{(\lambda)}_{(1)} - \mathbf{E}^{(\lambda)}_{(1)}.\mathbf{E}^{(0)}_{(1)}) + \epsilon_1(\mathbf{D}^{(\lambda)}_{(2)} - \mathbf{E}^{(\lambda)}_{(2)})]:\nabla\mathbf{u}\,dV \\ &\qquad + \kappa\frac{\tilde{\lambda}}{\lambda}\int_{\tilde{V}_f}[\tilde{\mathbf{D}}^{(0)}_{(1)}.\tilde{\mathbf{D}}^{(\lambda)}_{(1)} + \tilde{\mathbf{D}}^{(\lambda)}_{(1)}.\tilde{\mathbf{D}}^{(0)}_{(1)} + \tilde{\epsilon}_1\tilde{\mathbf{D}}^{(\lambda)}_{(2)}]:\nabla\tilde{\mathbf{u}}\,dV \\ &\qquad + \int_{V_f}[\epsilon_2, \epsilon_3, \epsilon_4 \text{ terms}]^{(0)}:\nabla\mathbf{u}\,dV + \kappa\left(\frac{\tilde{\lambda}}{\lambda}\right)^2\int_{\tilde{V}_f}[\tilde{\epsilon}_2, \tilde{\epsilon}_3, \tilde{\epsilon}_4 \text{ terms}]^{(0)}:\nabla\tilde{\mathbf{u}}\,dV. \end{aligned} \tag{7.4}$$

Once again, the integrand of the surface integral over A_d is identically zero. Furthermore, using the Newtonian solutions in conjunction with (5.24) for the $O(\lambda)$ velocity field, we can easily show that the integrands of the volume integrals over V_f and $\tilde{V}_f$ are all odd in x_1 and therefore integrate to zero. Hence there will be no migration at

this order. This conclusion is reached without any assumptions about wall effects and shear gradients, and will therefore be true for all unidirectional shear flows. This means that, to this order, the shear-dependence of viscosity yields no contribution to the migration of a spherical drop. Parenthetically, we may note that a similar result may be proved rigorously for any *purely-viscous* fluid model; i.e. for any fluid in which the only non-Newtonian property is a shear-dependent viscosity. This latter conclusion follows trivially from the 'mirror-symmetry time-reversal' theorem of Bretherton (1962), which takes into account the invariant nature of the Navier–Stokes equations (cf. Chan 1979).

Finally, the $O(\lambda\delta)$ and $O(\delta^2)$ contributions can be considered in the same manner. By keeping only relevant terms from the governing equations of §3, we obtain expressions for these two cases that are analogous to (7.1)–(7.4). Again, the integrands are odd in x_1. Hence there will be *no* correction to the migration velocity at any of the orders, $O(\lambda^2)$, $O(\lambda\delta)$ and $O(\delta^2)$.

8. Discussion

We now wish to compare our calculations from the last three sections with the available experimental results of Mason and his co-workers (Goldsmith & Mason 1962; Karnis & Mason 1966, 1967; Gauthier *et al.* 1971*a*, *b*) for the motion of a deformable drop in a non-Newtonian fluid undergoing Couette or three-dimensional Poiseuille flow. First, we consider the migration of a rigid sphere (i.e. $\kappa \to \infty$) due to normal stresses alone. For a Couette flow, we have noted earlier that the profile curvature in a typical Couette device is usually small and hence the asymptotically dominant profile curvature contribution, which is $O(\zeta^3)$, may actually be numerically dominated by the $O(\zeta^4)$ wall interaction effect. On this basis, our theory predicts an equilibrium position quite near the centre-line, in contrast to the observations of Karnis & Mason (1966) for sphere migration in a 4 % solution of PAA in water. It is, in fact, striking that the experimental observations seem to agree qualitatively with the predicted migration rate and direction from the profile curvature effect with no account taken of wall interactions. For example, by integrating (5.21) alone, we obtain in dimensional variables (defined in §5.3)

$$R_0^6 - R_0^6(0) = \left[-\frac{\phi_3}{\mu_0}(5+13\epsilon_1)\right][\tfrac{1}{3}\tfrac{0}{}A_2^2 a^2]\,T, \tag{8.1}$$

where T is the elapsed time. This equation can be compared with the data in figure 8 of Karnis & Mason (1966). In particular, we may obtain an estimate of the rheological constant ϕ_3/μ_0 for 4 % PAA in water, simply by fitting their data with (8.1). Thus, in figure 6, we plot R_0^6 as a function of T. From the slopes of the best fit straight lines, we estimate values for the parameter $-\phi_3/\mu_0(5+13\epsilon_1)$ of 22·8, 47·3, 18·1 and 98·7 s. These are quite reasonable for 4 % PAA in water [cf. the estimates by Leal (1975) for 3 % PAA in water]. In addition, it should be noted that PAA in water is strongly viscoelastic, in contrast to the 'near Newtonian' second-order fluid behaviour on which the present theory is based. A reasonable inference is thus that non-Newtonian contributions to particle motion, due to profile curvature, are reasonably well 'predicted' by the theory for an unbounded second-order fluid; on the other hand, it appears that the wall interaction effects, which are dominant in a second-order fluid,

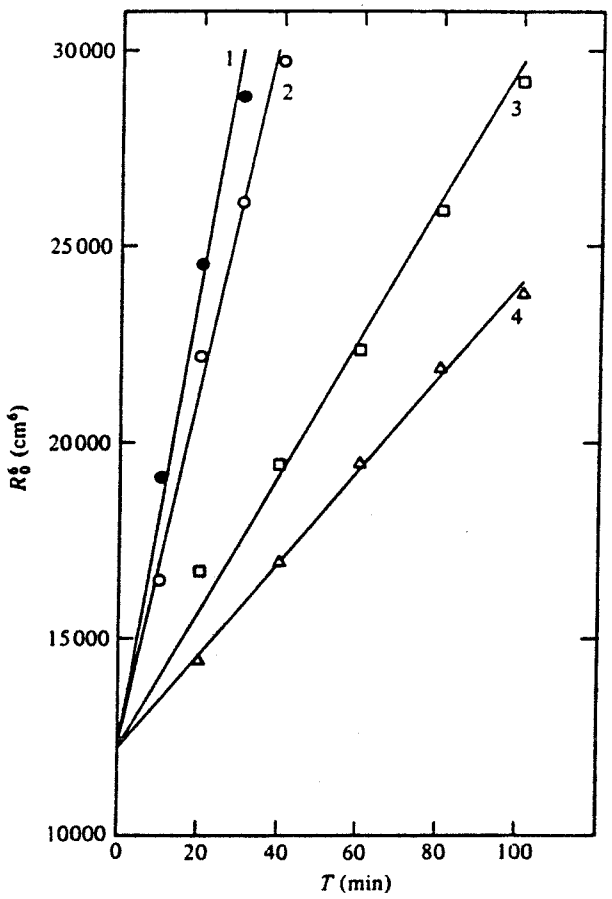

FIGURE 6. R_0^6 *vs.* T for a rigid sphere in a Couette flow ($R_1 = 4{\cdot}644$ cm, $R_2 = 5{\cdot}795$ cm) of 4 % PAA solution in water, observed by Karnis & Mason (1966). ●, case 1: $a = 0{\cdot}065$ cm, $\Omega_1 = -0{\cdot}092$ rad s^{-1}; ○, case 2: $a = 0{\cdot}065$ cm, $\Omega_1 = 0{\cdot}0563$ rad sec^{-1}; □, case 3: $a = 0{\cdot}065$ cm, $\Omega_2 = 0{\cdot}0563$ rad s^{-1}; △, case 4: $a = 0{\cdot}014$ cm, $\Omega_1 = -0{\cdot}092$ rad s^{-1}.

are greatly over-estimated when an attempt is made to extend the theory to the case of a *strong* viscoelastic liquid. Further experiments are presently being performed in our laboratory in an attempt to shed some light on these admittedly speculative ideas for the case of migration in a 'narrow' gap Couette device.

For a Poiseuille flow, in contrast to the narrow-gap Couette flow, the profile curvature is not 'small' and thus for small particles (i.e. $\zeta \ll 1$) the $O(\zeta^3)$ profile curvature contribution to the migration velocity is asymptotically *and* numerically dominant over the $O(\zeta^4)$ wall-particle hydrodynamic interaction effects. In the limit of $\kappa \to \infty$, (5.13) reduces to

$$(\hat{U}_s^{(\lambda)})_3 = \tfrac{1}{15}\beta\gamma(11 + 31\epsilon_1). \tag{8.2}$$

By dividing this expression with the axial velocity and then integrating, we obtain an equation for the trajectory of the sphere. In dimensional variables, we have

$$\left[\frac{D^2}{2B_0^2} - \left(1 - \frac{2}{3}\frac{a^2}{B_0^2}\right)\ln\frac{D}{B_0}\right] - \left[\frac{D(0)^2}{2B_0^2} - \left(1 - \frac{2}{3}\frac{a^2}{B_0^2}\right)\ln\frac{D(0)}{B_0}\right]$$
$$= \left[-\frac{\phi_3}{\mu_0}(11 + 31\epsilon_1)\right]\left[\frac{V^*_{\max}a^2}{9B_0^4}\right][L - L(0)], \tag{8.3}$$

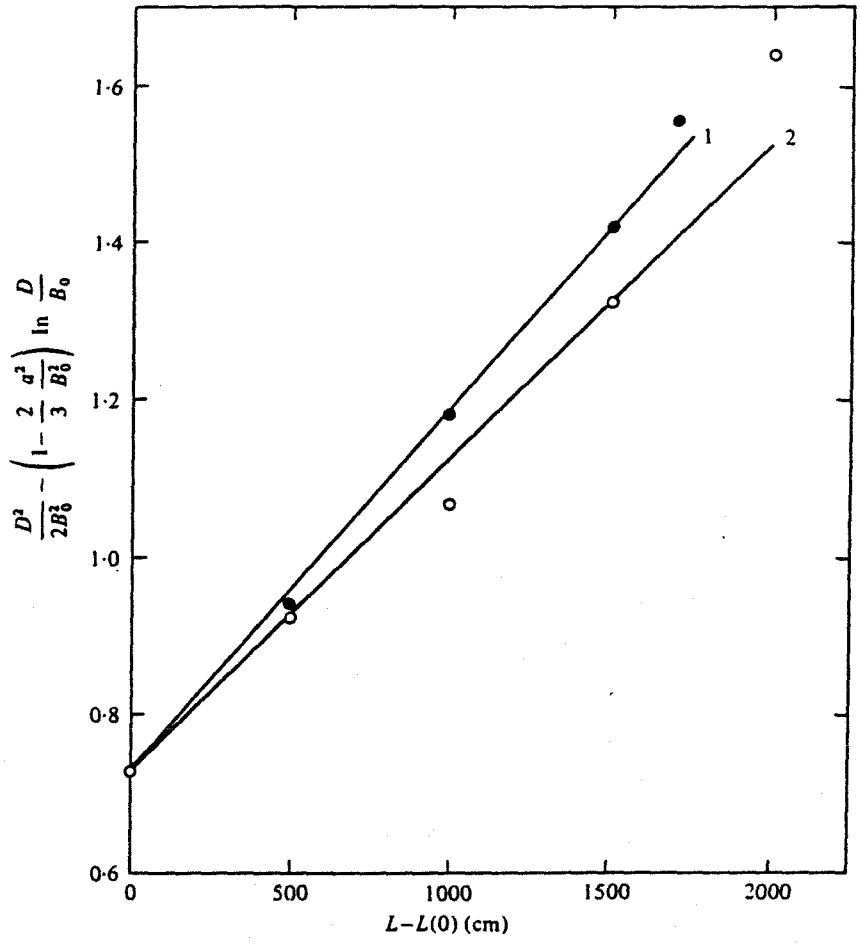

FIGURE 7. $D^2/2B_0^2-(1-\frac{2}{3}a^2/B_0^2)\ln(D/B_0)$ *vs.* $L-L(0)$ for a rigid sphere in a three-dimensional Poiseuille flow ($B_0 = 0{\cdot}3$ cm, $V^*_{max} = 0{\cdot}487$ cm s^{-1}) of 6 % PIB solution in Decalin, observed by Karnis & Mason (1966). ●, case 1: $a/B_0 = 0{\cdot}037$; ○, case 2: $a/B_0 = 0{\cdot}027$; ——, best linear fit with data.

where $L-L(0)$ is the axial distance travelled by the sphere; all other variables are again defined in § 5.3. In figure 7, we plot $D^2/2B_0^2-(1-\frac{2}{3}a^2/B_0^2)\ln(D/B_0)$ as calculated from the data in figure 4 of Karnis & Mason (1966) for sphere migration in a 6 % solution of PIB in Decalin, as a function of $L-L(0)$ for particles with $a/B_0 = 0{\cdot}037$ and 0·027 respectively. The parameter $-\phi_3(11+31\epsilon_1)/\mu_0$ is estimated to be 0·91 and 0·56 s. These values are certainly reasonable for 6 % PIB in Decalin, but we have no direct rheological data for comparison. The difference between the two cases is believed by us to result from the change in particle size. It will be recalled that the present theory is strictly applicable only in the limit $a/B_0 \to 0$. In particular, direct contributions to the migration rate due to hydrodynamic interaction between the particle and tube walls is *not* included in (8.2) – this effect will become more important for larger a/B_0 and thus lead to faster migration or increasing apparent values for $-(\phi_3/\mu_0)(11+31\epsilon_1)$ as a function of a/B_0. In order to estimate the magnitude of this effect, one would have to extend the present theory to include wall reflexions for a quadratic velocity profile (recall, that we have so far included wall reflexions only

for a linear profile, where they provide the only non-zero contribution to the migration rate). A second factor, also associated with the particle size, which may influence the apparent magnitude of $-(\phi_3/\mu_0)(11+31\epsilon_1)$, is the fact that the local strain-rates (i.e. those associated with the particle-induced disturbance flow) will depend upon a. Obviously, it is very difficult to estimate the contribution of this effect. However, it seems to go in the same direction as the change which is observed, since ϕ_3 is a decreasing function of shear-rate.

Let us now turn to the trajectory for a deformable Newtonian drop in a Newtonian suspending fluid. In this case, all of the rheological constants can be measured, and hence our predictions can be compared directly with known experimental observations. For a Couette flow, the migration rate again includes contributions from the interaction of the particle with the bounding walls [toward the centre-line, cf. (6.13)], and also from the shear gradient of a Couette device [toward the inner cylinder, cf. (6.15)]. Thus, the drop is expected to attain, in general, an equilibrium position between the centre-line and the inner cylinder, where the two effects cancel each other. For the experimental conditions of Karnis & Mason (1967), the wall contributions always dominate numerically, and hence the predicted equilibrium position is quite near the centre-line, in agreement with their experimental observations. To obtain the predicted trajectories, we add the two contributions and then integrate to obtain

$$T = \frac{d\sigma}{\mu_0}\int_{s_0}^{s}\frac{ds}{Z(s)}, \tag{8.4}$$

where

$$Z(s) = \frac{a^4}{d^2}\left(A_1-\frac{A_2}{R_0^2}\right)^2\frac{3(16+19\kappa)(54+97\kappa+54\kappa^2)}{4480(1+\kappa)^3}\left[\frac{1}{s^2}-\frac{1}{(1-s)^2}+2(1-2s)\right]$$
$$-\frac{2(4+61\kappa+85\kappa^2+25\kappa^3)}{7(2+3\kappa)(1+\kappa)^2}\frac{A_2^2a^3}{R_0^5}. \tag{8.5}$$

We now evaluate (8.4) numerically and then plot the predicted trajectory of the drop in figure 8 for the various conditions of Karnis & Mason's (1967) experiments, together with the measured trajectory data. For cases 1 and 2, the measured rates are larger than our calculations, but the inverse is true for case 3. Furthermore, the predicted equilibrium positions of $s = 0{\cdot}474$, $0{\cdot}484$ and $0{\cdot}487$ for cases 1, 2 and 3 [obtained by solving $Z(s) = 0$] agree well with the experimental observations (for example, the measured equilibrium position for case 3 is at approximately $s = 0{\cdot}47$).

For the sake of comparison, we have also calculated the corresponding theoretical results from Chaffey *et al.* (1965, 1967), which include only the interaction of the particle with one wall. These may be obtained approximately by dividing T by 11 for each value of s. As shown in case 1 (which offers their *best* fit with data), their agreement with experiment is obviously much poorer than for our present theory.

It should be remarked that the conditions of the experiments do *not* lend themselves well to a definitive comparison between experiment and theory. Aside from $\zeta = a/d \ll 1$, it is also inherently assumed in our theory that the drop is not close to either wall (i.e. $\zeta \ll s$ for $0 < s \leqslant 0{\cdot}5$; $\zeta \ll 1-s$ for $0{\cdot}5 < s < 1$). Now, the experimental values of ζ were $0{\cdot}0337$, $0{\cdot}0556$ and $0{\cdot}0772$ for cases 1, 2 and 3 respectively. In addition, the initial values of s (or $1-s$ for $0{\cdot}5 < s$) were $0{\cdot}0526$, $0{\cdot}0877$ and $0{\cdot}149$, which are twice

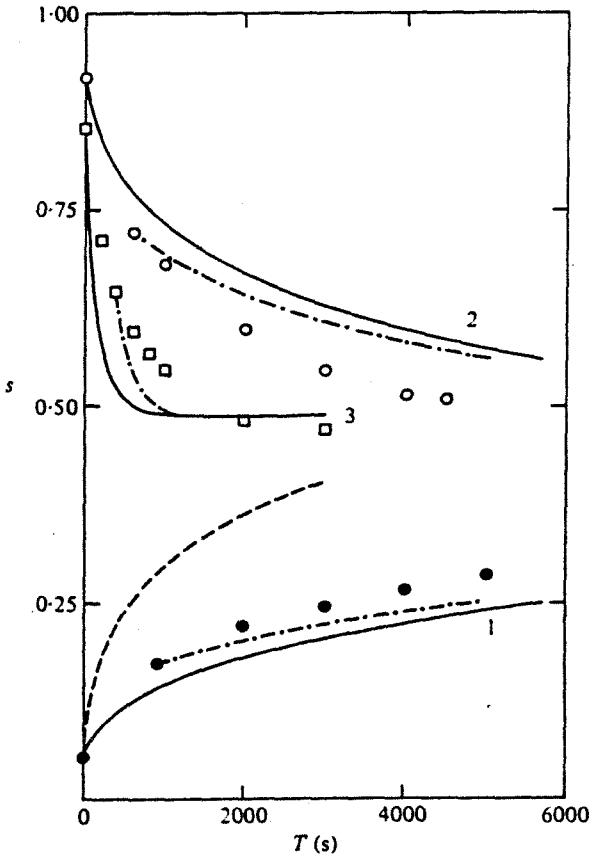

FIGURE 8. A comparison of experimental trajectory of a deformable drop in a simple shear flow with theory. From Karnis & Mason (1967), $\kappa = 2\times10^{-4}$, $\mu_0 = 50$ P, $d = 1{\cdot}869$ cm, $\sigma = 10$ dyne cm^{-1}. ●, case 1: $a = 0{\cdot}063$ cm, $V_w^* = 0{\cdot}662$ cm s^{-1}; ○, case 2: $a = 0{\cdot}104$ cm, $V_w^* = 0{\cdot}662$ cm s^{-1}; □, case 3: $a = 0{\cdot}135$ cm, $V_w^* = 1{\cdot}835$ cm s^{-1}; ——, present theory (8.3); –·–, present theory but with comparison restricted to $5\zeta < s$; – – –, Chaffey *et al.* (1965, 1967) theory.

as large. The value of ζ is obviously fixed for a particular experiment. The maximum values of s can, however, be varied to some degree by restricting our comparison only to those portions of the trajectories where the particle is 'near' to the centre-line, say $5\zeta \leqslant s$. Then, we see from figure 8 that the differences between theory and experiment are considerably reduced, with the best agreement occurring for the smallest drop used.

For a three-dimensional Poiseuille flow, we follow procedures analogous to those outlined by Wohl & Rubinow (1974) to obtain

$$\left[\frac{D^2}{2B_0^2}-\left(1-\frac{2\kappa}{2+3\kappa}\frac{a^2}{B_0^2}\right)\ln\frac{D}{B_0}\right]-\left[\frac{D(0)^2}{2B_0^2}-\left(1-\frac{2\kappa}{2+3\kappa}\frac{a^2}{B_0^2}\right)\ln\frac{D(0)}{B_0}\right]$$
$$=\frac{2V_{\max}^* a^3\mu_0}{B_0^4\sigma}\frac{1}{(1+\kappa)^2(2+3\kappa)}\left[\frac{3}{14}\times\frac{16+19\kappa}{2+3\kappa}(1-\kappa-2\kappa^2)\right.$$
$$\left.+\frac{10+11\kappa}{140}(8-\kappa+3\kappa^2)\right]\times[L-L(0)]. \tag{8.6}$$

Here, we compare the above expression with the experimental observations of

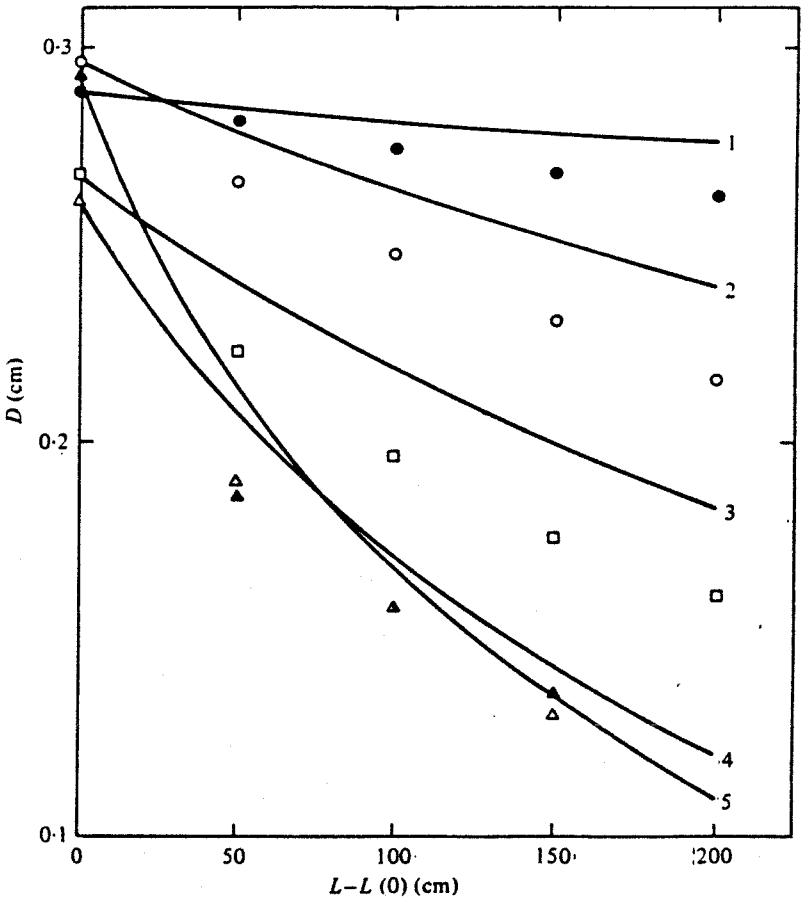

FIGURE 9. A comparison of experimental trajectory of a deformable drop in a three-dimensional Poiseuille flow with present theory (8.5) (——). From Goldsmith & Mason (1962), $\kappa = 2 \times 10^{-4}$, $\mu_0 = 50$ P, $B_0 = 0{\cdot}4$ cm, $\sigma = 29$ dyne cm^{-1}. ●, case 1: $a = 0{\cdot}0175$ cm, $V^*_{max} = 0{\cdot}142$ cm s^{-1}; ○, case 2: $a = 0{\cdot}0300$ cm, $V^*_{max} = 0{\cdot}142$ cm s^{-1}; □, case 3: $a = 0{\cdot}0390$ cm, $V^*_{max} = 0{\cdot}142$ cm s^{-1}; △, case 4: $a = 0{\cdot}0410$ cm, $V^*_{max} = 0{\cdot}283$ cm s^{-1}; ▲, case 5: $a = 0{\cdot}0350$ cm, $V^*_{max} = 0{\cdot}565$ cm s^{-1}.

Goldsmith & Mason (1962). From figure 9, we see that the agreement is good, although in all cases the observed rate of migration is slightly greater than the prediction. We believe that this discrepancy is due to wall effects which are neglected here and will tend to increase the rate. In support of this opinion is the fact that the error is largest for cases 1 and 2 in which the drop remains close to the boundary for a long time, but becomes smaller for cases 4 and 5 in which the drop migrates rapidly to the tube centre. In addition, Wohl & Rubinow (1974) have also compared their migration velocity with the experimental observations, and claimed that their agreement was good. However, from their figure 9, we see that the prediction is significantly greater than the measured rates in cases 3, 4 and 5. Furthermore, they have made an algebraic error, involving a factor of 2, in their calculations. (When calculating the centre-line velocity, they used $V^*_{max} = Q/\pi B_0^2$. The correct expression is $V^*_{max} = 2Q/\pi B_0^2$.) If this factor is introduced into the calculations, their theory will over-estimate the migration rate by an even wider margin.

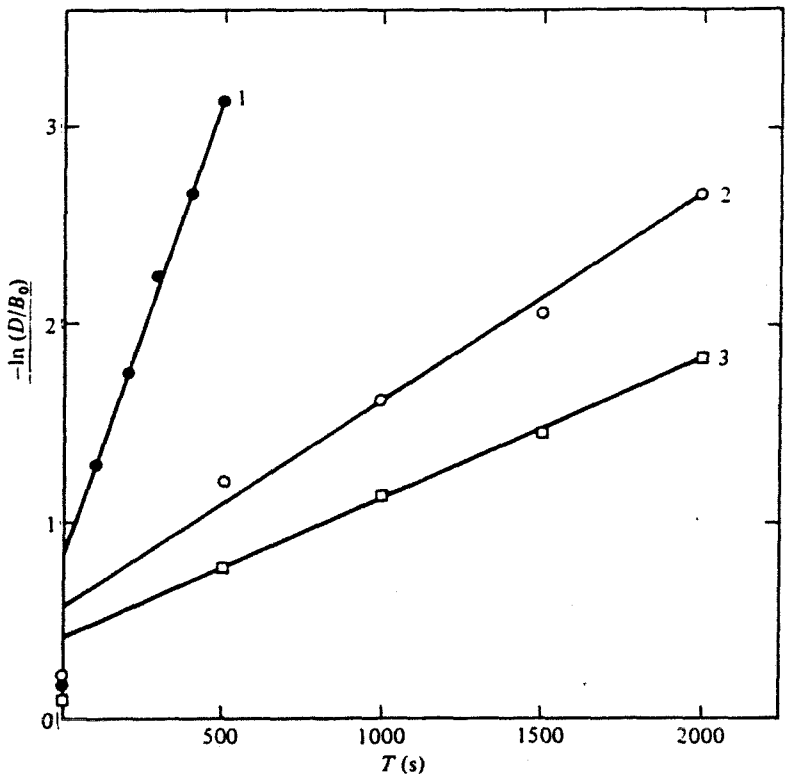

FIGURE 10. $-\ln(D/B_0)$ *vs.* T for a deformable drop in a three-dimensional Poiseuille flow ($B_0 = 0{\cdot}4$ cm) of 3 % PIB solution in Decalin, observed by Gauthier *et al.* (1971*b*). ●, case 1: $a = 0{\cdot}044$ cm, $V^*_{max} = 0{\cdot}253$ cm s^{-1}; ○, case 2: $a = 0{\cdot}044$ cm, $V^*_{max} = 0{\cdot}130$ cm s^{-1}; □, case 3: $a = 0{\cdot}021$ cm, $V^*_{max} = 0{\cdot}253$ cm s^{-1}; ——, best linear fit with data.

Finally, we consider the problem of a Newtonian deformable drop in a non-Newtonian fluid. In a Couette flow, Gauthier *et al.* (1971*a*) showed that a drop suspended in a 1·5 % solution of PAA in water migrates to an equilibrium position between the centre-line and the outer cylinder. Here, there will be separate independent contributions from deformation and non-Newtonian effects. It is obvious that deformation alone results in a lateral force toward the centre-line. Normal stresses, on the other hand, will cause migration toward the outer cylinder, if we assume as before that the contribution from the shear gradient in a Couette device dominates over that from the particle interaction with the walls, particularly for a *strong* viscoelastic suspending medium which is not well modelled as a second-order fluid. On this basis, our theory indeed predicts an intermediate equilibrium position where the deformation and viscoelastic effects cancel each other. However, owing to the speculative nature of the above ideas, we shall not attempt a detailed comparison of theory with experimental data here.

For a three-dimensional Poiseuille flow, our theory may be compared in detail with the data of Gauthier *et al.* (1971*b*) for a 3 % solution of PIB in Decalin. By integrating $\lambda(\hat{U}_s^{(\lambda)})_3 + \delta(\hat{U}_s^{(\delta)})_3$, we obtain (for $\kappa = 0$)

$$-\ln\frac{D}{B_0} + \ln\frac{D(0)}{B_0} = \left\{\left[-\frac{\phi_3}{\mu_0}(19+40\epsilon_1)\right]\left[\frac{4V^{*2}_{max}a^2}{63B_0^4}\right] + \frac{16V^{*2}_{max}a^3\mu_0}{7B_0^4\sigma}\right\}T. \qquad (8.7)$$

In figure 10, we plot $-\ln(D/B_0)$ versus T for three different cases. After subtracting the independent deformation contributions (i.e. $16V_{\max}^{*2}a^3\mu_0/7B_0^4\sigma$) from the slopes, we obtain numerical values for the parameter $-\phi_3(19+40\epsilon_1)/\mu_0$ which are 5·4, 3·2 and 5·4 s respectively. These values are apparently inconsistent with those obtained previously for a rigid sphere in a 6% solution of PIB in Decalin, since in general ϕ_3/μ_0 should decrease for decreasing concentrations of PIB (cf. Brodnyan, Gaskins & Philippoff 1957). However, it must be noted that our present procedure for calculating ϕ_3/μ_0 is incomplete, since the effect of the interaction of a deformed drop with the bounding walls has not been accounted for [recall that even (8.6) shows a slight discrepancy with the experiments]. In the present case, since large drops are used, this contribution is likely to be large and may even be of the same order of magnitude as the normal stress term which we obtain above. To put it in another way, we hypothesize that the contribution to migration which we have so far attributed to normal stresses may yet come from wall effects in drop deformation.

This work was supported by a grant from the National Science Foundation.

Appendix

We shall consider briefly the theoretical basis for generalization of the theory for motion of a deformable drop from a two-dimensional to *general* quadratic flow of a Newtonian fluid. The equations of motion are given in (4.2) and (6.1), with boundary conditions from (4.10*a*)–(4.10*c*) and (6.3*a*)–(6.3*c*). Following the same procedures as Chan & Leal (1977), we express the undisturbed velocity in index notation as

$$V_i = \alpha_i + e_{ij}x_j - \epsilon_{ijk}\Omega_k x_j + \psi_{ijk}x_k x_j - \tfrac{1}{3}(\epsilon_{ijl}\delta_{mk} + \tfrac{1}{2}\delta_{im}\epsilon_{ljk})\theta_{lm}x_k x_j + \tfrac{1}{10}(-\delta_{kl}\delta_{ij} - \delta_{jl}\delta_{ik} + 4\delta_{il}\delta_{jk})\tau_l x_k x_j - (\hat{U}_s)_i. \tag{A 1}$$

At $O(1)$, the translational velocity is

$$(\hat{U}_s^{(0)})_i = \alpha_i + \kappa\tau_i/(2+3\kappa). \tag{A 2}$$

An expression for the deformation of the drop (cf. also Haber & Hetsroni 1971) may be obtained at this stage by general tensorial arguments. In principle, it should include all linear terms from the six flow parameters. For our purpose, it is not necessary to obtain this expression in detail. However, we must note that eventually only e_{ij} and ψ_{ijk} will remain, since all other terms vanish in (4.10*c*).

By considering the force on the drop, the $O(\delta)$ migration velocity may also be obtained. Owing to the boundary conditions, it will in general include all terms that are quadratic in the flow parameters. Since the problem is spherically isotropic, we easily obtain

$$(\hat{U}_s^{(\delta)})_i = \frac{1+\kappa}{2\pi(2+3\kappa)}\{\hat{c}_1^{(1)}[\alpha_m - (\hat{U}_s^{(0)})_m]e_{mi} + \hat{c}_2^{(1)}\epsilon_{imn}[\alpha_m - (\hat{U}_s^{(0)})_m]\Omega_n + \hat{c}_3^{(1)}e_{nm}\psi_{mni} + \hat{c}_4^{(1)}\epsilon_{imn}e_{ml}\theta_{ln} + \hat{c}_5^{(1)}e_{im}\tau_m + \hat{c}_6^{(1)}\Omega_m\theta_{mi} + \hat{c}_7^{(1)}\epsilon_{imn}\Omega_n\tau_m\}. \tag{A 3}$$

By comparison with (6.6), we see that Ω_i cannot contribute to migration and hence $\hat{c}_2^{(1)}$, $\hat{c}_6^{(1)}$ and $\hat{c}_7^{(1)}$ are all zero. Combining $\hat{c}_2^{(1)}$ and $\hat{c}_5^{(1)}$, we finally simplify (A 3) to

$$(\hat{U}_s^{(\delta)})_i = \frac{1+\kappa}{2\pi(2+3\kappa)}\{\hat{c}_3^{(1)}e_{nm}\psi_{mni} + \hat{c}_4^{(1)}\epsilon_{imn}e_{ml}\theta_{ln} + \hat{c}_8^{(1)}e_{im}\tau_m\}. \tag{A 4}$$

The coefficients are obtained by a detailed comparison with our two-dimensional quadratic shear flow calculations, which then gives

$$\left.\begin{aligned} \hat{c}_3^{(1)} &= \frac{\pi}{14(1+\kappa)}\left[\frac{16+19\kappa}{1+\kappa}(6+7\kappa)-\frac{10+11\kappa}{1+\kappa}\left(\frac{8-\kappa+3\kappa^2}{1+\kappa}\right)\right], \\ \hat{c}_4^{(1)} &= -\frac{\pi}{6(1+\kappa)}\left[\frac{16+19\kappa}{1+\kappa}\left(\frac{2+2\kappa+\kappa^2}{4+\kappa}\right)\right] \\ \text{and} \quad \hat{c}_8^{(1)} &= -\frac{\pi}{10(1+\kappa)}\left[\frac{16+19\kappa}{1+\kappa}\left(\frac{6-4\kappa+3\kappa^2}{2+3\kappa}\right)\right]. \end{aligned}\right\} \tag{A 5}$$

For a Poiseuille flow in a pipe

$$\left.\begin{aligned} e_{nm}\psi_{mni} &= \tfrac{1}{5}\beta\gamma\delta_{3i}, \\ e_{imn}e_{ml}\theta_{ln} &= 0 \\ \text{and} \quad e_{im}\tau_m &= \beta\gamma\delta_{3i}. \end{aligned}\right\} \tag{A 6}$$

Thus, (6.10) is finally obtained by substitution of (A 5) and (A 6) into (A 4).

REFERENCES

Beavers, G. S. & Joseph, D. D. 1975 *J. Fluid Mech.* **69**, 475.

Bretherton, F. P. 1962 *J. Fluid Mech.* **14**, 284.

Brodnyan, J. G., Gaskins, F. H. & Philippoff, W. 1957 *Trans. Soc. Rheol.* **1**, 109.

Brunn, P. 1976 *Rheol. Acta* **15**, 589.

Chaffey, C. E., Brenner, H. & Mason, S. G. 1965 *Rheol. Acta* **4**, 64.

Chaffey, C. E., Brenner, H. & Mason, S. G. 1967 *Rheol. Acta* **6**, 100.

Chan, P. C.-H. 1979 Ph.D. thesis, California Institute of Technology.

Chan, P. C.-H. & Leal, L. G. 1977 *J. Fluid Mech.* **82**, 549.

Cox, R. G. & Brenner, H. 1968 *Chem. Engng Sci.* **23**, 147.

Frankel, N. A. & Acrivos, A. 1970 *J. Fluid Mech.* **44**, 65.

Gauthier, F., Goldsmith, H. L. & Mason, S. G. 1971*a* *Rheol. Acta* **10**, 344.

Gauthier, F., Goldsmith, H. L. & Mason, S. G. 1971*b* *Trans. Soc. Rheol.* **15**, 297.

Goldsmith, H. L. & Mason, S. G. 1962 *J. Colloid Sci.* **17**, 448.

Haber, S. & Hetsroni, G. 1971 *J. Fluid Mech.* **49**, 257.

Hadamard, J. 1911 *C. R. Acad. Sci. Paris* **152**, 1735.

Happel, J. & Brenner, H. 1973 *Low Reynolds Number Hydrodynamics.* Noordhoff.

Ho, B. P. & Leal, L. G. 1974 *J. Fluid Mech.* **65**, 365.

Ho, B. P. & Leal, L. G. 1976 *J. Fluid Mech.* **76**, 783.

Karnis, A. & Mason, S. G. 1966 *Trans. Soc. Rheol.* **10**, 571.

Karnis, A. & Mason, S. G. 1967 *J. Colloid Sci.* **24**, 164.

Leal, L. G. 1975 *J. Fluid Mech.* **69**, 305.

Peery, J. H. 1966 Ph.D. thesis, Princeton University.

Rybczynski, W. 1911 *Bull. Akad. Sci. de Cracovie*, A **40**.

Taylor, G. I. 1932 *Proc. Roy. Soc.* (London) A **138**, 41.

Taylor, G. I. 1934 *Proc. Roy. Soc.* (London) A **146**, 501.

Wohl, P. R. 1976 *Adv. Engng Sci.*, N.A.S.A. CP-2001. **4**, 1493.

Wohl, P. R. & Rubinow, S. I. 1974 *J. Fluid Mech.* **62**, 185.

APPENDIX A

We provide here a rigorous proof for omitting from (3.7) the terms $\int_{A_f} (\underline{\underline{S}} - \underline{\underline{I}})\cdot(\underline{u} + \underline{e}_3)\cdot\underline{n}dA$ and $\int_{A_f} \underline{\underline{t}}\cdot(\underline{U} - \underline{V})\cdot\underline{n}dA$, where A_f denotes an appropriate surface bounding the fluid. In general, A_f includes a fluid surface at infinity, A_∞, in addition to the solid bounding walls. The contribution from the latter is obviously zero since both $\underline{u} + \underline{e}_3$ and $\underline{U} - \underline{V}$ vanishes identically on the walls. On A_∞, we define "outer" variables $r' = \zeta r$ and describe the surface for the case of two parallel plane walls using cylindrical coordinates (ρ', x_3', θ) as $\{A_\infty: \rho' = (x_1'^2 + x_2'^2)^{1/2} \to \infty, -s \le x_3' \le 1 - s, r'^2 = \rho'^2 + x_3'^2\}$. Thus, on A_∞

$$dA = \zeta^{-2}\, \rho' dx_3'\, d\theta \tag{A1}$$

The "complementary" velocity and stress evaluated at A_∞ give [cf. (4.19a)]

$$\begin{aligned} &\underline{u} + \underline{e}_3 \sim O(r^{-1}) \sim O(\zeta\rho'^{-1}) \\ &\underline{\underline{t}} \sim O(\zeta^2\rho'^{-1}) \end{aligned} \tag{A2}$$

Next, we consider $\underline{U} - \underline{V}$ and $\underline{\underline{S}} - \underline{\underline{I}}$. The only Newtonian terms again come from the Stokeslet contribution to the disturbance velocity, which even for the general case of a <u>non</u>-neutrally buoyant sphere can go only as r^{-1}. Furthermore, additional corrections to the velocity field due to non-Newtonian rheology and drop shape deformation also go as r^{-1}. Thus

$$\underline{U} - \underline{V} \sim O(\zeta\rho'^{-1})$$

$$\underline{\underline{S}} - \underline{\underline{T}} \sim O(\zeta^2\rho'^{-1}) \tag{A3}$$

By substituting (A1) - (A3) into the original integrals, we obtain

$$\int_{A_f} (\underline{\underline{S}} - \underline{\underline{T}})\cdot(\underline{u} + \underline{e}_3)\cdot n dA \sim \zeta\rho'^{-1} \int_{A_\infty} O(1) dx_3' d\theta$$

$$\int_{A_f} \underline{\underline{t}}\cdot(\underline{U} - \underline{V})\cdot\underline{n} dA \sim \zeta\rho'^{-1} \int_{A_\infty} O(1) dx_3' d\theta \tag{A4}$$

Both integrals may be neglected as $\rho' \to \infty$.

APPENDIX B

We now evaluate the first integral in (5.7) for the case of a linear shear flow. As stated previously, the entire volume V_f is to be divided into "near-field" region V_1 and "far-field" region V_2. In V_1, the Newtonian velocity field $\underline{U}^{(o)}$ is given in (4.5) - (4.7), but there will be no shear gradient (i.e. γ) terms in (4.5). Thus,

$$
\begin{aligned}
&{}_1\underline{U}^{(o)} \sim O(\zeta) + O(\zeta^3) + \ldots \\
&{}_2\underline{U}^{(o)} \sim O(\zeta^3) + \ldots \\
&{}_3\underline{U}^{(o)} \sim O(\zeta^3) + \ldots
\end{aligned}
\tag{B1}
$$

For a neutrally buoyant fluid drop, the $O(\zeta^3)$ terms in these expressions, which come from the Stokeslet and potential doublet contributions to the velocity field, will add to zero. Hence

$$
\underline{U}^{(o)} \sim O(\zeta) + O(\zeta^4) + \ldots \tag{B2}
$$

Furthermore, for the "complementary" velocity field, we have

$$
\begin{aligned}
&{}_1\underline{u} \sim O(1) \\
&{}_2\underline{u} \sim O(\zeta) + O(\zeta^2) + \ldots \\
&{}_3\underline{u} \sim O(\zeta) + O(\zeta^2) + \ldots
\end{aligned}
\tag{B3}
$$

To evaluate the integrand, we now write

$$
\begin{aligned}
&(\underline{\underline{D}}^{(o)}_{(1)} \cdot \underline{\underline{D}}^{(o)}_{(1)} - \underline{\underline{E}}^{(o)}_{(1)} \cdot \underline{\underline{E}}^{(o)}_{(1)}) + \varepsilon_1(\underline{\underline{D}}^{(o)}_{(2)} - \underline{\underline{E}}^{(o)}_{(2)}) \sim O(\zeta^2) + O(\zeta^5) \\
&\nabla \underline{u} \sim O(1) + O(\zeta) + O(\zeta^2)
\end{aligned}
\tag{B4}
$$

By direct substitution of (B4) into (5.7), it is evident by symmetry arguments that all $O(\zeta^2)$ and $O(\zeta^3)$ terms in the dot product will vanish after integration. Thus, the leading contribution is $O(\zeta^4)$. Our calculation gives

$$\int_{V_1} \left[\left(\underline{\underline{D}}^{(o)}_{(1)} \cdot \underline{\underline{D}}^{(o)}_{(1)} - \underline{\underline{E}}^{(o)}_{(1)} \cdot \underline{\underline{E}}^{(o)}_{(1)}\right) + \varepsilon_1 \left(\underline{\underline{D}}^{(o)}_{(2)} - \underline{\underline{E}}^{(o)}_{(2)}\right)\right] : \nabla \underline{u} dV$$

$$= \frac{\pi \zeta \beta^2 J_2}{210(1+\kappa)^3} \left[(176 + 204\kappa + 312\kappa^2 + 95\kappa^3)\right.$$

$$\left. + \varepsilon_1 (704 + 1320\kappa + 1590\kappa^2 + 785\kappa^3)\right] \tag{B5}$$

In V_2, we again use "outer" variables defined as $r' = \zeta r$. In this case

$$\underline{\underline{U}}^{(o)}_{1} \sim O(1) + O(\zeta^3) + O(\zeta^4) + \ldots$$

$$\underline{\underline{U}}^{(o)}_{2} \sim O(\zeta^3) + O(\zeta^4) + \ldots$$

$$\underline{\underline{U}}^{(o)}_{3} \sim O(\zeta^4) + \ldots \tag{B6}$$

and

$$\underline{u}_1 \sim O(1) + O(\zeta) + O(\zeta^3) + \ldots$$

$$\underline{u}_2 \sim O(\zeta) + O(\zeta^2) + \ldots$$

$$\underline{u}_3 \sim O(\zeta^2) + \ldots \tag{B7}$$

Hence, we have

$$\left(\underline{\underline{D}}^{(o)}_{(1)} \cdot \underline{\underline{D}}^{(o)}_{(1)} - \underline{\underline{E}}^{(o)}_{(1)} \cdot \underline{\underline{E}}^{(o)}_{(1)}\right) + \varepsilon_1 \left(\underline{\underline{D}}^{(o)}_{(2)} - \underline{\underline{E}}^{(o)}_{(2)}\right) \sim O(\zeta^5) + O(\zeta^6)$$

$$\nabla \underline{u} \sim O(\zeta^2) + O(\zeta^3) \tag{B8}$$

The leading term in the dot product is therefore of $O(\zeta^7)$. However, dV

itself is of $O(\zeta^{-3})$, and hence the integral over V_2 is $O(\zeta^4)$. Using ${}_1\underline{U}^{(o)}$, ${}_2\underline{U}^{(o)}$, ${}_1\underline{u}$ and ${}_2\underline{u}$ in outer variables and integrating, we now obtain the contribution of region V_2 to the migration velocity. Quite surprisingly, most of the resulting terms cancel each other with the remainder coming only from ${}_1\underline{u}$ and ${}_1\underline{U}^{(o)}$. It can be expressed in a surprisingly simple form as

$$\int_{V_2} \left[\left(\underline{\underline{D}}^{(o)}_{(1)}\cdot\underline{\underline{D}}^{(o)}_{(1)} - \underline{\underline{E}}^{(o)}_{(1)}\cdot\underline{\underline{E}}^{(o)}_{(1)}\right) + \varepsilon_1\left(\underline{\underline{D}}^{(o)}_{(2)} - \underline{\underline{E}}^{(o)}_{(2)}\right)\right]:\nabla u\,dV$$

$$= \frac{\pi(2+5\kappa)}{3(1+\kappa)}\,\zeta\beta^2 J_2\cdot(1+4\varepsilon_1) \qquad \text{(B9)}$$

(B5) and (B9) are now substituted into (5.7) to give the first term in (5.9). The contribution from the drop fluid is obtained similarly by integrating $\tilde{\underline{U}}^{(o)}$ and $\tilde{\underline{u}}$ over $\tilde{V}_f$.

APPENDIX C

We estimate here the effect of the rotation of "particle coordinates". First, we define a fixed laboratory frame in which the position vector at any point R is denoted as $\underline{x}'$. The velocity measured in this frame is assumed to be steady in time, and denoted as $\underline{V}'$. The location of the sphere at any instant is given as $\underline{x}_o'$. Next, we choose particle coordinates fixed at the center of the sphere, translating with sphere velocity $\underline{U}_s$. We also assume that these coordinates may be rotating with an arbitrary angular velocity $\underline{\Omega}_f$. The position vector at point R is denoted as $\underline{x}$.

$\underline{V}'$ is now written in terms of the particle coordinates as

$$\underline{V}' = \underline{\alpha} + \underline{\underline{\beta}}\cdot\underline{x} + \underline{\underline{\underline{\gamma}}}:\underline{x}\underline{x} \tag{C1}$$

It should be noted that $\underline{\alpha}$, $\underline{\underline{\beta}}$ and $\underline{\underline{\underline{\gamma}}}$ as defined in the above expressions should be time-dependent, even though $\underline{V}'$ itself is assumed to be steady. To obtain their time derivatives, we first write[†]

$$\frac{d\underline{V}'}{dt'} = \frac{d\underline{V}'}{dt} + \underline{\Omega}_f \times \underline{V}' \tag{C2}$$

[†]For an arbitrary vector $\underline{u}$, we have $\underline{u} = u_i\underline{e}_i = u_i'\underline{e}_i'$. Thus $\frac{d\underline{u}}{dt'} = \underline{e}_i' \frac{du_i'}{dt'} = \frac{d}{dt'}(u_i\underline{e}_i) = \underline{e}_i \frac{du_i}{dt'} + u_i \frac{d\underline{e}_i}{dt'} = \underline{e}_i \frac{du_i}{dt} + u_i(\underline{\Omega}\times\underline{e}_i) = \frac{d\underline{u}}{dt} + \underline{\Omega}\times\underline{u}$.

By straightforward manipulations, we obtain

$$\frac{\partial \underline{V}'}{\partial t} = \frac{\partial \underline{V}'}{\partial t'} + (\underline{V}' - \underline{V})\cdot\nabla\underline{V}' - \underline{\Omega}_f \times \underline{V}' \tag{C3}$$

Clearly, $\frac{\partial \underline{V}'}{\partial t'} = 0$. Furthermore, $\underline{V}'$ and $\underline{V}$ differ only by the translation and rotation of the particle coordinates. Thus

$$\frac{\partial \underline{V}'}{\partial t} = (\underline{U}_s + \underline{\Omega}_f \times \underline{x})\cdot\nabla\underline{V}' - \underline{\Omega}_f \times \underline{V}' \tag{C4}$$

We now substitute (C1) into (C4) to give

$$\frac{\partial \underline{\alpha}}{\partial t} + \frac{\partial \underline{\underline{\beta}}}{\partial t}\cdot\underline{x} + \frac{\partial \underline{\underline{\gamma}}}{\partial t}:\underline{x}\underline{x} = (\underline{\underline{\beta}} + 2\underline{\underline{\gamma}}\cdot\underline{x})\cdot(\underline{U}_s + \underline{\Omega}_f \times\underline{x})$$

$$- \underline{\Omega}_f \times(\underline{\alpha} + \underline{\underline{\beta}}\cdot\underline{x} + \underline{\underline{\gamma}}:\underline{x}\underline{x}) \tag{C5}$$

By grouping terms into different powers of $\underline{x}$, we have

$$\frac{\partial \underline{\alpha}}{\partial t} = \underline{\underline{\beta}}\cdot\underline{U}_s - \underline{\Omega}_f \times\underline{\alpha}$$

$$\frac{\partial \underline{\underline{\beta}}}{\partial t}\cdot\underline{x} = 2\underline{\underline{\gamma}}\cdot\underline{x}\cdot\underline{U}_s + \underline{\underline{\beta}}\cdot(\underline{\Omega}_f \times\underline{x}) - \underline{\Omega}_f \times(\underline{\underline{\beta}}\cdot\underline{x})$$

$$\frac{\partial \underline{\underline{\gamma}}}{\partial t}:\underline{x}\underline{x} = 2\underline{\underline{\gamma}}\cdot\underline{x}\cdot(\underline{\Omega}_f \times\underline{x}) - \underline{\Omega}_f \times(\underline{\underline{\gamma}}:\underline{x}\underline{x}) \tag{C6}$$

which can be rewritten as

$$\frac{\partial \underline{\alpha}}{\partial t} = \underline{\underline{\beta}}\cdot\underline{U}_s - (\underline{\underline{\varepsilon}}\cdot\underline{\Omega}_f)\cdot\underline{\alpha}$$

$$\frac{\partial \underline{\underline{\beta}}}{\partial t} = 2\underline{\underline{\gamma}}\cdot\underline{U}_s + \underline{\underline{\beta}}\cdot(\underline{\underline{\varepsilon}}\cdot\underline{\Omega}_f) - (\underline{\underline{\varepsilon}}\cdot\underline{\Omega}_f)\cdot\underline{\underline{\beta}}$$

$$\frac{\partial \underline{\underline{\gamma}}}{\partial t} = 2\underline{\underline{\gamma}}\cdot(\underline{\underline{\varepsilon}}\cdot\underline{\Omega}_f) - (\underline{\underline{\varepsilon}}\cdot\underline{\Omega}_f)\cdot\underline{\underline{\gamma}} \tag{C7}$$

For $\underline{\Omega}_f \equiv 0$, the above equations clearly reduce to (2.12) of Chan and Leal

(1977) for the time derivatives of $\underline{\alpha}$, $\underline{\underline{\beta}}$ and $\underline{\underline{\gamma}}$ defined in a coordinate system which only translates with the particle velocity. The additional terms in our expressions are therefore due to the rotation of the coordinates.

The force and torque acting on the particle may now be obtained simply by tensorial arguments involving the flow parameters $\underline{\alpha} - \underline{U}_s$, $\underline{\underline{e}}$, $\underline{\Omega} - \underline{\Omega}_f$, $\underline{\underline{\psi}}$, $\underline{\underline{\theta}}$, $\underline{\tau}$, and boundary value $\underline{\omega}_s - \underline{\Omega}_f$ (cf. Chan and Leal 1977). For a rigid sphere, they are, at O(1)

$$\underline{F}^{(o)} = c_1^{(o)}\left[\underline{\alpha} - \underline{U}_s^{(o)}\right] + c_2^{(o)}\underline{\tau}$$

$$\underline{G}^{(o)} = d_1^{(o)}\left[\underline{\Omega} - \underline{\Omega}_f\right] + d_2^{(o)}\left[\underline{\omega}_s^{(o)} - \underline{\Omega}_f\right] \tag{C8}$$

Thus, for a neutrally buoyant sphere

$$\underline{U}_s^{(o)} = \underline{\alpha} + \frac{c_2^{(o)}}{c_1^{(o)}}\underline{\tau}$$

$$\underline{\omega}_s^{(o)} = \underline{\Omega} \tag{C9}$$

At $O(\lambda)$, we have

$$\underline{F}^{(\lambda)} = -c_1^{(o)}\,\underline{U}_s^{(1)} + \text{quadratic terms with no explicit time dependence}$$
$$+ \varepsilon_1\left\{\underline{\underline{t}}_A^1 \cdot \frac{\partial}{\partial t}\left[\underline{\alpha} - \underline{U}_s^{(o)}\right] + \underline{\underline{\underline{t}}}_A : \frac{\partial \underline{\underline{\psi}}}{\partial t} + \underline{\underline{\underline{t}}}_B : \frac{\partial \underline{\underline{\theta}}}{\partial t} + \underline{\underline{t}}_A^2 \cdot \frac{\partial \underline{\tau}}{\partial t}\right\} \tag{C10a}$$

$$\underline{G}^{(\lambda)} = d_2^{(o)}\,\underline{\omega}_s^{(1)} + \text{quadratic terms with no explicit time dependence}$$
$$+ \varepsilon_1\left\{\underline{\underline{r}}_B : \frac{\partial \underline{\underline{e}}}{\partial t} + \underline{\underline{r}}_A \cdot \frac{\partial}{\partial t}\left[\underline{\Omega} - \underline{\Omega}_f\right] + \underline{\underline{r}}_A^2 \cdot \frac{\partial}{\partial t}\left[\underline{\omega}_s^{(o)} - \underline{\Omega}_f\right]\right\} \tag{C10b}$$

To estimate the migration velocity, we use only (C10a). In Chan and Leal (1977), $\underline{\underline{\psi}}$ and $\underline{\underline{\theta}}$ are shown to be symmetric and completely irreducible tenors. Clearly, $\frac{\partial \underline{\underline{\psi}}}{\partial t}$ and $\frac{\partial \underline{\underline{\theta}}}{\partial t}$ should also have the same properties.

Thus, when dotted respectively with isotropic tensor $\underline{\underline{A}}^t$ and isotropic pseudotensor $\underline{\underline{B}}^t$, they both vanish. By (C9), we obtain

$$\underline{F}^{(\lambda)} = -C_1^{(o)} \underline{U}_s^{(1)} + \text{quadratic terms with no explicit time dependence} + \varepsilon_1 C^{(\lambda)} \frac{\partial \underline{\tau}}{\partial t} \tag{C11}$$

Using (C7), the above expression can be rewritten as

$$\underline{F}^{(\lambda)} = -C_1^{(o)} \underline{U}_s^{(1)} + \text{quadratic terms with no explicit time dependence} - \varepsilon_1 C^{(\lambda)} (\underline{\underline{\varepsilon}} \cdot \underline{\Omega}_f \cdot \underline{\tau}) \tag{C12}$$

Therefore, in general, there will be an additional contribution to the particle migration velocity due to the rotation of the coordinates. The significance of this term clearly depends on the value of $\underline{\Omega}_f$, i.e. if the coordinates are rotating "very slowly", this term may be neglected. We are primarily interested in estimating its contribution for a Couette flow. In this case, however, $\underline{\tau}$ is identically zero [cf. (5.19) of Chan and Leal (1979) and the definition of $\underline{\tau}$], regardless of the curvature of the Couette device. Thus, the rotation of the particle coordinates in the Couette flow problem has no effect.

APPENDIX D

It has been shown by Bretherton (1962) that for a rigid body moving in a given orbit in a steady unidirectional flow of a Newtonian fluid, there exists one for a body of opposite mirror-symmetry, obtained by reflexion in a plane perpendicular to the streamlines, but transversed in opposite senses. Here we repeat the same proof to show that a rigid sphere in a "purely-viscous" (e.g. Power-law) fluid will not migrate.

The equations of motion are written as

$$\nabla P = \nabla\cdot(\mu \underline{\underline{D}}) \tag{D1}$$

$$\nabla\cdot\underline{U} = 0$$

where $\underline{\underline{D}} = \nabla\underline{U} + (\nabla\underline{U})^T$ and $\mu = \mu(D)$

$$D = (\tfrac{1}{2}\,\underline{\underline{D}}:\underline{\underline{D}})^{\frac{1}{2}} \tag{D2}$$

The boundary conditions at large distance from the sphere is

$$\underline{U} \to V(x_2,x_3)\underline{e}_1 \quad \text{as} \quad |\underline{x}| \to \infty \tag{D3}$$

At any point O on the surface of the sphere, the coordinates are denoted as $\underline{r}(O,t)$ and the velocity as $\underline{U}_s(O,t)$. Thus

$$\underline{U}_s = \frac{d\underline{r}}{dt} \tag{D4}$$

Next, we define a sphere which is a mirror image of the original one by reflexion in the (x_2,x_3)-plane, and then we reverse the time. A point O' on the surface of this sphere will thus have coordinates

$$\underline{r}(O',t) = \hat{\underline{r}}(O,-t) \tag{D5}$$

where

$$\hat{r}_1 = -r_1 \ , \ \hat{r}_2 = r_2 \ , \ \hat{r}_3 = r_3 \tag{D6}$$

Furthermore, the new sphere will be moving in a velocity field

$$\underline{U}'(O',t) = -\hat{\underline{U}}(O,-t) \tag{D7}$$

where

$$\hat{U}_1 = -U_1, \hat{U}_2 = U_2, \hat{U}_3 = U_3 \tag{D8}$$

and

$$P'(O',t) = -P(O,-t) \tag{D9}$$

$\underline{U}'$ and P' can be shown to satisfy the equations of motion (D1) and the condition at infinity (D3). (In particular, we note that the shear rate D is not affected by reflexion, using (D2)).

Finally, on the sphere surface, the boundary condition becomes

$$\underline{U}'_s = \frac{d\underline{r}(O',t)}{dt} = \frac{d\hat{\underline{r}}(O,-t)}{dt} = -\hat{\underline{U}}_s \tag{D10}$$

where

$$(\hat{U}_s)_1 = -(U_s)_1, \ (\hat{U}_s)_2 = (U_s)_2, \ (\hat{U}_s)_3 = (U_s)_3 \tag{D11}$$

Thus, we have

$$(U'_s)_2 = -(U_s)_2 \quad \text{and} \quad (U'_s)_3 = -(U_s)_3 \tag{D12}$$

Clearly, in this case, no migration is possible. The only motion on the particle's surface is rigid body rotation.

CHAPTER III: A NOTE ON THE MOTION OF A SPHERICAL PARTICLE IN A GENERAL QUADRATIC FLOW OF A SECOND-ORDER FLUID

J. Fluid Mech. (1977), *vol.* 82, *part* 3, *pp.* 549–559
Printed in Great Britain

A note on the motion of a spherical particle in a general quadratic flow of a second-order fluid

By P. C.-H. CHAN AND L. G. LEAL
Department of Chemical Engineering, California Institute of Technology, Pasadena

(Received 12 July 1976 and in revised form 10 December 1976)

The migration of a rigid sphere in a two-dimensional unidirectional shear flow of a second-order fluid was considered by Ho & Leal (1976). It was found that the sphere would migrate in the direction of decreasing absolute shear rate. The present paper extends the previous results to a general quadratic flow, and also considers the case of a spherical drop.

1. Introduction

Brenner (1964) studied the Stokes resistance of an arbitrary rigid particle in an arbitrary field of flow. He showed that both the force and the torque relative to any given point O of the body can depend only linearly on certain vectorial or tensorial parameters that characterize the undisturbed bulk velocity distribution. In a general linear flow, these parameters are the translational velocity relative to that of the particle, the vorticity tensor as seen in a frame of reference which rotates with the particle, and the rate-of-strain tensor. Calculation of the force and torque from these quantities, for an arbitrary body, then reduces to the determination of six tensor coefficients which depend only on the shape of the body. Symmetry conditions for these tensors were discussed by Hinch (1972).

Application of these general ideas to the motion of an arbitrary rigid particle in a non-Newtonian fluid was first reported by Brunn (1976, 1977), who used an incompressible second-order fluid in a perturbation expansion about the Newtonian limit. As a consequence, the non-Newtonian contributions to the force and torque were found to depend only on quadratic combinations of the flow parameters. However, Brunn considered only a linear bulk velocity field and concluded that no migration would occur for neutrally buoyant rigid particles. In contrast, Ho & Leal (1976) recently reported detailed calculations for the motion of a rigid sphere in a two-dimensional, quadratic, unidirectional shear flow of a second-order fluid. In this case, it was found that the sphere would migrate in the direction of decreasing absolute shear rate.

The present paper extends the results of Ho & Leal (1976) to a *general* quadratic flow of a second-order fluid. In § 2 we outline the formulation of the problem. In § 3.1 general expressions are obtained for the translation and rotation of a rigid sphere, and numerical values for the geometry-dependent coefficients which appear are determined by comparison with the detailed calculation for the specific flow of Ho & Leal (1976). Finally, in § 3.2 we obtain analogous results for a spherical drop. As will be obvious later on, index notation is to be preferred over tensor notation for our analysis and will be used throughout this paper.

2. Formulation of the problem

We consider a rigid particle suspended in a second-order fluid which is undergoing some general quadratic motion. To non-dimensionalize, we define a characteristic (particle) length a, a characteristic velocity Ga and a characteristic pressure $\mu_0 G$, where G is an average shear rate for the bulk flow and μ_0 is the zero-shear viscosity. We adopt a *non-rotating* co-ordinate system which has its origin fixed at the centre of rotation of the particle, and thus translates with the particle velocity $(U_s)_i$ relative to a fixed laboratory reference frame. The position vector of a point R in this translating frame is denoted by x_i, whereas the position vectors for R and for the centre of rotation measured with respect to the fixed frame are x_i' and $(x_0(t))_i$, respectively. Thus

$$x_i = x_i' - (x_0(t))_i. \tag{2.1}$$

The complete dimensionless velocity and pressure distributions, including the disturbance motion induced by the particle, will be denoted by (U_i, P). The equations of motion, with inertia effects neglected, are then

$$\partial S_{ij}/\partial x_j = 0, \quad \partial U_i/\partial x_i = 0, \tag{2.2}$$

where

$$S_{ij} = -P\delta_{ij} + D_{(1)ij} + \lambda D_{(1)ik} D_{(1)kj} + \lambda\epsilon_1 D_{(2)ij}. \tag{2.3}$$

$D_{(1)ij}$ and $D_{(2)ij}$ are Rivlin–Ericksen tensors given by

$$D_{(1)ij} = \partial U_i/\partial x_j + \partial U_j/\partial x_i, \tag{2.4a}$$

$$D_{(2)ij} = \partial D_{(1)ij}/\partial t + U_k D_{(1)ij,k} + D_{(1)ik} U_{k,j} + D_{(1)kj} U_{k,i}, \tag{2.4b}$$

while λ and ϵ_1 are material parameters of the fluid. From a macroscopic point of view, λ is often defined as the ratio of a normal-stress function to the viscosity in the limit of zero shear; physically, it may be interpreted as the ratio of the intrinsic relaxation time scale of the fluid to the convective time scale of the flow problem (Caswell & Schwarz 1962). We assume here that the flow is slow (nearly Newtonian) compared with the intrinsic relaxation time (i.e. $\lambda \ll 1$) but that non-Newtonian effects are still more important than inertial effects (i.e. $Re \ll \lambda$). Similarly, the undisturbed bulk velocity and pressure fields (V_i, Q) may be assumed to satisfy the equations

$$\partial T_{ij}/\partial x_j = 0, \quad \partial V_i/\partial x_i = 0, \tag{2.5a, b}$$

where

$$T_{ij} = -Q\delta_{ij} + E_{(1)ij} + \lambda E_{(1)ik} E_{(1)kj} + \lambda\epsilon_1 E_{(2)ij} \tag{2.6}$$

with $E_{(n)ij}$ defined analogously to $D_{(n)ij}$, but using V_i.

We are interested primarily in the $O(\lambda)$ contribution to the translational velocity of the particle. For a unidirectional flow, this specifies the lateral migration as well as any $O(\lambda)$ contributions to motion in the direction of the undisturbed bulk flow. Ho & Leal (1976) showed rigorously, in the case of a sphere in a two-dimensional unidirectional flow, that the non-Newtonian migration is a 'near-field' effect caused by the disturbance velocity field in the vicinity of the sphere, provided of course that the sphere is small relative to the characteristic dimension of the flow d (i.e. $\zeta = a/d \ll 1$). In particular, the fluid can effectively be considered as unbounded, with no direct effect of the bounding walls other than their role in determining the undisturbed velocity profile. Any corrections to the infinite-domain disturbance flow to account for the

presence of boundaries give only higher-order corrections in ζ for the migration velocity. A rigorous proof that the non-Newtonian contributions to particle motion at $O(\lambda)$ are similarly dominated by 'near-field' effects for a general quadratic flow has not been constructed.† Nevertheless, we believe this result to hold true and shall therefore assume that the presence of any walls may be neglected. Hence we require that the complete velocity field U_i reduces to the undisturbed form at large distances from the particle, i.e.

$$U_i \to V_i \quad \text{as} \quad r = (x_j x_j)^{\frac{1}{2}} \to \infty. \tag{2.7}$$

On the surface of the particle, U_i satisfies

$$U_i = -\epsilon_{ijk}(\omega_s)_k x_j. \tag{2.8}$$

The undisturbed velocity relative to the laboratory-fixed reference frame, which we denote by V'_i, is assumed to be steady in time and representable, at any instant, by the general quadratic form

$$V'_i = \alpha'_i + \beta'_{ij} x'_j + \gamma'_{ijk} x'_k x'_j, \tag{2.9}$$

where α'_i, β'_{ij} and γ'_{ijk} are constant tensors. Thus, in the translating frame which we have adopted,

$$V_i = \alpha_i + \beta_{ij} x_j + \gamma_{ijk} x_k x_j - (U_s)_i, \tag{2.10}$$

where

$$\left.\begin{aligned} \alpha_i &= \alpha'_i + \beta'_{ij}(x_0)_j + \gamma'_{ijk}(x_0)_k (x_0)_j, \\ \beta_{ij} &= \beta'_{ij} + 2\gamma'_{ijk}(x_0)_k, \quad \gamma_{ijk} = \gamma'_{ijk}. \end{aligned}\right\} \tag{2.11}$$

The coefficient γ_{ijk} remains constant in time, but α_i and β_{ij} are time dependent, as a result of the motion of the reference frame. It follows easily from (2.11) that

$$\partial\alpha_i/\partial t = \beta_{ij}(U_s)_j, \quad \partial\beta_{ij}/\partial t = 2\gamma_{ijk}(U_s)_k. \tag{2.12a, b}$$

In deriving (2.11) and (2.12a, b), we have made use of the obvious symmetry condition

$$\gamma_{ijk} = \gamma_{ikj}. \tag{2.13}$$

It is also apparent from (2.5b) that β_{ij} and γ_{ijk} satisfy the additional constraints

$$\beta_{ii} = 0, \quad \gamma_{iki} = \gamma_{iik} = 0. \tag{2.14}$$

In this paper, tensors which give zero when contracted along *any* two indices will be termed *completely irreducible*.

Both β_{ij} and γ_{ijk} have to be decomposed into their respective irreducible components in order to be applied conveniently in a general expression for the force or torque. This decomposition was illustrated by Coope, Snider & McCourt (1965). Its main advantage for present purposes is that all the components of β_{ij} and γ_{ijk} are made to be completely irreducible and symmetric, and much simplification is then possible in the analysis. Besides, each component then has its own physical significance. The decomposition of β_{ij} is well known:

$$\beta_{ij} = \tfrac{1}{2}(\beta_{ij} + \beta_{ji}) + \tfrac{1}{2}(\beta_{ij} - \beta_{ji}). \tag{2.15}$$

Consequently

$$\beta_{ij} x_j = e_{ij} x_j - \epsilon_{ijk}\,\Omega_k x_j, \tag{2.16}$$

where

$$e_{ij} = \tfrac{1}{2}(\beta_{ij} + \beta_{ji}), \quad \Omega_k = \tfrac{1}{2}\epsilon_{kmn}\beta_{nm}. \tag{2.17}$$

† And, indeed, would be extremely difficult in this general problem.

The decomposition of γ_{ijk} is more complicated:

$$\begin{aligned}\gamma_{ijk} = [&\tfrac{1}{6}(\gamma_{ijk}+\gamma_{ikj}+\gamma_{kij}+\gamma_{kji}+\gamma_{jik}+\gamma_{jki})\\ &-\tfrac{1}{15}(\gamma_{imm}\delta_{jk}+\gamma_{jmm}\delta_{ik}+\gamma_{kmm}\delta_{ij})]+\tfrac{1}{3}[\epsilon_{ijl}(-\epsilon_{lmn}\gamma_{nmk}-\epsilon_{kmn}\gamma_{nml})\\ &+(-\tfrac{1}{2}\epsilon_{imn}\gamma_{nml}-\tfrac{1}{2}\epsilon_{lmn}\gamma_{nmi})\epsilon_{ljk}]+\tfrac{1}{10}[-\gamma_{kmm}\delta_{ij}-\gamma_{jmm}\delta_{ik}+4\gamma_{imm}\delta_{jk}].\end{aligned} \tag{2.18}$$

Consequently

$$\begin{aligned}\gamma_{ijk}x_kx_j = \psi_{ijk}x_kx_j &-\tfrac{1}{3}(\epsilon_{ijl}\delta_{mk}+\tfrac{1}{2}\delta_{im}\epsilon_{ljk})\theta_{lm}x_kx_j\\ &+\tfrac{1}{10}(-\delta_{kl}\delta_{ij}-\delta_{jl}\delta_{ik}+4\delta_{il}\delta_{jk})\tau_lx_kx_j,\end{aligned} \tag{2.19}$$

where

$$\left.\begin{aligned}\psi_{ijk} &= \tfrac{1}{6}(\gamma_{ijk}+\gamma_{ikj}+\gamma_{kij}+\gamma_{kji}+\gamma_{jik}+\gamma_{jki})\\ &\quad-\tfrac{1}{15}(\gamma_{imm}\delta_{jk}+\gamma_{jmm}\delta_{ik}+\gamma_{kmm}\delta_{ij}),\\ \theta_{ij} &= \epsilon_{imn}\gamma_{nmj}+\epsilon_{jmn}\gamma_{nmi},\quad \tau_i = \gamma_{imm}.\end{aligned}\right\} \tag{2.20}$$

Once again, we note that e_{ij}, ψ_{ijk} and θ_{ij} are all completely irreducible and symmetric. It is also important to observe that both

$$(\epsilon_{ijl}\delta_{mk}+\tfrac{1}{2}\delta_{im}\epsilon_{ljk})\theta_{lm} \quad \text{and} \quad (-\delta_{kl}\delta_{ij}-\delta_{jl}\delta_{ik}+4\delta_{il}\delta_{jk})\tau_l$$

in (2.19) are symmetric in j, k (the former condition is by no means obvious from a casual inspection) and therefore our decomposition is consistent with (2.13).

Intuitively, it is appealing to interpret θ_{ij} as the vorticity gradient, and to assume that ψ_{ijk} and τ_i specify the rate-of-strain gradient. To show that this intuitive 'guess' is indeed correct, we may re-express V_i as

$$\begin{aligned}V_i = \alpha_i+e_{ij}x_j-\epsilon_{ijk}\Omega_kx_j+\psi_{ijk}x_kx_j &-\tfrac{1}{3}(\epsilon_{ijl}\delta_{mk}+\tfrac{1}{2}\delta_{im}\epsilon_{ljk})\theta_{lm}x_kx_j\\ &+\tfrac{1}{10}(-\delta_{kl}\delta_{ij}-\delta_{jl}\delta_{ik}+4\delta_{il}\delta_{jk})\tau_lx_kx_j-(U_s)_i\end{aligned} \tag{2.21}$$

and follow the familiar argument based upon the rate of change of the length of a material line element (Fredrickson 1964) to get (using the results of last paragraph)

$$dV_i\frac{dx_i}{ds} = e_{ij}dx_j\frac{dx_i}{ds}+2\psi_{ijk}x_kdx_j\frac{dx_i}{ds}+\tfrac{1}{5}(-\delta_{kl}\delta_{ij}-\delta_{jl}\delta_{ik}+4\delta_{il}\delta_{jk})\tau_lx_kdx_j\frac{dx_i}{ds}. \tag{2.22}$$

Finally we observe that

$$dV_i(dx_i/ds) = \mathfrak{d}(ds)/\mathfrak{d}t, \tag{2.23}$$

where $\mathfrak{d}/\mathfrak{d}t$ is a convected time derivative expressed in terms of a fixed co-ordinate system, and therefore

$$\mathfrak{d}(ds)^2/\mathfrak{d}t = 2[e_{ij}+2\psi_{ijk}x_k+\tfrac{1}{5}(-\delta_{kl}\delta_{ij}-\delta_{jl}\delta_{ik}+4\delta_{il}\delta_{jk})\tau_lx_k]dx_jdx_i. \tag{2.24}$$

The argument for the vorticity is also well known and follows in a similar manner by consideration of the rate of rotation of a line element. For the sake of brevity, we shall omit the details here. As expected, the rotation depends only on Ω_i and θ_{ij}.

3. The migration velocity

We now attempt to obtain general expressions for the force and torque on the particle. To this end, we first note that the solution of (2.2), obtained by a straightforward perturbation expansion, shows that the $O(1)$ Newtonian contribution is

linear in the flow parameters $(\alpha_i - (U_s)_i)$, e_{ij}, Ω_i, ψ_{ijk}, θ_{ij} and τ_i and also the boundary value $(\omega_s)_i$. On the other hand, the $O(\lambda)$ non-Newtonian contribution consists of quadratic combinations of these seven parameters, from the time-independent terms in the non-Newtonian part of (2.3), and also additional linear terms arising from their time derivatives, due to particle translation. By this formulation, any contributions from the rate of change of orientation (i.e. rotation) of the particle are included automatically. Hence, if we now use the superscript (n) to denote contributions at $O(\lambda^n)$, the expressions for the force and torque are

$$\begin{aligned} F_i &= F_i^{(0)} + \lambda F_i^{(1)} \\ &= \{{}^tA^1_{ij}[\hat{\alpha}_j - \lambda(U_s^{(1)})_j] + {}^tA^1_{ijk}\, e_{kj} + {}^tB^1_{ij}\,\Omega_j + {}^tA^1_{ijkl}\,\psi_{lkj} + {}^tB^1_{ijk}\,\theta_{kj} \\ &\quad + {}^tA^2_{ij}\,\tau_j + {}^tB^2_{ij}[(\omega_s^{(0)})_j + \lambda(\omega_s^{(1)})_j]\} \\ &\quad + \lambda\{28 \text{ terms from all possible quadratic combinations among} \\ &\quad \hat{\alpha}_i,\ e_{ij},\ \Omega_i,\ \psi_{ijk},\ \theta_{ij},\ \psi_i,\ \tau_i,\ (\omega_s^{(0)})_i\} \\ &\quad + \lambda\epsilon_1\{4 \text{ terms from time derivatives of } \hat{\alpha}_i,\ e_{ij},\ \Omega_i,\ (\omega_s^{(0)})_i\}, \end{aligned} \tag{3.1a}$$

$$\begin{aligned} G_i &= G_i^{(0)} + \lambda G_i^{(1)} \\ &= \{{}^rB^1_{ij}[\hat{\alpha}_j - \lambda(U_s^{(1)})_j] + {}^rB^1_{ijk}\, e_{kj} + {}^rA^1_{ij}\,\Omega_j + {}^rB^1_{ijkl}\,\psi_{lkj} + {}^rA^1_{ijk}\,\theta_{kj} \\ &\quad + {}^rB^2_{ij}\,\tau_j + {}^rA^2_{ij}[(\omega_s^{(0)})_j + \lambda(\omega_s^{(1)})_j]\} + \lambda\{\ldots\} + \lambda\epsilon_1\{\ldots\}. \end{aligned} \tag{3.1b}$$

Here, we have used $\hat{\alpha}_i$ to denote the combination $\alpha_i - (U_s^{(0)})_i$. The ${}^tA$'s and ${}^rA$'s are second- and higher-rank *time-dependent* material tensors that depend upon the particle geometry, i.e. its shape and its orientation with respect to our non-rotating co-ordinate frame. By contrast, the ${}^tB$'s and ${}^rB$'s are second- and higher-rank *time-dependent* pseudo-tensors. This distinction between tensors and pseudo-tensors is necessary because vorticity and torque are pseudo-quantities. The time dependence of these coefficients reflects the changing geometry as the particle rotates, and is therefore not present when the particles are spheres.†

So far, the shape of the particle has not been specified. Brunn (1977) considered the case of a transversely isotropic particle, i.e. a body of revolution with fore–aft symmetry. All odd-rank tensors and even-rank pseudo-tensors are then identically zero, while the rest depend on the orientation of the symmetry axis. The expressions for the force and torque to $O(1)$ and $O(\lambda)$ are then

$$\left.\begin{aligned} F_i^{(0)} &= {}^tA^1_{ij}\,\hat{\alpha}_j + {}^tA^1_{ijkl}\,\psi_{lkj} + {}^tB^1_{ijk}\,\theta_{kj} + {}^tA^2_{ij}\,\tau_j, \\ G_i^{(0)} &= {}^rB^1_{ijk}\, e_{kj} + {}^rA^1_{ij}\,\Omega_j + {}^rA^2_{ij}(\omega_s^{(0)})_j, \end{aligned}\right\} \tag{3.2}$$

$$\begin{aligned} F_i^{(1)} = &-{}^tA^1_{ij}(U_s^{(1)})_j + \{{}^tB^2_{ijk}\,\hat{\alpha}_k\,\Omega_j + {}^tB^3_{ijk}\,\hat{\alpha}_k(\omega_s^{(0)})_j \\ &+ {}^tB^4_{ijk}\,\Omega_k\,\tau_j + {}^tB^5_{ijk}(\omega_s^{(0)})_k\,\tau_j + {}^tA^2_{ijkl}\,\hat{\alpha}_l\, e_{kj} \\ &+ 7 \text{ more terms involving quadratic combinations of } e_{ij},\ \psi_{ijk}, \\ &\theta_{ij},\ \tau_i,\ \Omega_i,\ (\omega_s^{(0)})_i \text{ with coefficients which are even-rank tensors or} \\ &\text{odd-rank pseudo-tensors}\} + \epsilon_1\{{}^tA^2_{ij}\,\partial\hat{\alpha}_j/\partial t\}, \end{aligned} \tag{3.3a}$$

† Indeed, for analysis of non-spherical geometry it is more convenient to allow the co-ordinate frame to translate *and* rotate with the particle. We are mainly concerned in the present communication with spheres (equation (3.4) onwards) and so choose a non-rotating frame for our analysis.

$$G_i^{(1)} = {}^rA^2_{ij}(\omega_s^{(1)})_j + \{{}^rB^2_{ijk}\hat{\alpha}_k\hat{\alpha}_j + {}^rB^3_{ijk}\hat{\alpha}_k\tau_j + {}^rB^4_{ijk}\Omega_k\Omega_j$$
$$+ 13 \text{ more terms involving quadratic combinations of } \hat{\alpha}_i,\ e_{ij},$$
$$\psi_{ijk},\ \theta_{ij},\ \tau_i,\ \Omega_i,\ (\omega_s^{(0)})_i \text{ with coefficients which are even-rank}$$
$$\text{tensors or odd-rank pseudo-tensors}\}$$
$$+\epsilon_1\left\{{}^rB^5_{ijk}\frac{\partial}{\partial t}e_{kj} + {}^rA^3_{ij}\frac{\partial}{\partial t}\Omega_j + {}^rA^4_{ij}\frac{\partial}{\partial t}(\omega_s^{(0)})_j\right\}. \tag{3.3b}$$

3.1. *The rigid sphere*

To simplify further the calculations of this section, we consider the particular case of a neutrally buoyant rigid sphere in the absence of any externally applied torque. The non-zero material tensors and pseudo-tensors are then spherically isotropic and expressed in the most general form are

$$\left.\begin{aligned} A_{ij} = a_0\delta_{ij}, \quad B_{ijk} = b_0\epsilon_{ijk}, \\ A_{ijkl} = a_1\delta_{ij}\delta_{kl} + a_2\delta_{ik}\delta_{jl} + a_3\delta_{il}\delta_{jk}. \end{aligned}\right\} \tag{3.4}$$

Expressions for the higher-order tensor and pseudo-tensor coefficients follow in a similar manner but are excessively cumbersome, and will not be given here.

Equations (3.2) can now be further simplified. In particular

$${}^tA^1_{ijkl}\psi_{lkj} = 0, \quad {}^tB^1_{ijk}\theta_{kj} = {}^rB^1_{ijk}e_{kj} = 0, \tag{3.5}$$

whereas for the other terms we may write

$$\left.\begin{aligned} {}^tA^1_{ij}\hat{\alpha}_j = c_1^{(0)}\hat{\alpha}_i, \quad {}^tA^2_{ij}\tau_j = c_2^{(0)}\tau_i, \\ {}^rA^1_{ij}\Omega_j = d_1^{(0)}\Omega_i, \quad {}^rA^2_{ij}(\omega_s^{(0)})_j = d_2^{(0)}(\omega_s^{(0)})_i. \end{aligned}\right\} \tag{3.6}$$

Since the force and torque on the particle arc zero to the present level of approximation, we finally obtain

$$(U_s^{(0)})_i = \alpha_i + \frac{c_2^{(0)}}{c_1^{(0)}}\tau_i, \quad (\omega_s^{(0)})_i = \left(-\frac{d_1^{(0)}}{d_2^{(0)}}\right)\Omega_i. \tag{3.7a,b}$$

To simplify the $O(\lambda)$ expressions, we use (2.12b) for the time derivative of β_{ij} [$\hat{\alpha}_i$ being constant with time by (3.7a)], relationships analogous to (3.5) and (3.6), and also (3.7b). This leads to

$$(U_s^{(1)})_i = (c_1^{(0)})^{-1}\{c_1^{(1)}\hat{\alpha}_m e_{mi} + c_2^{(1)}\epsilon_{imn}\hat{\alpha}_m\Omega_n + c_3^{(1)}e_{nm}\psi_{mni} + c_4^{(1)}\epsilon_{imn}e_{ml}\theta_{ln} + c_5^{(1)}e_{im}\tau_m$$
$$+ c_6^{(1)}\Omega_m\theta_{mi} + c_7^{(1)}\epsilon_{imn}\Omega_n\tau_m\}, \tag{3.8a}$$

$$(\omega_s^{(1)})_i = -(d_2^{(0)})^{-1}\{d_1^{(1)}\hat{\alpha}_m\theta_{mi} + d_2^{(1)}e_{im}\Omega_m + d_3^{(1)}\psi_{imn}\theta_{nm}$$
$$+ d_4^{(1)}\theta_{im}\tau_m + d_5^{(1)}(U_s^{(0)})_m\theta_{mi} + d_6^{(1)}\epsilon_{imn}(U_s^{(0)})_m\tau_n\}. \tag{3.8b}$$

Equations (3.7a, b) and (3.8a, b) are the main results of this section. $(U_s^{(0)})_i$ and $(\omega_s^{(0)})_i$ are the translational and angular velocities of a sphere in an unbounded Newtonian fluid. The scalars $c_1^{(0)}$, $c_2^{(0)}$, $d_1^{(0)}$ and $d_2^{(0)}$ in (3.6) are

$$c_1^{(0)} = 6\pi, \quad c_2^{(0)} = 2\pi, \quad d_1^{(0)} = -d_2^{(0)} = 8\pi. \tag{3.9}$$

Hence, as expected, the angular velocity is equal to the local undisturbed vorticity, whereas the translational velocity shows the anticipated dependence on the undisturbed fluid velocity α_i plus an additional term related to the existence of a gradient

in the rate of strain. These well-known results are of course completely consistent with, and derivable from, Faxén's laws (Brenner 1964).

The $O(\lambda)$ non-Newtonian contributions to the translational and angular velocities of the sphere are given by (3.8*b*). To make these equations useful, we need of course to obtain $c_i^{(1)}$ and $d_i^{(1)}$. To this end, we may simply follow the reciprocal theorem outlined by Ho & Leal (1976). However, since they have already performed the migration calculations for a two-dimensional unidirectional flow, we need only a careful comparison of the general equation (3.8*a*) with their specific results to determine completely the coefficients $c_i^{(1)}$. The flow parameters for the two-dimensional case are

$$\alpha_i = \delta_{1i}\alpha, \quad \beta_{ij} = \delta_{1i}\delta_{3j}\beta, \quad \gamma_{ijk} = \delta_{1i}\delta_{3j}\delta_{3k}\gamma. \tag{3.10}$$

For the purpose of comparing (3.8*a*) term by term with the migration-velocity expression of Ho & Leal (1976), it is important to distinguish the separate contributions of ψ_{ijk}, θ_{ij} and τ_i in the original two-dimensional calculation. After some work, we finally obtain

$$c_1^{(1)} = 6\pi(1+2\epsilon_1), \quad c_2^{(1)} = 6\pi\epsilon_1, \quad c_3^{(1)} = \tfrac{5}{3}\pi(5+13\epsilon_1),$$

$$c_4^{(1)} = \tfrac{2}{9}\pi(1+11\epsilon_1), \quad c_5^{(1)} = 2\pi(2+5\epsilon_1), \quad c_6^{(1)} = 0, \quad c_7^{(1)} = 2\pi\epsilon_1. \tag{3.11}$$

To illustrate further the physical significance of the $O(\lambda)$ translational-migration expression, we substitute (3.7*a*), (3.9) and (3.11) into (3.8*a*) to obtain

$$(U_s^{(1)})_i = \tfrac{5}{18}(5+13\epsilon_1)\,e_{nm}\psi_{mni} + \tfrac{1}{27}(1+11\epsilon_1)\,\epsilon_{imn}\,e_{ml}\theta_{ln} + \tfrac{1}{3}(1+3\epsilon_1)\,e_{im}\tau_m. \tag{3.12}$$

Qualitatively, we see for the case of a neutrally buoyant rigid sphere that $(U_s^{(1)})_i$ is generated only from the interaction between the pure straining part of the linear contribution to V_i and either a strain-rate gradient or a vorticity gradient. The constant vorticity Ω_i has no effect. The accepted value for ϵ_1 is (Ho & Leal 1976)

$$-0{\cdot}6 < \epsilon_1 < -0{\cdot}5 \tag{3.13}$$

and therefore the coefficients in (3.12) are all negative. In general, it is not possible to predict the direction of motion without specific knowledge of the flow parameters e_{ij}, ψ_{ijk}, θ_{ij} and τ_i. However, we observe, after some straightforward algebra, that the absolute shear rate for the bulk flow is given by

$$e_{im}\,e_{mi} + [4e_{nm}\psi_{mni} + \tfrac{2}{3}\epsilon_{imn}\,e_{ml}\theta_{ln} + \tfrac{6}{5}e_{im}\tau_m]\,x_i + \ldots. \tag{3.14}$$

By inspection, we see then that in general each separate term in (3.12) tends to induce $O(\lambda)$ migration in the direction of decreasing absolute shear rate, in agreement with the conclusions of Ho & Leal (1976).

The above results (3.8*a*) and (3.12) are particularly important when $(U_s^{(1)})_i$ represents the first non-zero (though $O(\lambda)$) contribution to the motion of the sphere in the lateral direction. This happens when, in the Newtonian limit, the sphere translates only in the direction of the bulk translational velocity (i.e. $\epsilon_{ijk}\alpha_k\tau_j = 0$), as is always the case when the bulk flow itself is unidirectional. If it does not, then we see from (3.7*a*) that the first lateral motion still occurs at $O(\lambda)$ if $(U_s^{(1)})_i$ has a component orthogonal to the α_i, τ_i plane (i.e. $\epsilon_{ijk}\alpha_k\tau_j(U_s^{(1)})_i \neq 0$). Meanwhile the components of $(U_s^{(1)})_i$ in the α_i, τ_i plane represent only small non-Newtonian corrections to the translational motion of the particle.

3.2. *The spherical drop*

Let us now turn to the interesting case where the particle is a non-Newtonian drop with zero-shear viscosity $\tilde{\mu}_0$. To non-dimensionalize the equations of motion inside the drop, we use a characteristic pressure $\tilde{\mu}_0 G$ with all other characteristic quantities as defined in § 2. The equations become

$$\partial \tilde{S}_{ij}/\partial x_j = 0, \quad \partial \tilde{U}_i/\partial x_i = 0, \tag{3.15}$$

where

$$\tilde{S}_{ij} = -\tilde{P}\delta_{ij} + \tilde{D}_{(1)ij} + \tilde{\lambda}\tilde{D}_{(1)ik}\tilde{D}_{(1)kj} + \tilde{\lambda}\tilde{\epsilon}_1\tilde{D}_{(2)ij}. \tag{3.16}$$

The boundary conditions in this case are more complicated. In particular it will be futile to define an angular velocity of the drop analogous to (2.8). On the surface of the neutrally buoyant drop, the boundary conditions are

$$U_i = \tilde{U}_i \quad \text{(matching velocity)}, \tag{3.17a}$$

$$U_i n_i = \tilde{U}_i n_i = 0 \quad \text{(kinematic condition)}, \tag{3.17b}$$

$$S_{ij} n_j = \kappa \tilde{S}_{ij} n_j + \frac{1}{\delta}\left(\frac{1}{R_1} + \frac{1}{R_2}\right) n_i \quad \text{(matching stress)}. \tag{3.17c}$$

Here $\kappa = \tilde{\mu}_0/\mu_0$, $\delta = a\mu_0 G/\sigma$, where σ is the interfacial tension, and R_1 and R_2 are the principal radii of curvature.

In contrast to a rigid particle, it is not possible in the case of a drop to obtain general expressions for the particle motion simply by force and torque considerations alone. Since no angular velocity can be defined, a torque expression will be useless. We note, however, that the condition of no torque on the particle is already implied by (3.17*c*).

The translational migration velocity can still be obtained. By considering the force alone, we get, for the case of an *undeformed* spherical drop (i.e. $\delta = 0$),

$$(\hat{U}_s^{(0)})_i = \alpha_i + (\hat{c}_2^{(0)}/\hat{c}_1^{(0)})\tau_i, \tag{3.18}$$

$$\begin{aligned}(\hat{U}_s^{(1)})_i = (\hat{c}_1^{(0)})^{-1}\{&\hat{c}_1^{(1)}[\alpha_m - (\hat{U}_s^{(0)})_m]e_{mi} + \hat{c}_2^{(1)}\epsilon_{imn}[\alpha_m - (\hat{U}_s^{(0)})_m]\Omega_n \\ &+ \hat{c}_3^{(1)}e_{nm}\psi_{mni} + \hat{c}_4^{(1)}\epsilon_{imn}e_{ml}\theta_{ln} + \hat{c}_5^{(1)}e_{im}\tau_m + \hat{c}_6^{(1)}\Omega_m\theta_{mi} + \hat{c}_7^{(1)}\epsilon_{imn}\Omega_n\tau_m\}.\end{aligned} \tag{3.19}$$

Again, $\hat{c}_1^{(0)}$ and $\hat{c}_2^{(0)}$ in (3.18) are well known, and given by

$$\hat{c}_1^{(0)} = 2\pi\left(\frac{2+3\kappa}{1+\kappa}\right), \quad \hat{c}_2^{(0)} = 2\pi\left(\frac{\kappa}{1+\kappa}\right). \tag{3.20}$$

As for the $O(\lambda)$ expression (3.19), we get, again by comparison with a detailed reciprocal-theorem calculation (Chan & Leal 1977),

$$\begin{aligned}\hat{c}_1^{(1)} = \frac{2\pi}{5(1+\kappa)^3}&[(12+32\kappa+40\kappa^2+15\kappa^3) + \epsilon_1(22+61\kappa+80\kappa^2+30\kappa^3)] \\ &+ \eta\frac{12\pi}{5(1+\kappa)^3}[1+2\tilde{\epsilon}_1],\end{aligned} \tag{3.21a}$$

$$\hat{c}_2^{(1)} = \frac{2\pi}{(1+\kappa)^2}\epsilon_1(2+4\kappa+3\kappa^2) + \eta\frac{2\pi}{(1+\kappa)^2}\tilde{\epsilon}_1, \tag{3.21b}$$

$$\begin{aligned}\hat{c}_3^{(1)} = \frac{\pi}{63(1+\kappa)^3}&[(256+816\kappa+1238\kappa^2+525\kappa^3) \\ &+ \epsilon_1(592+2112\kappa+3254\kappa^2+1365\kappa^3)] + \eta\frac{8\pi}{21(1+\kappa)^3}[8+17\tilde{\epsilon}_1],\end{aligned} \tag{3.21c}$$

$$\hat{c}_4^{(1)} = \frac{2\pi}{27(4+\kappa)(1+\kappa)^2}[(16+60\kappa+11\kappa^2+3\kappa^3)+\epsilon_1(64+204\kappa+173\kappa^2+33\kappa^3)]+\eta\frac{4\pi}{9(4+\kappa)(1+\kappa)^2}[-5+\tilde{\epsilon}_1], \quad (3.21d)$$

$$\hat{c}_5^{(1)} = \frac{2\pi}{5(1+\kappa)^3}[(4+11\kappa+22\kappa^2+10\kappa^3)+\epsilon_1(8+28\kappa+56\kappa^2+25\kappa^3)]+\eta\frac{12\pi}{5(1+\kappa)^3}[1+2\tilde{\epsilon}_1], \quad (3.21e)$$

$$\hat{c}_6^{(1)} = 0, \quad \hat{c}_7^{(1)} = \frac{2\pi}{(1+\kappa)^2}\epsilon_1\kappa^2+\eta\frac{2\pi}{(1+\kappa)^2}\tilde{\epsilon}_1, \quad (3.21f, g)$$

where $\eta = (\tilde{\lambda}/\lambda)\kappa$. These results of course agree with those for a rigid sphere when κ approaches infinity.

If we now substitute (3.18), (3.20) and (3.21) into (3.19), an expression analogous to (3.12) can be obtained. For the sake of brevity, we shall omit the cumbersome expression which results. However, we note, in contrast to the previous case of a rigid sphere, that constant vorticity will also contribute to the migration velocity of a neutrally buoyant drop. It is also obvious, since both fluids can make 'independent' contributions to the drop motion at $O(\lambda)$ [cf. (3.21)], that migration will still occur even if only the drop fluid is non-Newtonian.

4. Discussion

In the preceding section, we have derived expressions from which the first non-Newtonian contributions to the motion of spherical particles or drops can be calculated *exactly* for a general quadratic flow of a second-order fluid. An *approximate* scheme which might appear to be an attractive alternative for unidirectional shear flows is simply to assume that the undisturbed flow is *locally* two-dimensional so that the results of Ho & Leal (1976) can be adopted directly. In this section we compare the exact and approximate predictions for the case of a rigid sphere in a pressure-driven flow through a straight tube of elliptical cross-section.

A cross-sectional view of the configuration which we consider is shown in figure 1. We assume the unidirectional flow to be in the X_1' direction, so that the undisturbed velocity profile is given by†

$$V_i' = V_{\max}\left(1-\frac{X_2'^2}{A_0^2}-\frac{X_3'^2}{B_0^2}\right)\delta_{1i}, \quad (4.1)$$

where A_0 and B_0 are the major and minor semi-axes respectively. We let $(\bar{x}_2, \bar{x}_3)$ be the components of the position vector for any material point in a co-ordinate system non-dimensionalized with the sphere radius a and fixed at the sphere centre. The sphere itself is at a radial distance D from the tube axis. Hence

$$X_2' = D\sin\theta + a\bar{x}_2, \quad X_3' = D\cos\theta + a\bar{x}_3. \quad (4.2)$$

By straightforward substitution into (4.1), we may express the undisturbed velocity V_i relative to the sphere as

$$V_i = V_{\max}\{[1-s^2(p^2\sin^2\theta+\cos^2\theta)]-2s\zeta(p^2\sin\theta\bar{x}_2+\cos\theta\bar{x}_3)-\zeta^2(p^2\bar{x}_2^2+\bar{x}_3^2)\}\delta_{1i}-(U_s)_i, \quad (4.3)$$

† This approximation can be shown to be accurate to $O(\lambda^4)$ in the retarded-motion, nth-order fluid expansion, cf. Langlois & Rivlin (1963).

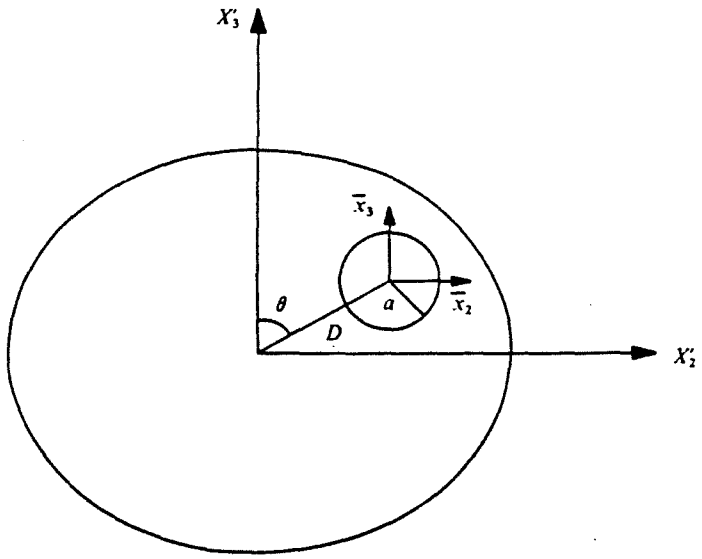

FIGURE 1. A cross-sectional view of a sphere in an elliptical tube.

where $p = B_0/A_0$, $s = D/B_0$ and $\zeta = a/B_0$. The parameter p is zero for the limiting case of two parallel plates and unity for a circular tube, whereas s is $O(1)$. The basic theory neglects wall effects and hence implicitly assumes ζ to be small.

To consider the migration velocity of the sphere, it is most convenient to use co-ordinates (x_2, x_3) defined by the orthogonal transformation

$$\left.\begin{aligned} \bar{x}_2 &= (p^4\sin^2\theta+\cos^2\theta)^{-\frac{1}{2}}(\cos\theta\, x_2+p^2\sin\theta\, x_3),\\ \bar{x}_3 &= (p^4\sin^2\theta+\cos^2\theta)^{-\frac{1}{2}}(-p^2\sin\theta\, x_2+\cos\theta\, x_3).\end{aligned}\right\} \tag{4.4}$$

The undisturbed velocity may then be expressed as

$$V_i = [\alpha+\beta x_3+\gamma(x_3^2+\phi_1 x_2 x_3+\phi_2 x_2^2)]\,\delta_{1i}-(U_s)_i, \tag{4.5}$$

where

$$\left.\begin{aligned} \alpha &= V_{\max}[1-s^2(p^2\sin^2\theta+\cos^2\theta)],\quad \beta = V_{\max}[-2s\zeta(p^4\sin^2\theta+\cos^2\theta)^{\frac{1}{2}}],\\ \gamma &= V_{\max}\left[-\frac{\zeta^2(p^6\sin^2\theta+\cos^2\theta)}{p^4\sin^2\theta+\cos^2\theta}\right]\end{aligned}\right\} \tag{4.6}$$

and

$$\phi_1 = \frac{2p^2(p^2-1)\sin\theta\cos\theta}{p^6\sin^2\theta+\cos^2\theta},\quad \phi_2 = \frac{p^2(p^2\sin^2\theta+\cos^2\theta)}{p^6\sin^2\theta+\cos^2\theta}. \tag{4.7}$$

Equation (4.5) is in the most advantageous form for our present analysis. The 'cross-stream' direction, in which uniform shearing occurs, is now denoted by x_3 and ϕ_1 and ϕ_2 are parameters which reduce to zero for the limiting case of two parallel plates.

The approximate procedure which we outlined at the beginning of this section is to assume the undisturbed flow to be *locally* two-dimensional so that the results of Ho & Leal (1976) can be adopted directly. The most natural implementation of this scheme in the present case is to take the x_1, x_3 plane as the (local) plane of shear, i.e. to neglect completely the ϕ_1 and ϕ_2 contributions to the shear gradient. The analysis of Ho & Leal (1976) then gives

$$(U_s^{(1)})_i = \beta\gamma[\tfrac{5}{9}(1+3\epsilon_1)]\,\delta_{3i}. \tag{4.8}$$

This is to be compared with the *exact* result for the migration velocity, which may be calculated using (3.12) in conjunction with (4.5)–(4.7). After some algebra, we obtain

$$(U_s^{(1)})_i = \beta\gamma \left\{ \left[\tfrac{5}{9}(1+3\epsilon_1) + \frac{\phi_2}{18}(1+\epsilon_1) \right] \delta_{3i} + \frac{\phi_1}{36}(9+29\epsilon_1)\,\delta_{2i} \right\}. \tag{4.9}$$

The above expresson, with parameters β and γ, clearly reduces in the limit as p approaches zero to that of Ho & Leal (1976) for the case of two parallel plates. Furthermore, comparison of (4.8) and (4.9) shows, in general, that the attempt to adapt *directly* the two-dimensional results of Ho & Leal to the elliptical-tube problem [i.e. use (4.8) as an approximation] leads to a predicted migration velocity which not only has an error in magnitude, but is also in a slightly incorrect direction [cf. the ϕ_1 term in (4.9)]. This difference in direction is zero for the particular case of a circular tube, but is significant when the parameter p is about 0·7. For the circular tube, we see from (4.4) that x_3 corresponds exactly to the radial direction and hence the sphere migrates in a straight line towards the tube centre. The difference in magnitude between (4.8) and (4.9) is then less than 10 %, assuming $\epsilon_1 = -0{\cdot}55$ [cf. (3.13)]. For the elliptical tube, however, the sphere usually describes a curved trajectory in the x_2', x_3' plane which, at any instant, depends on its radial distance D and *orientation* relative to the tube centre. (On the major and minor axes, the trajectories will be straight lines.) Intuitively, it is reasonable to assume that the sphere will move *towards* the centre, but we shall not attempt to provide a rigorous proof here.

The authors thank Dr H. Brenner for two very interesting seminars and subsequent discussions, which inspired this paper. This work was supported by NSF Grant ENG74-17590.

REFERENCES

Brenner, H. 1964 *Chem. Engng Sci.* **19**, 703.

Brunn, P. 1976 *Rheol. Acta* **15**, 163.

Brunn, P. 1977 *J. Fluid Mech.* **82**, 529.

Caswell, B. & Schwarz, W. H. 1962 *J. Fluid Mech.* **13**, 417.

Chan, P. C.-H. & Leal, L. G. 1977 The motion of a deformable drop in a second-order fluid. In preparation.

Coope, J. A. R., Snider, R. F. & McCourt, F. R. 1965 *J. Chem. Phys.* **43**, 2269.

Fredrickson, A. G. 1964 *Principles and Applications of Rheology*. Prentice-Hall.

Hinch, E. J. 1972 *J. Fluid Mech.* **54**, 423.

Ho, B. P. & Leal, L. G. 1976 *J. Fluid Mech.* **76**, 783.

Langlois, W. E. & Rivlin, R. S. 1963 *Rend. Mat. Appl. Univ. Roma, Inst. Naz. Alta Mat.* **22**, 169.

AN EXPERIMENTAL STUDY OF DROP MIGRATION IN SHEAR FLOW BETWEEN CONCENTRIC CYLINDERS

Paul C.-H. Chan† and L. G. Leal
Department of Chemical Engineering
California Institute of Technology

†Present address: Department of Chemical Engineering, University of Rochester, Rochester, N.Y. 14627.

Abstract

The phenomenon of migration of liquid drops in Couette flow between concentric cylinders due to non-Newtonian fluid properties and shape deformation has been studied experimentally. The results agree very well with the theory of Chan and Leal, which included the effect of hydrodynamic interaction with the bounding walls, and that of velocity profile curvature in a Couette device. Significant observations that were not reported in previous studies include the migration of a deformable Newtonian drop to an equilibrium position between the centerline and the inner rotor, and the competition between normal stresses and shape deformation effects for the case of a Newtonian drop in a non-Newtonian fluid.

Introduction

Previous investigations conducted in our research group have examined the dynamics of particle migration in shearing flows. In our recent paper (1), the roles of non-Newtonian rheology and shape deformation on the motion of a fluid drop were examined, based upon the assumptions of second-order fluid behavior, and weak deformation. It was found that the qualitative effects of these two mechanisms depend on the nature of the primary flow. For Poiseuille flow in a pipe, both contributions were predicted to produce particle motion towards the centerline. For planar Poiseuille flow, the qualitative effect of non-Newtonian fluid properties was predicted to remain the same, whereas that of drop deformation was found to depend on the value of the viscosity ratio between the two phases with the result that the drop might migrate either towards or away from the walls. For a Couette flow, the migration mechanism is even more complicated. In this case, both the non-Newtonian rheology and shape deformation effects are found to include two terms: one from hydrodynamic interaction between the particle and the walls, and a second due to the presence of velocity profile curvature in the Couette device. For non-Newtonian rheology alone, the net effect of these terms is predicted to be particle motion towards an equilibrium position between the centerline and the outer cylinder. On the other hand, the two contributions from drop deformation are predicted to result in an equilibrium position for the particle between the centerline and the inner rotor.

Although our theory for Poiseuille flows agrees very well with exist-

ing experimental observations (2,3), the predictions for Couette flow have yet to be verified. In particular, the prediction that profile curvature will tend to cause a deforming Newtonian drop in a Newtonian suspending fluid to migrate inwards (i.e. towards the inner rotor) has not been demonstrated experimentally. In fact, inward migration in Couette flow has never even been predicted in any previous theory, regardless of the mechanism of migration that was considered, and has been observed in experiments only for rigid spheres in a 'pseudoplastic' fluid. Since our prediction corresponds to drop motion towards the region of largest shape deformation, whereas all existing experimental observations show migration towards the region of smallest shape deformation, we feel that it is of fundamental interest to experimentally demonstrate the existence of inward migration for a deformable drop in a Couette flow.

In addition, our earlier theory also considered the effect of migration of a spherical drop due to non-Newtonian rheology of the suspending fluid or the drop, or both. It was concluded that the drop would migrate in any of these cases to an equilibrium position between the outer cylinder and the centerline. The prediction that non-Newtonian rheology of the drop fluid alone would lead to particle migration is new. The predicted migration of a spherical Newtonian drop in a viscoelastic suspending fluid is also new, though the limiting case of a rigid spherical particle has been considered by several authors (4 - 6). However, in this limiting case, the theory is in apparent disagreement with existing experimental observations (7).

Finally, for situations which include both non-Newtonian rheology and drop shape deformation, our theory for a slightly non-Newtonian suspending fluid appears to be in qualitative agreement with the experiments by Gauthier, Goldsmith and Mason (8) who studied Newtonian drops in a viscoelastic suspending fluid. However, their experiments involved only one system of fluids, and in particular considered only large drop viscosities where the contribution of deformation to migration is always small compared to the non-Newtonian contribution. In addition, there have so far been no experiments on migration which involve non-Newtonian drops, and in spite of the fact that the contribution from non-Newtonian rheology is predicted to be numerically small in this case compared to that due to shape deformation, this is another area of interest for experimental study.

In the present paper, we report on experiments that were performed in our laboratory for the purpose of considering a number of these problem areas which have not previously been studied experimentally. The objective of these experiments was both to test the predictions of Chan and Leal under conditions where the theory should be applicable, and to determine the range of applicability of the theory by extension to the domains of stronger viscoelasticity and deformation. For each system of fluids, we varied the drop sizes and gap widths, as well as the shear rates. A general description of the experiments is given in the next section, followed by the results and discussions.

Experimental Part

1. Description of the Apparatus

The Couette device used in the experiments is illustrated in Fig. 1. It consisted of a 25 cm section of precision-bore glass cylinder (I.D.

12.0 cm) fitted onto an aluminum base and sealed with commercial silicone sealant RTV. A set of four solid aluminum cylinders (radii 1.27 cm, 2.54 cm, 3.81 cm, 4.60 cm respectively) were prepared as inner rotors. With one of these embedded in the aluminum base by means of a bearing, a plexiglass lid was fitted onto the top. By precisely matching each individual component, we were able to achieve accurate alignment of the apparatus while at the same time allowing it to be easily dismantled for maintenance or change of inner rotors. Only the inner cylinder was designed to rotate; this was accomplished by directly coupling it to a variable-speed motor and control system, as illustrated, which was capable of rotation at a constant speed (without fluctuations) at very low rates of revolution.

To set up the experiment, a 1 cm layer of mercury was poured onto the bottom of the tank, which was then filled with the suspending fluid, leaving only a small air gap between the top of the fluid and the lid on the concentric cylinder apparatus. The mercury acted as a nearly inviscid layer and was used in order to avoid secondary flows and to minimize any axial variations in the primary flow. The drops were injected through a slit in the top of the apparatus using a 4 in. long hypodermic needle (17 gague) that was fed from a precision micrometer syringe. The drop sizes in our experiments varied from 5 μl to 50 μl. It was important that the drop sizes be measured accurately, since the migration velocity varies approximately linearly with the volume of the drop. The micrometer syringe which we used was accurate to 0.1 μl. However, an additional source of error was due to fluid loss when the tip of the syringe was actually pulled

away from the drop. By direct observation of the radius of the residual droplets compared to that of the main drop, we estimated that the resulting uncertainty in the drop volume was always less than five percent.

At the end of each experiment, the fluid drop was allowed to settle to the bottom of the apparatus (or rise to the top if it was lighter than the suspending fluid), where it would not affect other runs. Although we had attempted to find fluid systems with closely matched densities, a small density difference (not larger than 1/200 gm cm^{-3}) almost always existed, and hence the drop was often found to settle (or rise) out of the test region within approximately three hours.* In those few situations where the densities were 'identical', the drops had to be removed manually by suction using a large syringe. Thus, in all cases, the suspending fluid could be reused a number of times before it was replaced.

It should be noted that our apparatus was designed, for simplicity, without a constant temperature bath. However, the fluctuations in temperature are always small in our laboratory. In addition, viscous dissipation was clearly negligible at the low shear rates used in our experiments. Thus, the lack of a temperature control device in our apparatus is not believed to significantly affect the measured results.

Observation of the position of the drop during the experiment was

*It may be noted, however, that these small density differences are not significant insofar as the migration phenomenon is concerned, and the fluid drop can still be considered as neutrally buoyant for the purpose of comparing experimental results for migration with theoretical predictions. Obviously, this observation is correct only if the sedimentation velocity is small compared to the characteristic velocity, Ga, of the primary flow, as was always the case in our experiments.

achieved using a mirror inclined at 45^{o} and positioned directly above the gap between the concentric cylinders. The plane of the mirror was parallel to a radial axis of the Couette device. Measurements were made by looking horizontally into the mirror using a cathetometer as a telescopic device. The cathetometer was mounted on a platform which could be moved in the radial direction, and thus we could observe the migration of the drop by adjusting the position of the cathetometer each time the drop came into view. The position of its center was then measured using a linear scale placed directly on the plexiglass top of the apparatus. The margin of error for this method was approximately 0.02 cm. For comparison, we note that the drop usually travelled a radial distance of no less than 0.5 cm in the course of a typical run.

2. Materials

Previous experiments by Mason and his co-workers (2,3,7-9) on the migration of deformable drops were performed using various systems of drop and suspending fluids. In our case, however, the selection of fluids was considerably more difficult because the drops used in our experiments were generally larger (as we shall see in the following subsection, this was necessary to compensate for the wider gaps between the concentric cylinders when the smaller of the inner rotors was employed), and hence the densities of the fluids had to be more closely matched to minimize the velocity of drop sedimentation. As shown in Table I, each system consisted of an aqueous phase and an immiscible oil phase. It should be noted that we used Ucon oil LB-1715 throughout as our Newtonian suspending fluid because of its desirable physical properties and easy availability.

Separan AP-30 (polyacrylamide manufactured by Dow Chemical Co.) dissolved in water was chosen as the non-Newtonian suspending fluid in order to facilitate comparisons with the previous results by Gauthier, Goldsmith and Mason (8), who used Cyanamer P-250 (another brand of PAA).

To compare our experimental observations with theoretical predictions, it was necessary to estimate the interfacial tension and fluid viscosities for each system listed in Table I. The interfacial tension was obtained by determining the shape of the drop for one run at low shear rates, and calculating the interfacial tension using the formula for drop shape due to Taylor (10). For this purpose, a camera was used to record the experiment on videotape, after which the lengths of the drop's major and minor axes were measured. The velocity gradient in the Couette device at the radial position of the drop center, R_o, was calculated from the formula

$$\frac{\Omega_1 R_1^2}{R_2^2 - R_1^2}\left(1 \mp \frac{R_2^2}{R_o^2}\right)$$

for a device with appreciable curvature (1).† Although this procedure was somewhat inaccurate, as we shall discuss in more detail below, the fluid systems used in our experiments all had closely matched densities, and thus 'conventional' methods of measuring interfacial tension could not be applied directly. In particular, both the pendant drop and spinning drop

†For the remainder of this paper, we adopt the same notation as used in (1).

methods involve expressions for the interfacial tension which are linear in the density difference between the two fluids, and will therefore not give accurate results if the density difference is extremely small. The du Nouy ring method cannot be used for the simple reason that a 'good' interface cannot often be formed between two fluids with nearly equal densities. In these cases, the interfacial tension must be obtained by the tedious procedure of extrapolating from measurements on fluids with nonzero density differences, as shown, for example, by the recent work of Kovitz and Yannimaras (11). In contrast, the calculation of interfacial tension from a measured drop shape is obviously much simpler. However, the procedure is, at best, an approximate technique since Taylor's theory assumed linear shear flow and Newtonian rheology, whereas profile curvature and non-Newtonian fluid properties were both present in our experiments to determine interfacial tension. As a partial justification of its use here, it may be noted that Taylor's expression suffices as a valid first approximation for the drop shape, provided that the particle size-to-gap width ratio is small, and the viscoelastic effect is weak (1). Both conditions were satisfied in the experiments which were used to determine the interfacial tension, and the value of the deformation parameter $\delta \equiv a\mu_0 G/\sigma$ was always less than 0.2. In addition, it was shown by Gauthier, Goldsmith and Mason (8) that the discrepancy between theory and experiment for the deformation of a slightly non-Newtonian drop (1.5% polyacrylamide in water) in a linear shear flow was only approximately 10% for values of the deformation parameter δ up to 0.2, in qualitative agreement with our predictions. Finally, the results obtained here for systems 3 and 5 are consistent with the values obtained

independently in our laboratory using the du Nouy tensiometer for a similar system of 1% Separan AP-30 and Ucon Oil LB-135 (σ = 5 dyne cm^{-1}), which has a nonzero density difference (12). Thus, although it is difficult to quantify the accuracy of interfacial tension values listed in Table I, we believe that they are always within at least 15% of the exact value.

The viscosity of each fluid was measured using a Cannon-Fenske viscometer. This device is clearly adequate for Newtonian materials; on the other hand, for fluids with shear-dependent viscosities, there may be some doubt as to the correct interpretation of the measurements. We estimate that the shear rate that applies for a typical Cannon-Fenske viscometer is always less than 0.1 s^{-1}, and hence most measured values may be taken as the viscosities of the fluids in the limit of zero shear.

The theory of Chan and Leal (1) assumed that the viscoelastic fluids could be modelled as second-order fluids. In our case, there are no reported measurements in the literature on the rheological properties of aqueous Carbopol to test the applicability of this assumption. However, for 1% Separan AP-30, it appears (8, 13, 14) that the viscosity actually reaches a constant value at a shear rate of 1 s^{-1} or less, which was always satisfied in our experiments. In addition, rod climbing experiments performed by Beavers and Joseph (15) for 1.5% Cyanamer P-250 in a glycerine-water mixture were well correlated by their second-order fluid theory for rotation rates of less than 10 s^{-1}. Thus, it appears that 1% Separan AP-30 should behave as a second-order fluid under the conditions of our experiments. However, as we shall show later, this assumption appears to break down in the vicinity of the walls.

The zero-shear viscosities of Separan AP-30 solutions measured in

this study (listed on Table I) were lower than those published by Leal, Skoog and Acrivos (13), and by Blanks, Park, Patel and Hawley (14), but 'agreed' with those of Gauthier, Goldsmith and Mason (8). In addition all three batches of solutions that were used had different viscosities, depending on the degree of agitation during mixing. However, it is well known that the rheological parameters of polymer solutions may change if the modes of preparation are different. Thus, the observed variations are not surprising, and the material properties of all three batches of Separan AP-30 in our experiments are qualitatively consistent with one another.

3. Conditions of the Experiments

One of the objectives of our present investigation was to observe the qualitative effect of velocity profile curvature on the migration of a fluid drop in Couette flow. Thus, for each system listed in Table I, we performed migration experiments using several different inner cylinders. When the largest rotor (R_1 = 4.60 cm) was used, the fluid's motion in the Couette apparatus could be approximated as a linear shear flow, i.e. the effect of profile curvature, though nonzero, was small. With decreasing rotor size, curvature became increasingly important. In fact, when the smallest rotor (R_1 = 1.27 cm) was used, the shear rate varied by a factor of ten across the gap, with the result that a drop which was nearly spherical when released near the outer wall would be increasingly deformed if its migration was toward the inner wall. Indeed, with too high rotor speeds, and an inward direction of migration, some drops even broke up before reaching their equilibrium position. We did not measure the value of the deformation parameter δ at which breakup occurred for each different system listed in Table I, but for the case of

a non-Newtonian drop in a Newtonian suspending fluid, it was estimated that the critical value of δ was approximately 0.6. This agrees with the observations of Gauthier, Goldsmith and Mason (8) for a moderate viscosity ratio $\kappa \left(= \frac{\tilde{\mu}_0}{\mu_0}\right)$, but it is generally agreed that the critical value will be much higher if κ is quite large or quite small. For our systems, when breakup occurred, the drops usually deformed into long threads which extended around the inner rotor, and then separated into smaller droplets when the apparatus was stopped.

In the theory of Chan and Leal (1), both the deformation parameter δ and the non-Newtonian parameters λ and $\tilde{\lambda}$ were assumed to be much less than unity. For each particular experiment, we could calculate directly the value of δ. However, we did not measure the normal stress coefficient ϕ_3; rather, λ (or $\tilde{\lambda}$) was estimated by comparing the equilibrium positions predicted with those actually obtained (cf. Section 2 in 'Results and Discussion'). In practice, the inferred magnitudes of λ (or $\tilde{\lambda}$) were often of order unity, though the corresponding theory is only valid for $\lambda << 1$. One main reason for relaxing the conditions of small δ, λ and $\tilde{\lambda}$ in the experiments was that they had to be carried out in a finite period of time, before secondary effects (e.g. drop sedimentation, partial solubility between the two fluid phases) became important. In addition, it was desired to test the usefulness of our theory beyond the asymptotic regime of $\delta \to 0$, $\lambda \to 0$, $\tilde{\lambda} \to 0$ for which it is strictly valid. The values of δ, λ and $\tilde{\lambda}$ evaluated at the centerline of the Couette device for each experiment are listed in the captions to the figures.

In addition to δ and λ, the size of the drop must also be small relative to the width of the gap in order for the theory to be applicable.

Using the micrometer syringe, it was not possible to inject drops that were smaller than 5 μl in volume. Thus, the drop radius was always larger than 0.1 cm. When the largest rotor was used, the drop size to gap width ratio was approximately 0.1. For a larger gap, the size of the drops, as well as the angular velocity of the rotor, was also increased so that the migration velocity would remain finite, though in no case did the drop radius-to-gap width ratio ever exceed 0.1.

It is clear that flow instabilities (e.g. Taylor vortices) must not be allowed to occur in the Couette apparatus. For systems 1-3 in Table I where the suspending fluid was Newtonian (Ucon oil), the maximum Taylor number was approximately 30, well below the established critical value of 3390. When the suspending fluid was Separan AP-30, the effect of viscoelasticity on stability must be considered. In these experiments, inertial effects were negligible compared to non-Newtonian fluid rheology, and the relevant stability analysis is that of Giesekus (16) for a viscoelastic fluid. Since the non-Newtonian parameter λ was always below its predicted critical value of approximately 3.5, no instability should be expected and, indeed, no evidence of an instability was observed.

Results and Discussion

1. A Newtonian Drop in a Newtonian Fluid

Previous experiments on the migration of a Newtonian drop suspended in a Couette flow of a Newtonian fluid were reported by Karnis and Mason

(9) for water drops in silicone oil. For a narrow gap, the drop was observed to migrate to an equilibrium position which was very close to the centerline of the Couette device. However, no equilibrium positions were reported for larger gap widths. Since the theory of Chan and Leal (1) predicts that profile curvature is an important factor in determining the equilibrium position of a drop in Couette flow, we have repeated the Karnis and Mason experiments using water drops suspended in Ucon oil LB-1715 (which had the advantage over the previous systems that the densities were more closely matched) in order to study carefully the effect of profile curvature by systematically altering the size of the inner rotor, while holding the size of the outer cylinder fixed.

In all cases, the drops were observed to migrate towards an equilibrium position which was between the centerline and the inner cylinder. Furthermore, the equilibrium position was near the centerline only for the case of a 'narrow gap' Couette device. As the profile curvature increased, the equilibrium position moved closer to the inner cylinder. These observations are in qualitative agreement with the predictions of our theory. In Fig. 2, we plot the experimentally measured and theoretically predicted trajectories of the drops for each rotor size. The solid lines were obtained by summing the wall reflexion and profile curvature contributions, and then integrating to give [cf. (8.4) and (8.5) of Chan and Leal (1)],

$$T = \frac{d\sigma}{\mu_o} \int_{s_o}^{s} \frac{ds}{Z(s)} \qquad [1]$$

where

$$Z(s) = \frac{\Omega_1^2 R_1^4 R_2^4}{(R_2^2 - R_1^2)^2} \left\{ \frac{a^4}{d^2} \left(\frac{1}{R_o^2} + \frac{1}{R_2^2} \right)^2 \frac{3(16 + 19\kappa)(54 + 97\kappa + 54\kappa^2)}{4480(1 + \kappa)^3} \right.$$

$$\left. \left[\frac{1}{s^2} - \frac{\Gamma}{(1 - s)^2} + 2(1 - 2s) \right] - \frac{2(4 + 61\kappa + 85\kappa^2 + 25\kappa^3)}{7(2 + 3\kappa)(1 + \kappa)^2} \frac{a^3}{R_o^5} \right\} \qquad [2]$$

The material parameters σ, μ_o, κ were already listed in Table I, whereas a, R_1, R_2, R_o, d were all measurable for any particular Couette flow geometry. Thus, for each migration experiment, we could predict the trajectory of the drop after numerically integrating [1]. Under ideal conditions (asymptotically small drop deformation and velocity profile curvature) when our theory is expected to be valid, the accuracy of the prediction depends mainly on the accuracies to which the interfacial tension σ and the drop volume can be measured. Thus, for each predicted trajectory, the value of T as a function of position is accurate to within 20%. In addition, the actual measurement of (dimensionless) drop position s may have an error of $\pm$ 0.02.

We have plotted the measured and predicted trajectory for each migration experiment in Figs. 2a-2d. The corresponding value of the deformation parameter, δ, is listed in the captions. For cases 2a and 2b where the gap of the Couette device is small, the agreement between theory and experiment is extremely good, even though δ is as large as 0.684. We conclude, from this, that our deformation theory for a quadratic shear flow between two parallel plane walls is valid at least up to $\delta \sim 0.7$. On the other hand, when

smaller inner rotors were used (cases 2c and 2d), the theory begins to break down, as expected, even for smaller values of δ. Clearly, in these cases, the wall reflexions procedure for two parallel plane walls is no longer valid, in spite of the fact that the qualitative agreement between theory and experiment is still quite good. Furthermore, it should be noted that the predicted inward migration rate for these cases is always smaller than the experimentally measured values. This discrepancy may be attributed in part to the fact that the contribution to migration from hydrodynamic interaction with the inner rotor is overestimated when the radius of the inner rotor is small, since our calculation is based on two parallel plane walls. In addition, it seems likely that the effect of the outer cylinder will actually be larger than that predicted for a plane wall located at the same distance.

2. A Viscoelastic Drop in a Newtonian Fluid

There have been no previous experiments on the migration of a viscoelastic drop suspended in Couette flow of a Newtonian fluid. For the present investigation, we chose two aqueous polymer solutions as drops and Ucon oil LB-1715 as the suspending phase (Systems 2 and 3 in Table I). The migration effects for these systems were expected to result from a combination of drop deformation and non-Newtonian rheology.

Qualitatively, it was found that there were no changes in the behavior of the drops from the previous Newtonian case where the only migration mechanism is shape deformation, i.e. they migrated to an equilibrium position which was between the centerline and the inner cylinder.

However, by comparing the experimentally measured equilibrium positions with those predicted by the Newtonian deformation theory, it is evident that the non-Newtonian properties of the drop fluid were playing a non-trivial role in the migration process. The predicted magnitude of this contribution for a second-order fluid is given by (5.10) and (5.20) of Chan and Leal (1). If we sum the separate deformation and non-Newtonian terms (letting $\tilde{\varepsilon}_1 \simeq -0.60$; our results are not sensitive to the exact magnitude of $\tilde{\varepsilon}_1$, as long as it is within the generally accepted range of -0.5 to -0.6 as discussed in Leal (17)), and integrate, we again obtain [1], where in this case

$$Z(s) = \frac{\Omega_1^2 R_1^4 R_2^4}{(R_2^2 - R_1^2)^2}\left\{\frac{a^4}{d^2}\left(\frac{1}{R_o^2} + \frac{1}{R_2^2}\right)^2 \frac{3}{4480(1+\kappa)^3}\left[(16 + 19\kappa)(54 + 97\kappa + 54\kappa^2)\right.\right.$$
$$\left. + 8(33.8 + 63\kappa)\frac{\tilde{\phi}_3^{\sigma}}{a\mu_o^2}\right]\left[\frac{1}{s^2} - \frac{1}{(1-s)^2} + 2(1-2s)\right] - \frac{2}{21(2+3\kappa)(1+\kappa)^2}$$
$$\left.\cdot\left[3(4 + 61\kappa + 85\kappa^2 + 25\kappa^3) - 8.8\frac{\tilde{\phi}_3^{\sigma}}{a\mu_o^2}\right]\frac{a^3}{R_o^5}\right\}. \qquad [3]$$

In the above expression, the first term is due to the presence of the bounding walls, and will always contribute to migration towards the center of the Couette device. The second term comes from profile curvature, and has two contributions which tend to oppose each other, with the net effect

depending on the parameter $\frac{\tilde{\phi}_3\sigma}{a\mu_o^2}$ $\left(= \frac{\kappa\,\tilde{\lambda}}{\delta}\right)$, which measures the relative importance of deformation and non-Newtonian effects. Under 'normal' conditions, it can be shown that the deformation term will always dominate numerically. Thus, despite the fact that the parameter $\frac{\tilde{\phi}_3\sigma}{a\mu_o^2}$ itself was quite large in our experiments (cf. values of δ and $\tilde{\lambda}$ in Figs. 3 and 4), the equilibrium position is again predicted to be between the centerline and the inner cylinder, in agreement with the experimental observations.

In order to predict the detailed trajectory of the drop, we still need a quantitative estimate for the parameter $\frac{\tilde{\phi}_3\sigma}{\mu_o^2}$. This may be accomplished by measuring $\tilde{\phi}_3$ directly for any particular non-Newtonian fluid that is used (e.g. using a Weissenberg rheogoniometer or by means of rod climbing experiments). However, an alternate method which we have used here is to observe that the function Z(s) is zero when the drop is at its equilibrium position, so that $\tilde{\phi}_3$ may be estimated indirectly from [3], all other variables being measurable experimentally. Although this means that the predicted and measured equilibrium positions are forced to coincide, the theory is still subjected to two reasonably stringent tests by this procedure. First, the inferred values of $\tilde{\phi}_3$ can be compared with existing literature estimates obtained via normal stress or other measurements. Second, the measured trajectories can be compared with [1] and [3]. The fact that the final equilibrium position is forced to coincide does not insure that the rest of the trajectory will be correctly predicted unless the theory is, in fact, correct. For 1% Separan AP-30 solution (batch a), we find that a value of $\tilde{\phi}_3$ equal to 54 dyne sec^2 cm^{-2} provides a good fit to the experimental

data for the present case of a viscoelastic drop in a Newtonian fluid, as well as for the next case of a Newtonian drop in a viscoelastic fluid. This value is consistant with existing estimates of the normal stress coefficient of Separan, as we shall show in the next section. In addition, the fact that one value of $\tilde{\phi}_3$ can be used to match the trajectories of both sets of experiments is an extremely stron confirmation of the theory and of its applicability under conditions of the present experiments. The predicted trajectories for a Separan drop in Ucon oil, using $\tilde{\phi}_3 = 54$ dyne sec^2 cm^{-2}, are compared with experimentally observed ones in Fig. 3. With the exception of two cases in (3b) and (3c), the fit between data and predictions is excellent. In the latter two cases, the experimentally measured inward migration rates were <u>smaller</u> than our theoretical predictions, in contrast to our observations in the Newtonian-Newtonian problems of the previous subsection. Hence, this discrepancy must clearly be attributed to non-Newtonian effects alone. In addition, it should be noted that the disagreement between theory and experiment is large only when a wide gap Couette device is used, <u>and</u> when the shear rate (hence the value of $\tilde{\lambda}$) is high. Since the wall reflexion procedure in our theory depends critically on the assumption of two parallel plane walls, it may be hypothesized that the predicted wall contribution to the migration of a non-Newtonian drop in a wide gap Couette device is suspect (and, in fact, always <u>overestimates</u> the wall effect) when $\tilde{\lambda}$ is larger than 1.5. This hypothesis will be discussed in more detail in the final section of this paper.

For 0.1% Carbopol in water, the procedures outlined above yield an estimate for $\frac{\tilde{\phi}_3 \sigma}{\mu_o^2}$ of 1.4 cm, in which case $\tilde{\phi}_3$ is approximately 22 dyne sec^2 cm^{-2}.

This is certainly a reasonable value of $\tilde{\phi}_3$ for a dilute polymer solution, although there are no previous experiments that we could locate on the rheological properties of Carbopol in water. The predicted trajectories with $\tilde{\phi}_3$ = 22 dyne sec^2 cm^{-2} are plotted together with the observed trajectories in Fig. 4. From the apparent consistency between theory and experiment, it appears that our second-order theory for drop migration is applicable even though there are no definitive indications (from rheological measurements) that 0.1% Carbopol in water should obey the second-order fluid model at the shear rates used in the experiments. Once again, the discrepancy between theory and experiment becomes larger when the shear rate and curvature are increased, which is consistent with our previous observations.

3. A Newtonian Drop in a Viscoelastic Fluid

To supplement the previous work by Gauthier, Goldsmith and Mason (8) on drop migration in Couette flow of a non-Newtonian fluid, we have performed additional experiments using fluids of different viscosities and a systematic variation in the size of the inner rotor. The predicted trajectories of the drop are again obtained as before. In this case, for $\varepsilon_1 \simeq -0.6$, we have

$$Z(s) = \frac{\Omega_1^2 R_1^4 R_2^4}{(R_2^2 - R_1^2)^2} \left\{ \frac{a^4}{d^2} \left(\frac{1}{R_o^2} + \frac{1}{R_2^2} \right)^2 \frac{1}{4480(1+\kappa)^3} \left[3(16 + 19\kappa)(54 + 97\kappa + 54\kappa^2) \right.\right.$$

$$\left. + 2(324.8 + 1234.8\kappa + 1700.4\kappa^2 + 866\kappa^3) \frac{\phi_3 \sigma}{a\mu_o^2} \right] \left[\frac{1}{s^2} - \frac{1}{(1-s)^2} + 2(1 - 2s) \right]$$

$$- \frac{1}{63(2 + 3\kappa)(1 + \kappa)^2} \left[18(4 + 61\kappa + 85\kappa^2 + 25\kappa^3) \right.$$

$$\left.\left. - (99.2 + 451.2\kappa + 714.4\kappa^2 + 294\kappa^3) \frac{\phi_3 \sigma}{a\mu_o^2} \right] \frac{a^3}{R_o^5} \right\} . \qquad [4]$$

In contrast to our conclusions in the previous two subsections where the contribution due to drop deformation is numerically dominant, in the present systems the effects of deformation and non-Newtonian rheology are comparable in magnitude, and hence the equilibrium position of the drop (whether it is closer to the inner or outer wall) will critically depend on the material properties of the fluids. In fact, for a given viscosity ratio κ, we may calculate a value of the parameter $\frac{\phi_3\sigma}{a\mu_o^2}$ at which the second term in [4] changes sign, with the result that the equilibrium position of the drop moves from one side of the centerline to the other. These critical values for $\frac{\phi_3\sigma}{a\mu_o^2}$ are listed as a function of κ in Table 2.

Our experimental results were in fact in good agreement with the predicted trajectories. Indeed, by comparing the measured and predicted trajectories, we estimate that ϕ_3 is approximately 60 dyne sec^2 cm^{-2} for batch b of 1% Separan AP-30 in water, and 68 dyne sec^2 cm^{-2} for batch c. These estimates, together with the value of 54 dyne sec^2 cm^{-2} for batch a, which is used here as well as in the last subsection, appear to be self-consistent since the intrinsic time scales of <u>all three</u> batches (i.e. $\frac{\phi_3}{\mu_o}$) are then approximately 2 sec. Furthermore, they are also consistent with the measurements by Bartram, Goldsmith and Mason (<u>18</u>) for 2.5% PAA in water [cf. Leal (<u>17</u>)], and with the calculations by Chan and Leal (<u>1</u>) for the 4% solution. The experimental data and predicted trajectories for Systems 4 and 5 are shown in Figs. 5 and 6.

It should be noted, for some situations in which a silicone oil drop (System 4) migrated outwards at the start of the experiment, that it would <u>reverse</u> its direction of motion after approximately half an hour. We

attribute this occurence to a change in the relative magnitudes of the deformation and non-Newtonian contributions, which is reflected in a decrease of the parameter $\frac{\phi_3\sigma}{\mu_0^2}$. Clearly, a change in the temperature within the Couette device could cause this phenomenon; however, viscous dissipation is negligible in the present experiments. A much more plausible explanation, based upon observations of the shape of the drop at different time intervals, is that the interfacial tension between Separan AP-30 and silicone oil 510 fluid is gradually decreasing during the experiments. Most probably, this change in interfacial tension is due to a very slight solubility of polyacrylamide molecules in the silicone oil. Since the relative magnitudes of the deformation and non-Newtownian rheology contributions to the migration velocity are closely competitive in the present situation, a slight decrease in the value of the interfacial tension could easily cause a 'reversal' in the direction of migration. Estimates of the interfacial tension from photographs of the drop shape at the point of reversal indicated that the decrease in interfacial tension was as large as 20% before reversal occurred. It may be noted that a much larger decrease (threefold) had been reported by Grace (19) for another presumably immiscible system. In any case, we have omitted the portions of the trajectories where reversal occurred from Fig. 5.

It may appear at first that our results in this subsection are in qualitative disagreement with those of Gauthier, Goldsmith and Mason (8), who for a similar system always observed equilibrium positions which were between the centerline and the outer cylinder, with no reversal in the direction of particle motion. However, we note that the radii of the

drops in the previous experiments were smaller than ours by a factor of three, plus the viscosity of the suspending fluid (1.5% PAA in water) was also considerably lower. In their case, then, the contribution due to drop shape deformation was clearly minimized, as evidenced by a larger value of $\frac{\phi_3\sigma}{a\mu_o^2}$. Thus, Mason's experiments were carried out in a regime where non-Newtonian rheology was dominant, so that the equilibrium position of the drop was between the centerline and the outer wall, as expected. Our experiments, on the other hand, included both non-Newtonian rheology and drop shape deformation effects of comparable magnitude (cf. the values of δ and λ listed in the captions to Figs. 5 and 6), and hence the equilibrium positions could be on either side of the centerline. This observation may perhaps be best illustrated by considering specifically Figs. 5a and 6c, where the experimental conditions were identical except for the viscosity ratios $\frac{\tilde{\mu}_o}{\mu_o}$ and the values of the parameter $\frac{\phi_3\sigma}{a\mu_o^2}$. For silicone oil 510 fluid ($\tilde{\mu}_o$ = 1.1p), $\frac{\phi_3\sigma}{a\mu_o^2}$ equals 1.92, which is greater than its critical value of 0.98, and hence the equilibrium position is closer to the outer cylinder, as expected. The inverse was true for Ucon oil LB-1715. Thus, in spite of the fact that the observed equilibrium positions for our systems are different from Mason's, the results are not contradictory as might first appear to be the case. In fact, both Mason's results and the present results are qualitatively consistent with the predictions of Chan and Leal (1). The case of dominant drop deformation was considered in the previous two subsections.

Concluding Comments

We have performed experiments on drop migration in Couette flow which

have been compared with the theoretical predictions of Chan and Leal (1). For the case of a deformable Newtonian drop in a Newtonian fluid, the equilibrium position was always between the centerline and the inner wall. If non-Newtonian rheology was then included, the equilibrium position moved outwards. The effect of velocity profile curvature was to determine quantitatively how this would occur, i.e. for larger profile curvature, the equilibrium position was further away from the centerline. Of course, the rate of migration depends on the numerical values of all the material parameters of the fluids in any system that is used.

In spite of the qualitative success of the drop migration theory, one important difficulty remains to be resolved, namely the fact that the wall contribution to non-Newtonian migration appears to be always overestimated. This discrepancy manifests itself most distinctly in the limiting case of migration of a rigid sphere in a viscoelastic fluid, where Karnis and Mason (7) observed migration to the outer wall for a sphere in 4% PAA in water, whereas our theory predicts an equilibrium position between the outer wall and the centerline. Recent experiments performed in our laboratory using polystyrene spheres and 1% Separan AP-30 showed the same behavior as the earlier results of Karnis and Mason. Another apparent manifestation of the same difficulty is the apparent discrepancy between theory and experiment for the migration rates of drops when λ (or $\tilde{\lambda}$) is not vanishingly small, as we noted earlier in this paper. Indeed, careful examination of the results of Gauthier, Goldsmith and Mason (8) also shows the same problem. One plausible explanation of the apparent difficulty with the theory for estimating wall effects in a viscoelastic fluid is

that the influence of viscoelasticity is greatly increased near the walls, so that the second-order fluid expansion may not be expected to be valid in that neighborhood even though the flow is 'slow' in the domain far from the walls. Flow visualization experiments by Sigli and Coutanceau (20) for sphere sedimentation near finite boundaries in a tube tend to support this hypothesis since the viscoelastic effects were found to be large even though the nominal Weissenberg numbers were extremely small.

Acknowledgements

The authors thank Mr. William Fong for performing some of the experiments reported in this paper. This work was supported by a grant from the National Science Foundation. Experimental materials were generously donated by the Union Carbide Corp., B. F. Goodrich Co. and Dow Corning Co.

References

1. Chan, P. C.-H. and Leal, L. G. 1979 J. Fluid Mech. 92, 131.
2. Goldsmith, H. L. and Mason, S. G. 1962 J. Colloid Sci. 17,448.
3. Gauthier, F., Goldsmith, H. L. and Mason, S. G. 1971 Trans. Soc. Rheol. 15, 197.
4. Ho, B. P. and Leal, L. G. 1976 J. Fluid Mech. 76, 783.
5. Brunn, P. 1976 Rheol. Acta 15, 163.
6. Brunn, P. 1976 Rheol. Acta 15, 589.
7. Karnis, A. and Mason, S. G. 1966 Trans. Socl. Rheol. 10, 571.
8. Gauthier, F. Goldsmith, H. L. and Mason, S, G. 1971 Rheol. Acta 10, 344.
9. Karnis, A. and Mason, S. G. 1967 J. Colloid Sci. 24, 164.
10. Taylor, G. I. 1932 Proc. Roy. Soc. (London) A 138, 41.
11. Kovitz, A. A. and Yannimaras, D. 1979 "Interfacial Tension Measurements with a Mensical Breakoff Tensiometer", presented at the 31st meeting of the American Physical Society, Division of Fluid Dynamics.
12. Olbricht, W. and Leal, L. G. 1979 "The Motion of Liquid Drops Through a Converging-Diverging Tube of Comparable Diameter", presented at the Golden Jubilee Meeting of the Society of Rheology.
13. Leal, L. G., Skoog, J. and Acrivos, A. 1971 Can. J. Chem. E. 49, 569.
14. Blanks, R. F., Park, H. C., Patel, D. R. and Hawley, M. C. 1974 Polymer Eng. & Sci. 14, 16.
15. Beavers, G. S. and Joseph, D. D. 1975 J. Fluid Mech. 69, 475.
16. Giesekus, H. 1966 Rheo. Acta 5, 239.
17. Leal, L. G. 1975 J. Fluid Mech. 69, 305.

18. Bartram, E., Goldsmith, H. L. and Mason, S. G. 1975 Rheol. Acts 14, 776.

19. Grace, H. P. 1971 "Dispersion Phenomena in High Viscosity Immiscible Fluid Systems and Application of Static Mixers as Dispersion Devices in Such Systems". Du Pont Report AN-15937.

20. Sigli, D. and Coutanceau, M. 1977 J. non-Newtonian Fluid Mech. 2, 1.

Table I

	Suspending Phase	Suspended Phase	σ(dyne cm^{-1})
1	Newtonian: Ucon oil LB-1715 (μ_o = 9.0p)	water ($\tilde{\mu}_o$ = 0.01p)	2.3
2		1% Separan AP-30 ($\tilde{\mu}_o$ = 24.8p; batch a)	6.0
3		0.1% carboxyvinyl polymer in water ($\tilde{\mu}_o$ = 6.1p)	5.1
4	non-Newtonian: 1% Separan AP-30	Silicone oil 510 fluid ($\tilde{\mu}_o$ = 1.1p)	6.6
5	μ_o = 24.8p (batch a); 30.0p (batch b); 42.5p (batch c)	Ucon oil LB-1715 ($\tilde{\mu}_o$ = 9.0p)	4.9

Table II

κ	$\left(\frac{\phi_3 \sigma}{a\mu_o^2}\right)_{cr}$
0.01	0.80
0.1	1.30
1	2.02
10	1.66

Figure Captions

Fig. 1: Schematic view of Couette flow device. a: precision bore glass cylinder; b: aluminum rotor; c: aluminum base; d: brass supporting rods; e: bearings; f: mercury layer; g: suspending fluid; h: plexiglass lid; i: scale; j: coupling; k: variable speed motor; l: wood panel.

Fig. 2: A comparison of experimental trajectory with theory (—) for System 1. (a) R_1 = 4.60 cm. □, a = 0.134 cm, Ω_1 = 0.269 s^{-1}, δ = 0.459. (b) R_1 = 3.81 cm. ■, a = 0.134 cm, Ω_1 = 0.269 s^{-1}, δ = 0.238; Δ, a = 0.139 cm, Ω_1 = 0.537 s^{-1}, δ = 0.684. (c) R_1 = 2.54 cm. □, a = 0.134 cm, Ω_1 = 1.05 s^{-1}, δ = 0.358; ▲, a = 0.193 cm, Ω_1 = 0.537 s^{-1}, δ = 0.263. (d) R_1 = 1.27 cm. Δ, a = 0.193 cm, Ω_1 = 2.11 s^{-1}, δ = 0.278; o, a = 0.229 cm, Ω_1 = 2.11 s^{-1}, δ = 0.330.

Fig. 3: A comparison of experimental trajectory with theory (—) for System 2 (assuming $\tilde{\phi}_3$ = 54 dyne s^2 cm^{-2}). (a) R_1 = 3.81 cm. □, a = 0.134 cm, Ω_1 = 0.537 s^{-1}, δ = 0.182, $\tilde{\lambda}$ = 1.97; ■, a = 0.134 cm, Ω_1 = 0.269 s^{-1}, δ = 0.091, $\tilde{\lambda}$ = 0.98; ▲, a = 0.193 cm, Ω_1 = 0.537 s^{-1}, δ = 0.262, $\tilde{\lambda}$ = 1.97. (b) R_1 = 2.54 cm. □, a = 0.134 cm, Ω_1 = 0.537 s^{-1}, δ=0.070, $\tilde{\lambda}$ = 0.759; Δ, a = 0.193 cm, Ω_1 = 1.05 s^{-1}, δ = 0.197, λ = 1.49. (c) R_1 = 1.27 cm. Δ, a = 0.193 cm, Ω_1 = 1.05 s^{-1}, δ = 0.053, $\tilde{\lambda}$ = 0.399; o, a = 0.229 cm, Ω_1 = 2.11 s^{-1}, δ = 0.127, $\tilde{\lambda}$ = 0.803; ◇, a = 0.229 cm, Ω_1 = 5.11 s^{-1}, δ = 0.307, $\tilde{\lambda}$ = 1.94.

Fig. 4: A comparison of experimental trajectory with theory (—) for System 3 (assuming $\tilde{\phi}_3$ = 22 dyne s^2 cm^{-2}). (a) R_1 = 4.6 cm. ∇, a = 0.106 cm, Ω_1 = 0.269 s^{-1}, δ = 0.164, $\tilde{\lambda}$ = 3.16; ■, a = 0.134 cm, Ω_1 = 0.269 s^{-1}, δ = 0.207, $\tilde{\lambda}$ = 3.16. (b) R_1 = 3.81 cm. ▼, a = 0.106 cm, Ω_1 = 0.269 s^{-1}, δ = 0.085, $\tilde{\lambda}$ = 1.64; ∇, a = 0.106 cm, Ω_1 = 0.537 s^{-1}, δ = 0.169, $\tilde{\lambda}$ = 3.27; ◆, a = 0.161 cm, Ω_1 = 0.537 s^{-1}, δ = 0.257, $\tilde{\lambda}$ = 3.27. (c) R_1 = 2,54 cm. □, a = 0.134 cm, Ω_1 = 1.05 s^{-1}, δ = 0.161, $\tilde{\lambda}$ = 2.46; ▲, a = 0.193 cm, Ω_1 = 0.537 s^{-1}, δ = 0.119, $\tilde{\lambda}$ = 1.26; Δ, a = 0.193 cm, Ω_1 = 1.05 s^{-1}, δ = 0.232, $\tilde{\lambda}$ = 2.46. (d) R_1 = 1.27 cm. Δ, a = 0.193 cm, Ω_1 = 2.11 s^{-1}, δ = 0.126, $\tilde{\lambda}$ = 1.33; o, a = 0.229 cm, Ω_1 = 5.11 s^{-1}, δ = 0.361, $\tilde{\lambda}$ = 3.22.

Fig. 5: A comparison of experimental trajectory with theory (—) for System 4. (a) R_1 = 2.54 cm. Batch b (ϕ_3 = 60 dyne s^2 cm^{-2}). a = 0.229 cm, ●, Ω_1 = 0.0524 s^{-1}, δ = 0.035, λ = 0.068; ◆, Ω_1 = 0.105 s^{-1}, δ = 0.071, λ = 0.136; ▲, Ω_1 = 0.262 s^{-1}, δ = 0.177, λ = 0.340. (b) R_1 = 1.27 cm. Batch c (ϕ_3 = 68 dyne s^2 cm^{-2}). ▼, a = 0.106 cm, Ω_1 = 2.01 s^{-1}, δ = 0.240, λ = 0.562; ●, a = 0.229 cm, Ω_1 = 1.03 s^{-1}, δ = 0.265, λ = 0.288; ◆, a = 0.229 cm, Ω_1 = 0.524 s^{-1}, δ = 0.135, λ = 0.147.

Fig. 6: A comparison of experimental trajectory with theory (—) for System 5. (a) R_1 = 4.60 cm. Batch a (ϕ_3 = 54 dyne s^2 cm^{-2}). ∇, a = 0.106 cm, Ω_1 = 0.0524 s^{-1}, δ = 0.092, λ = 0.371. (b) R_1 = 3.81 cm. Batch a, □, a = 0.134 cm, Ω_1 = 0.105 s^{-1}, δ = 0.120, λ = 0.386; ▲, a = 0.193 cm, Ω_1 = 0.0524 s^{-1},

$\delta = 0.086$, $\lambda = 0.192$; b, $a = 0.229$ cm, $\Omega_1 = 0.0524\ s^{-1}$, $\delta = 0.102$, $\lambda = 0.192$. (c) $R_1 = 2.54$ cm. Batch b ($\phi_3 = 60$ dynes^2 cm^{-2}). $a = 0.229$ cm, ●, $\Omega_1 = 0.0524\ s^{-1}$, $\delta = 0.048$, $\lambda = 0.068$; o, $\Omega_1 = 0.262\ s^{-1}$, $\delta = 0.239$, $\lambda = 0.340$.

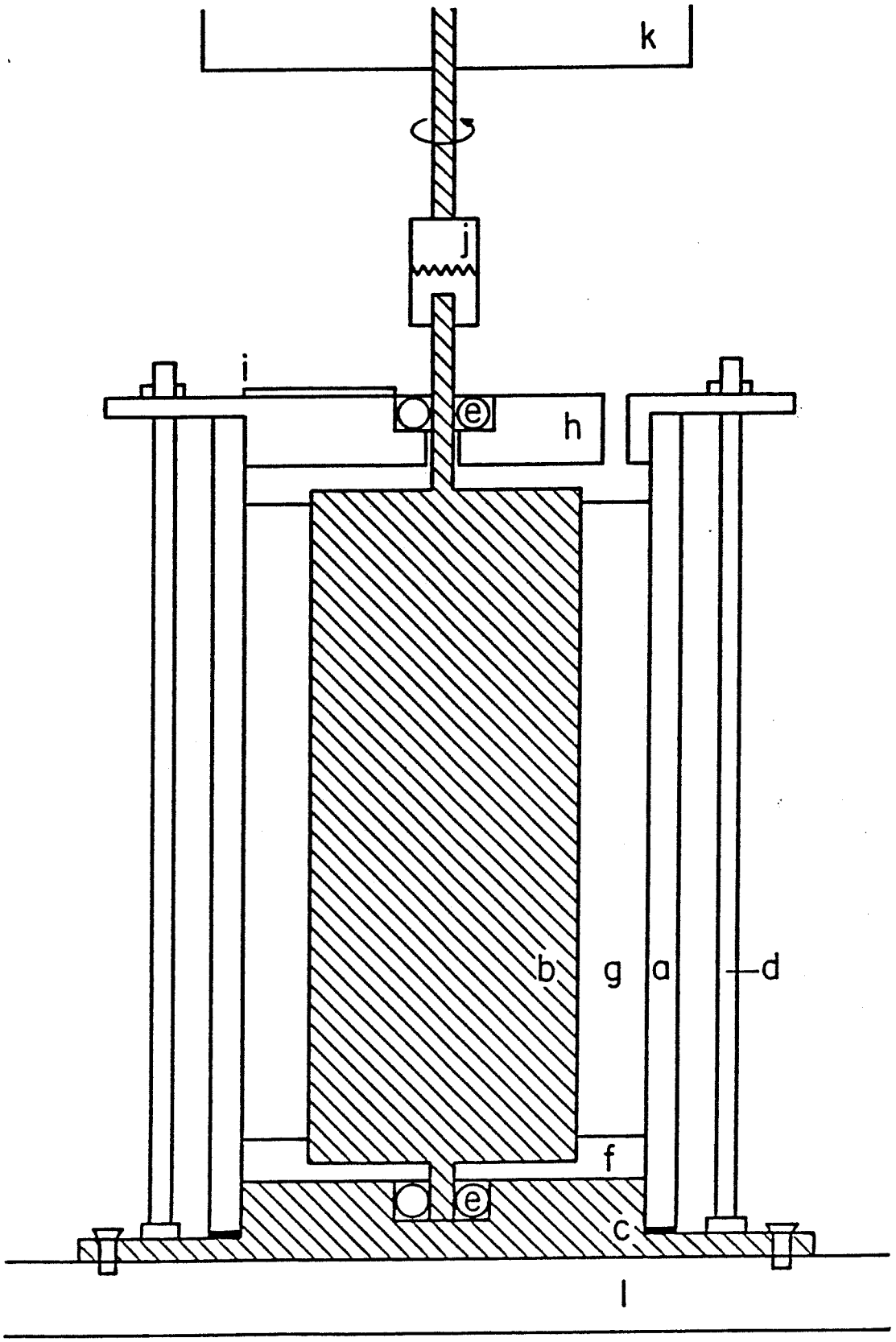

Figure 1

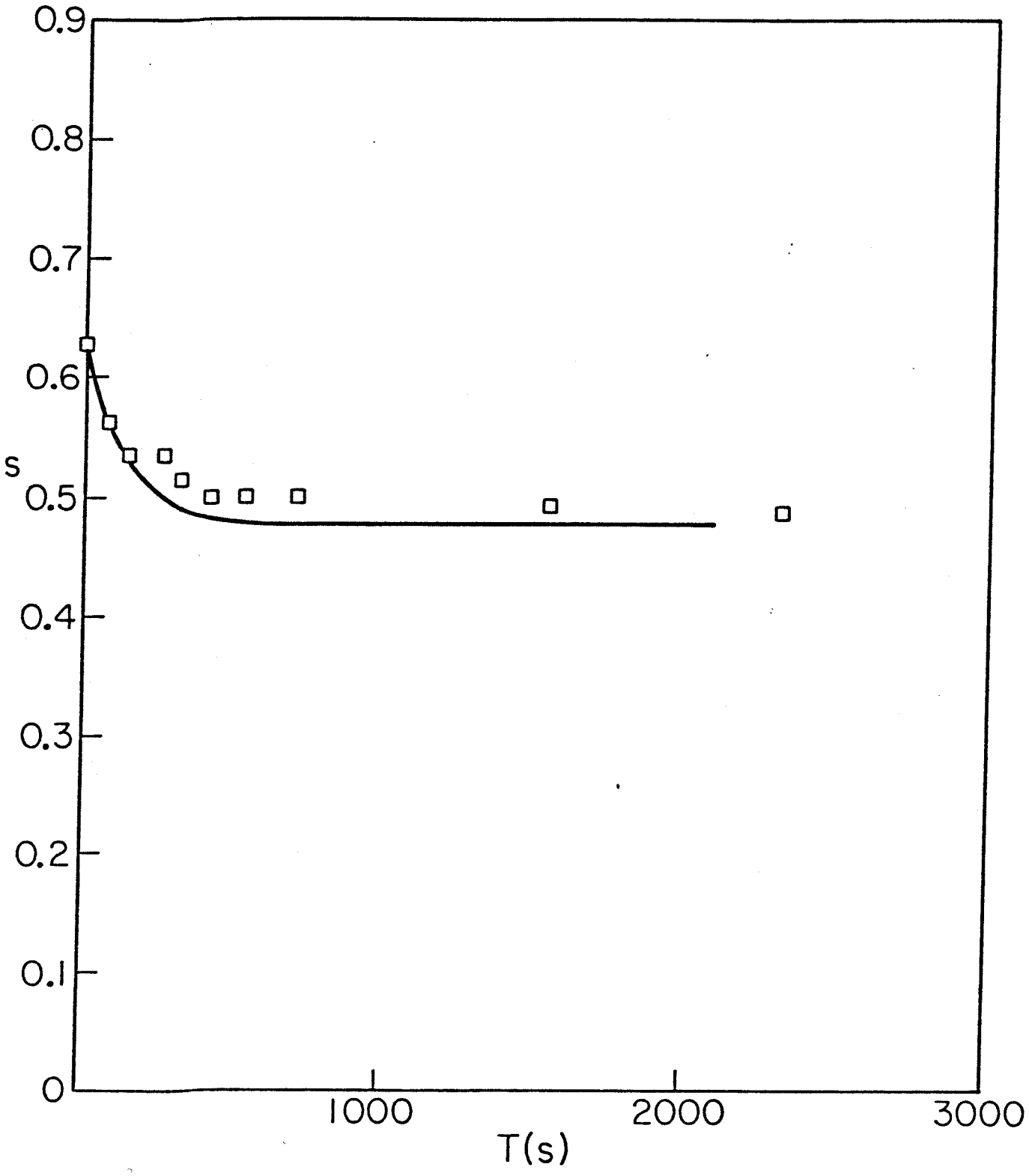

Figure 2a

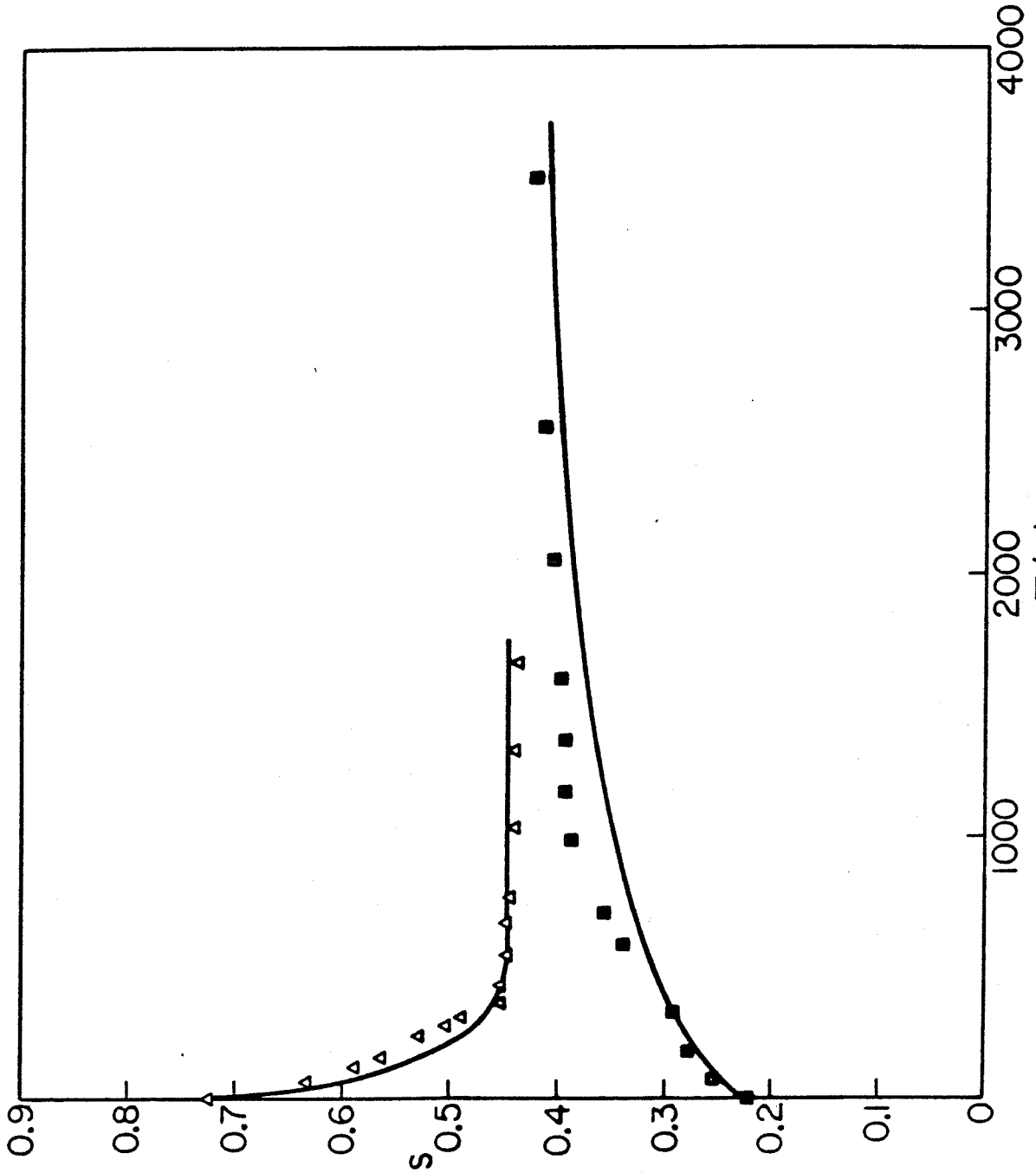

Figure 2b

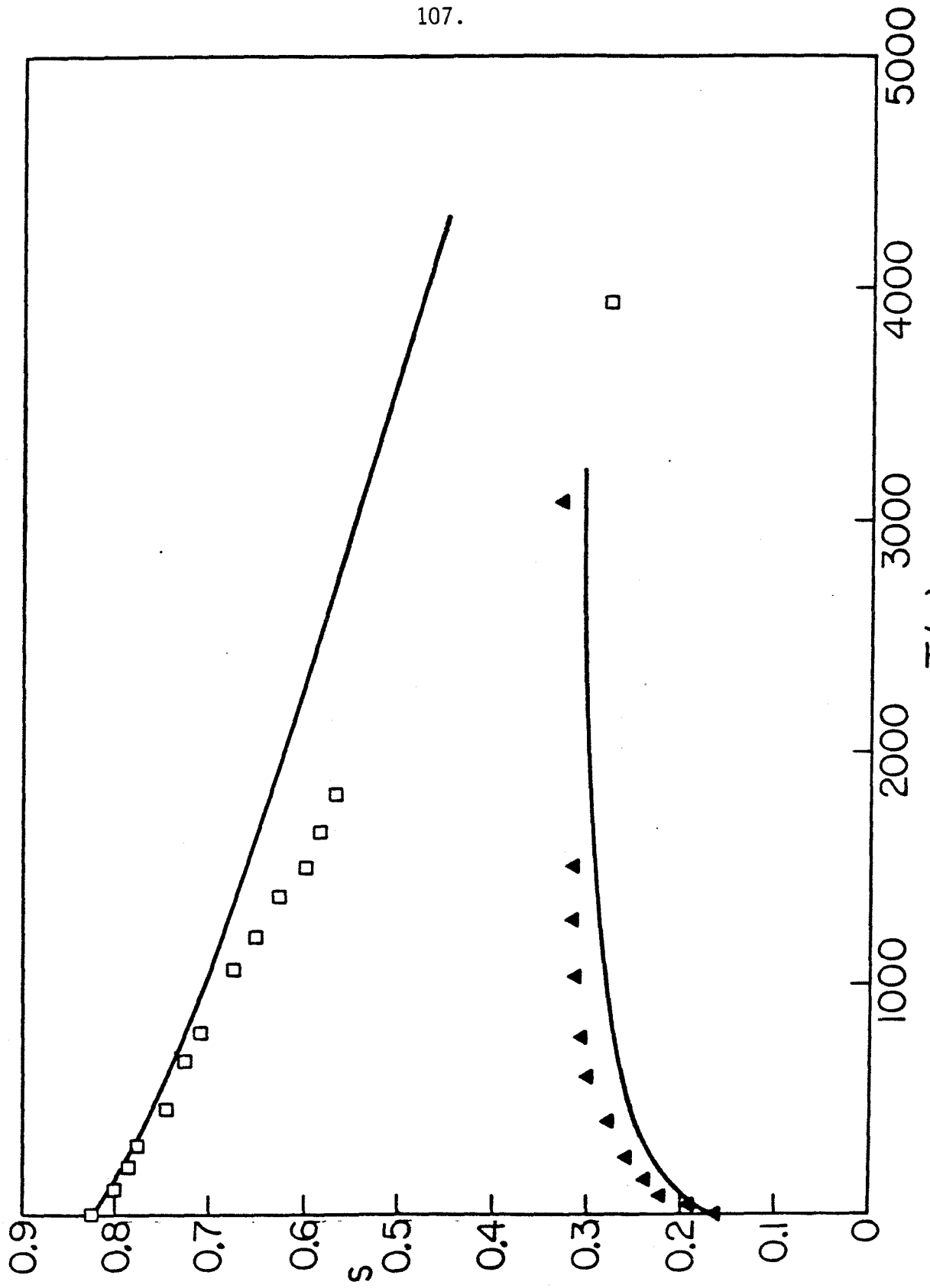

Figure 2c

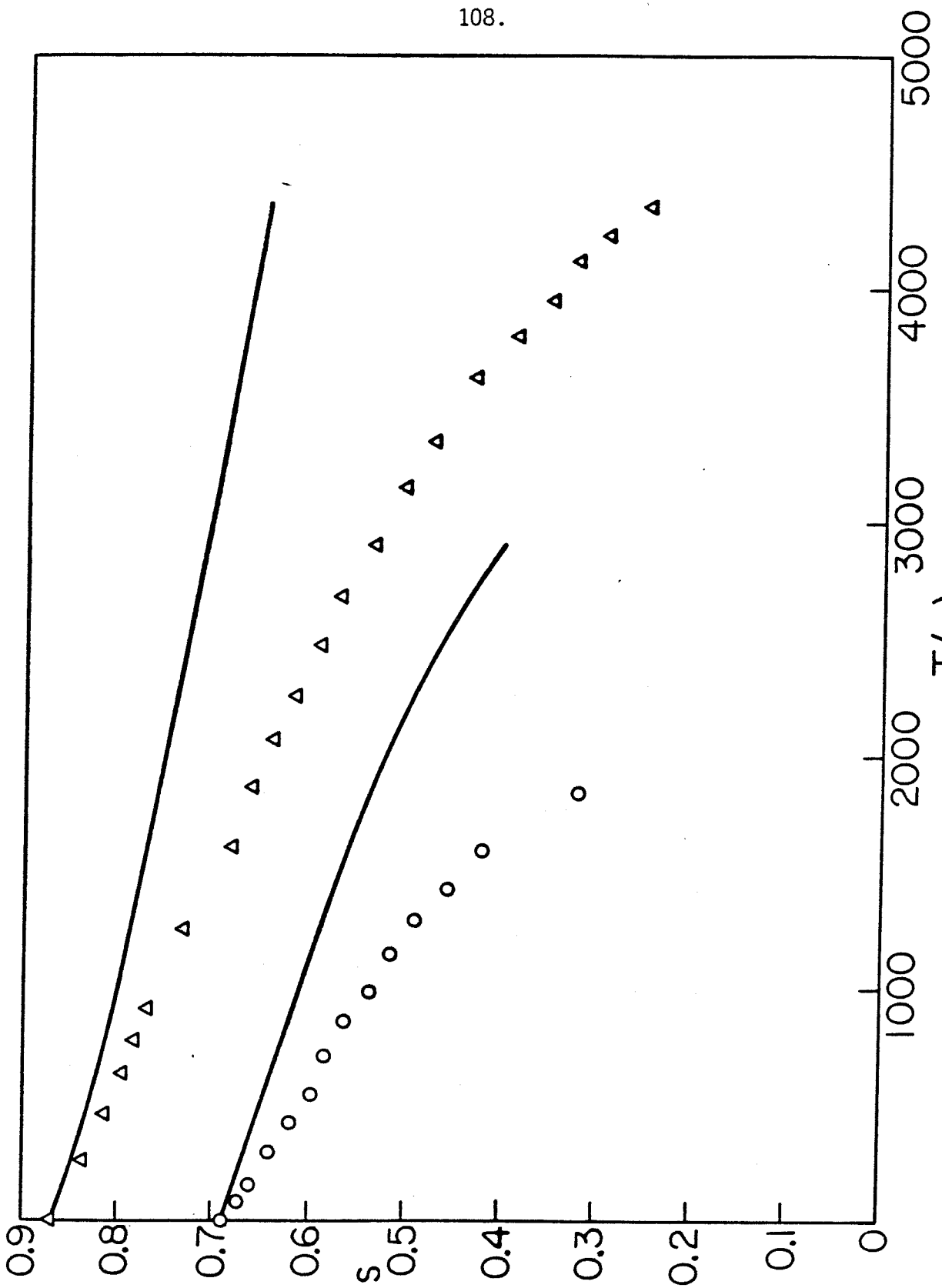

Figure 2d

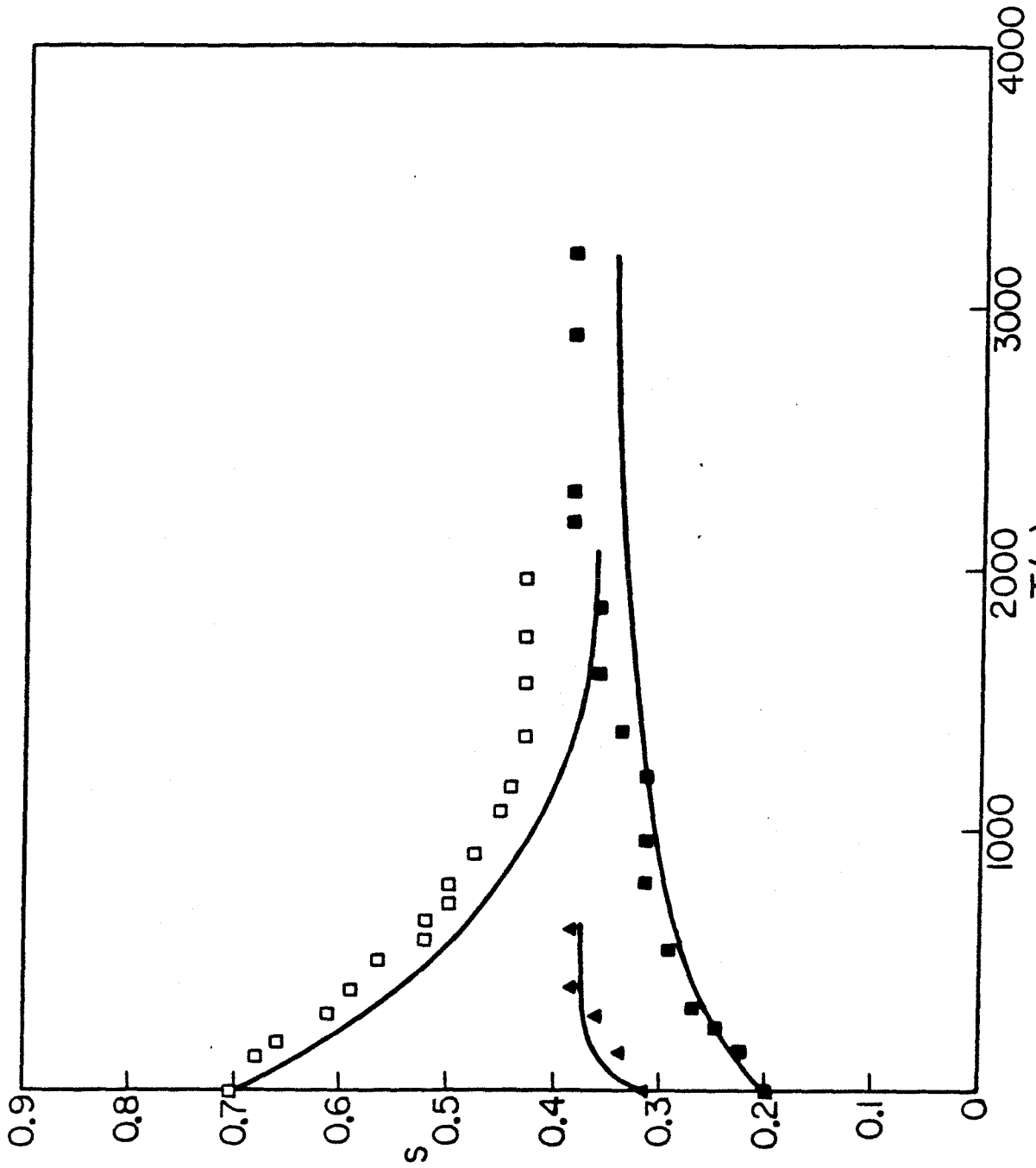

Figure 3a

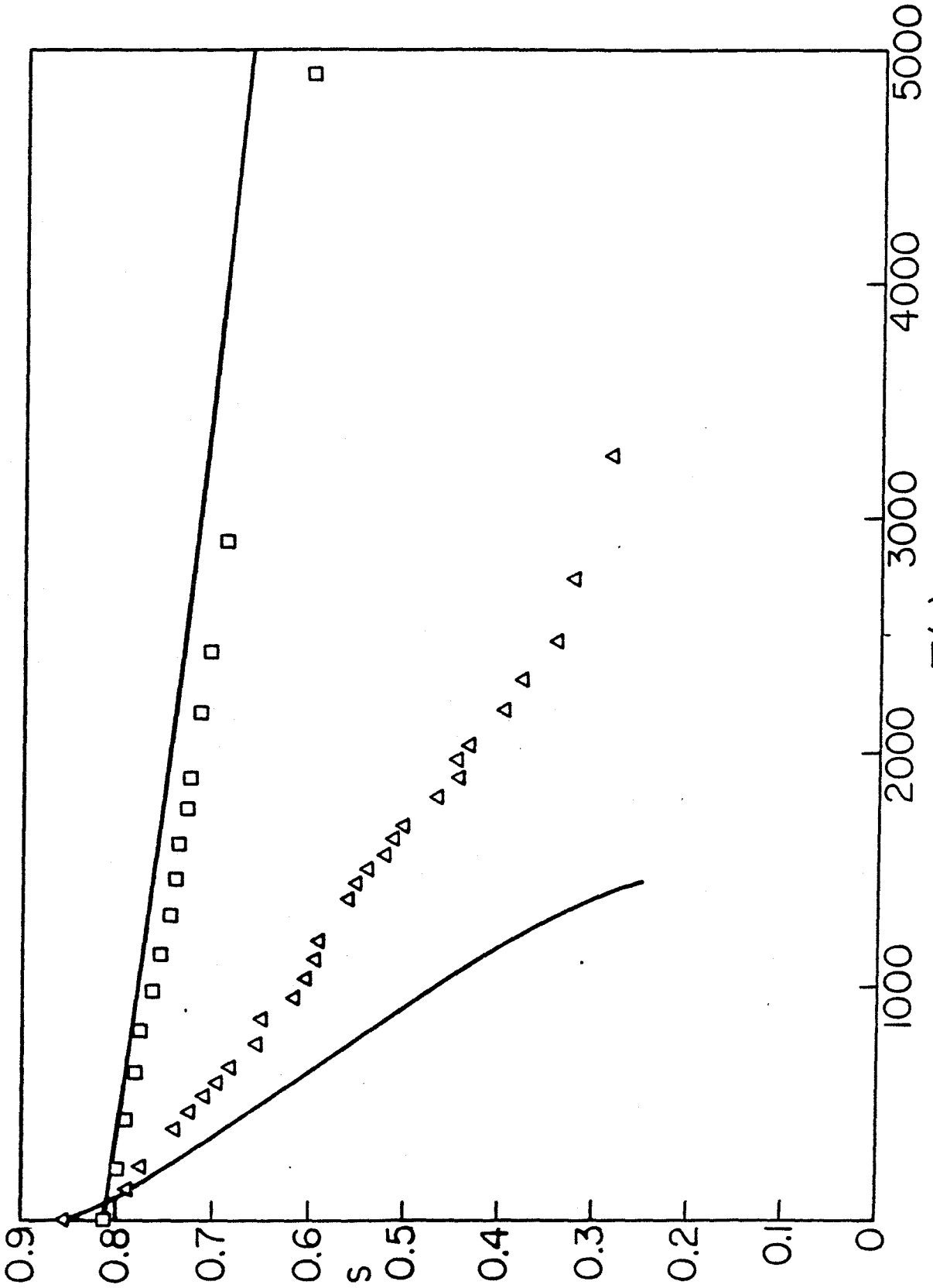

Figure 3b

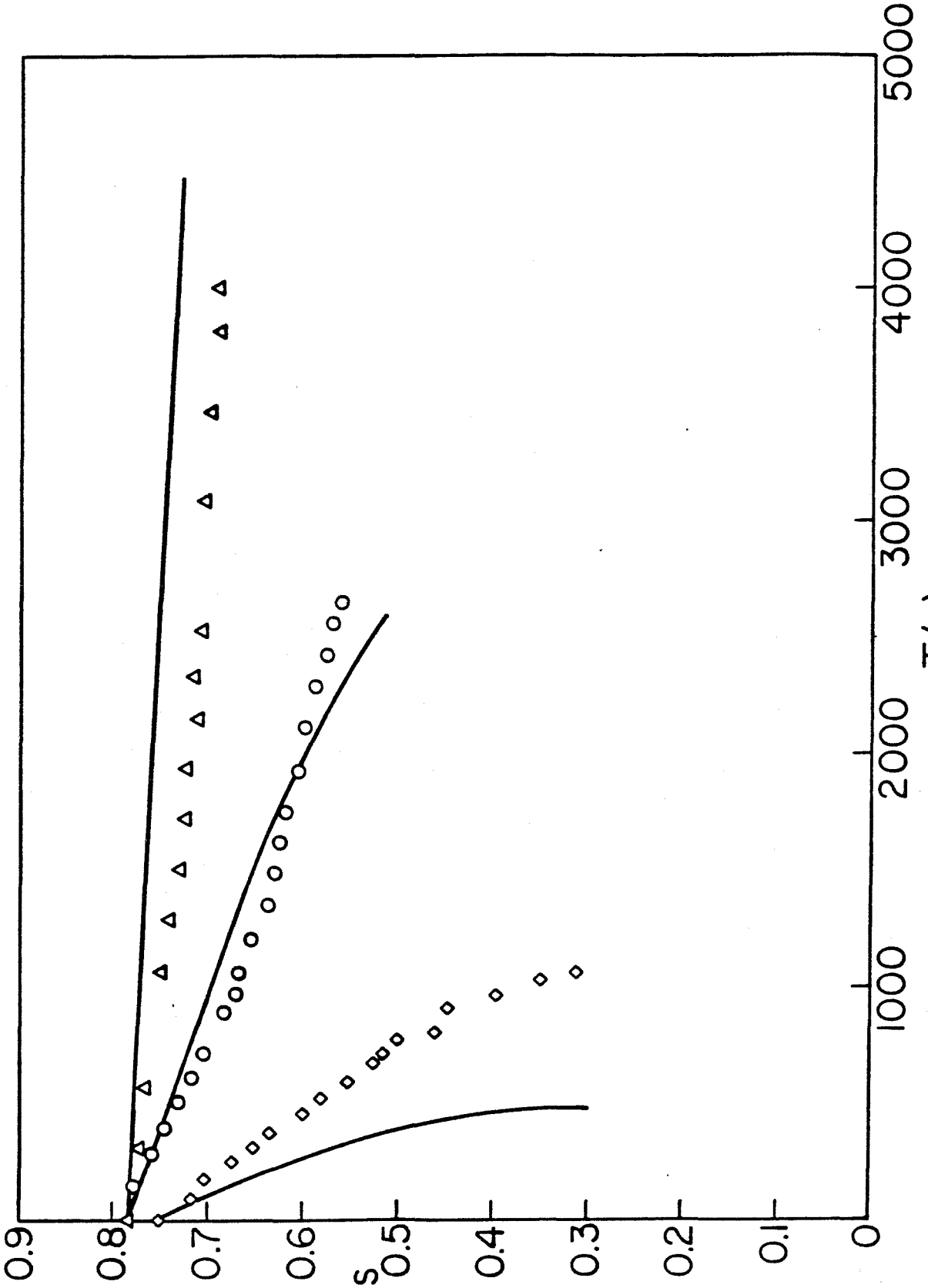

Figure 3c

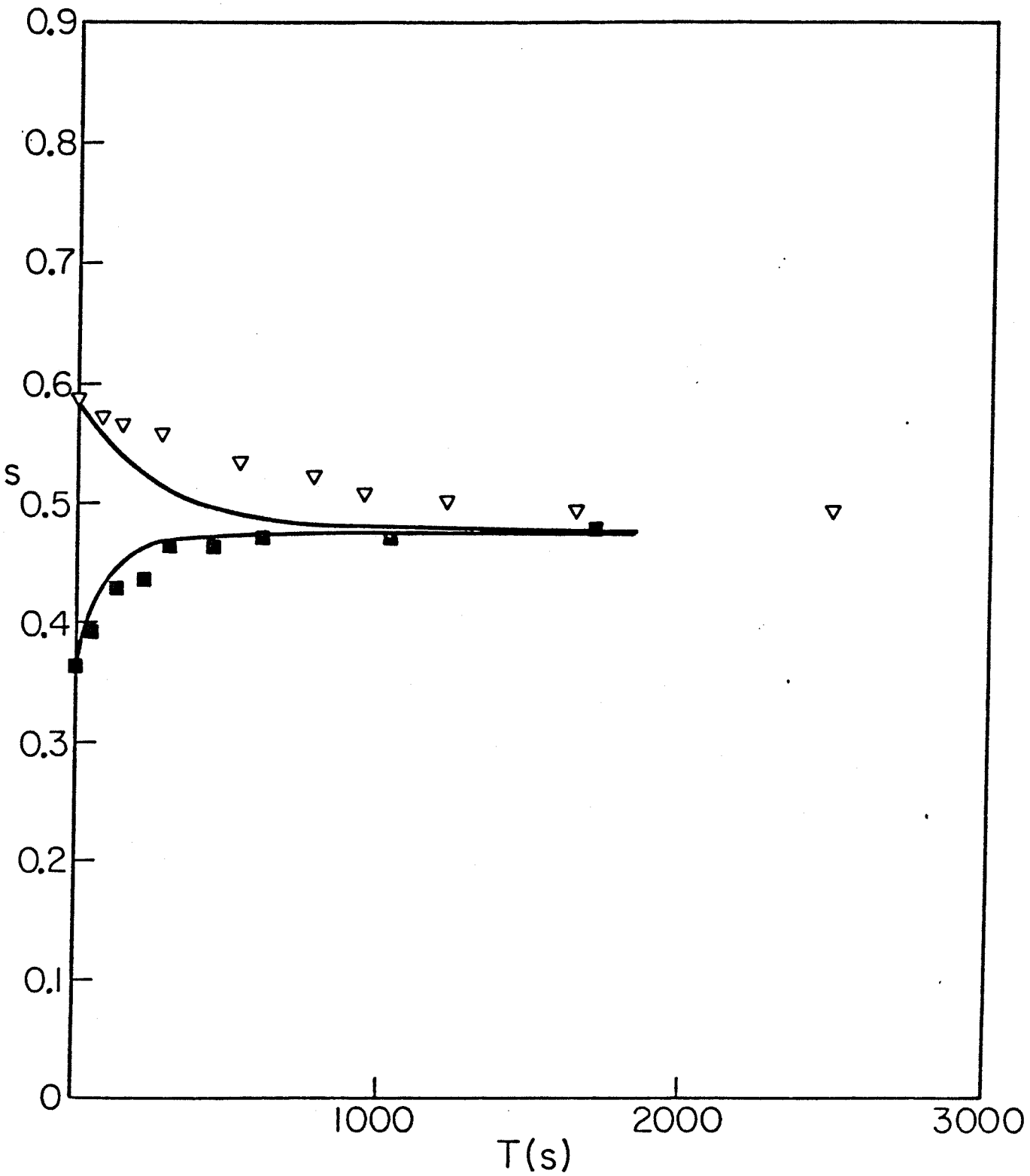

Figure 4a

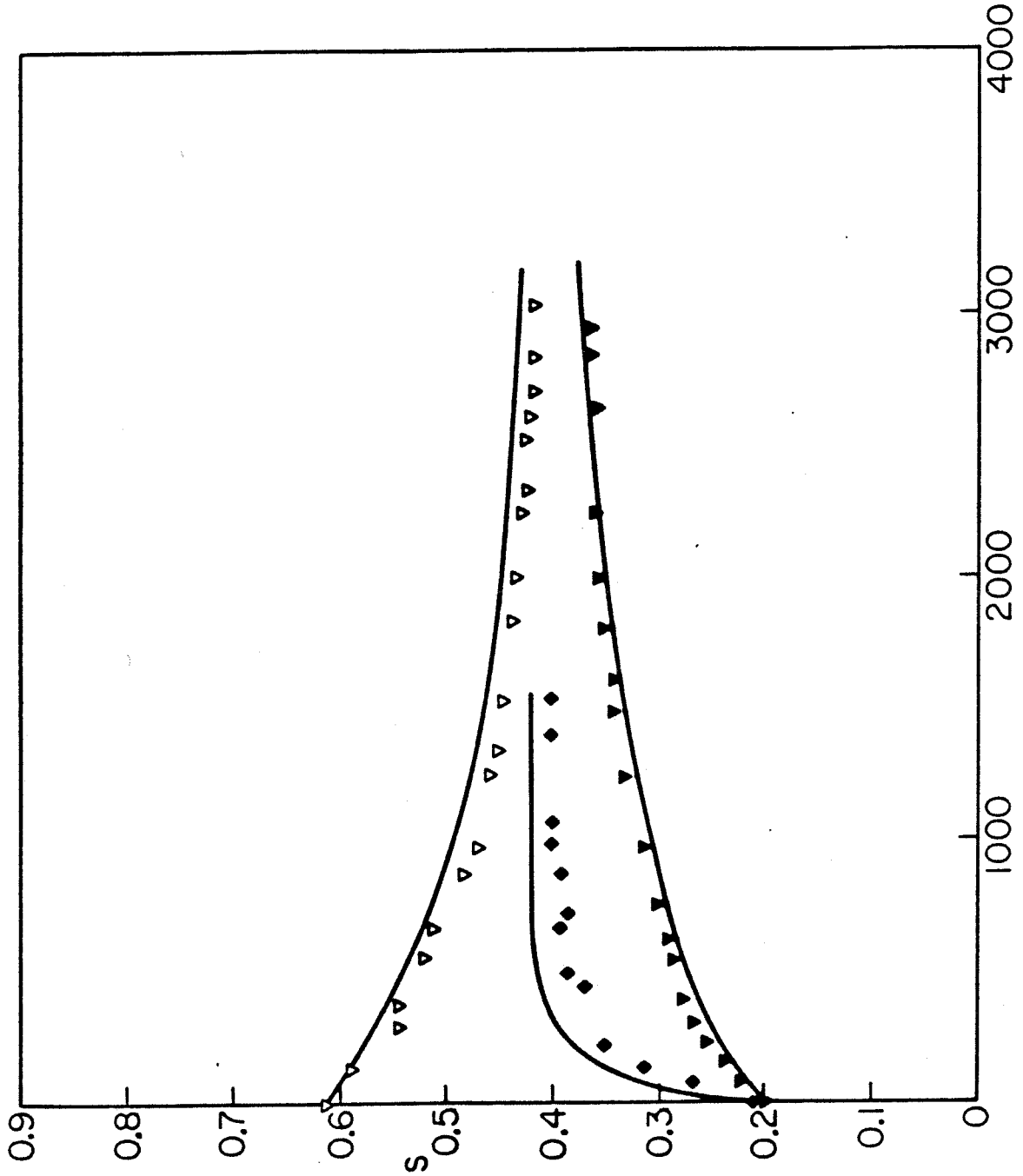

Figure 4b

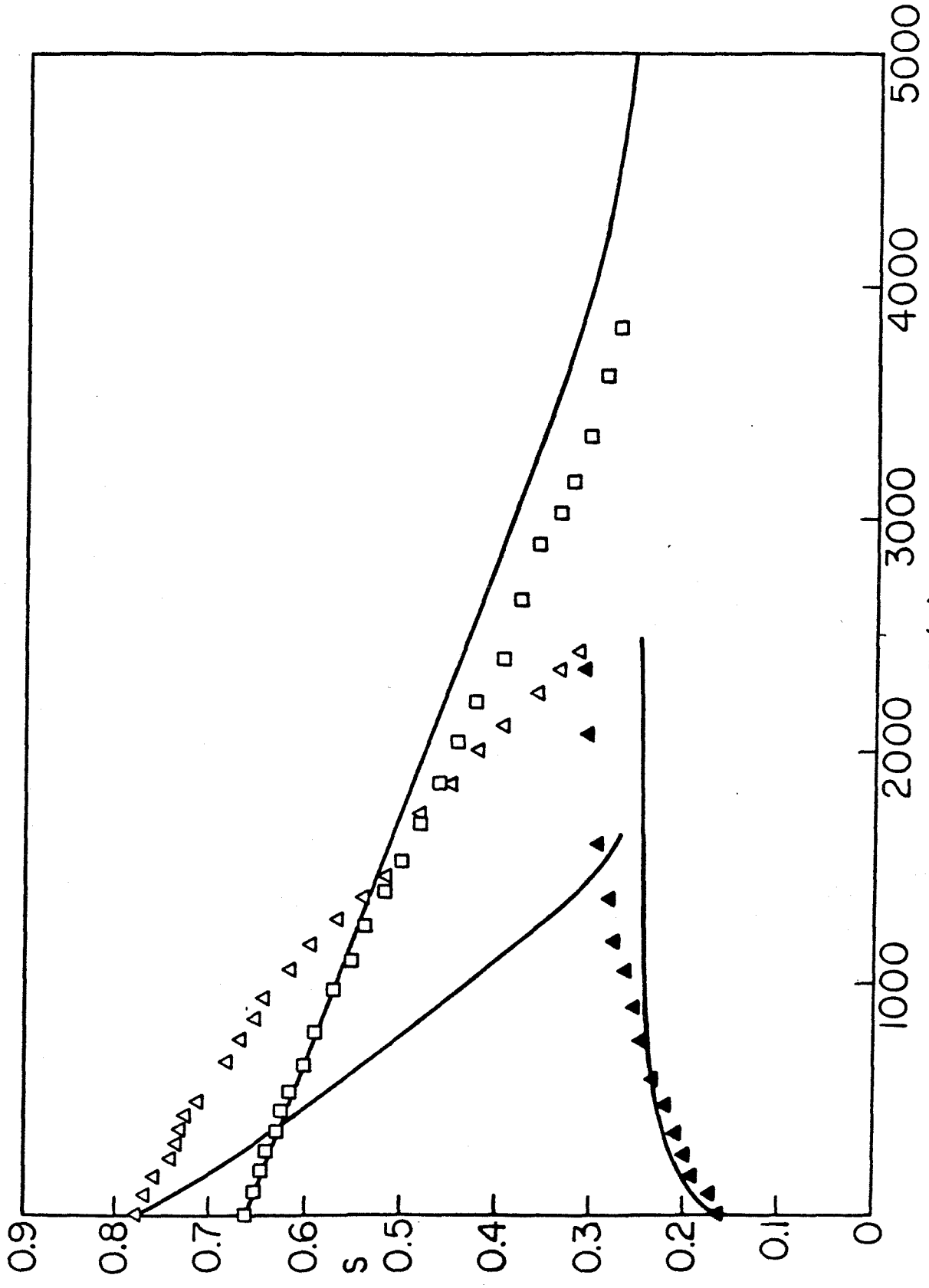

Figure 4c

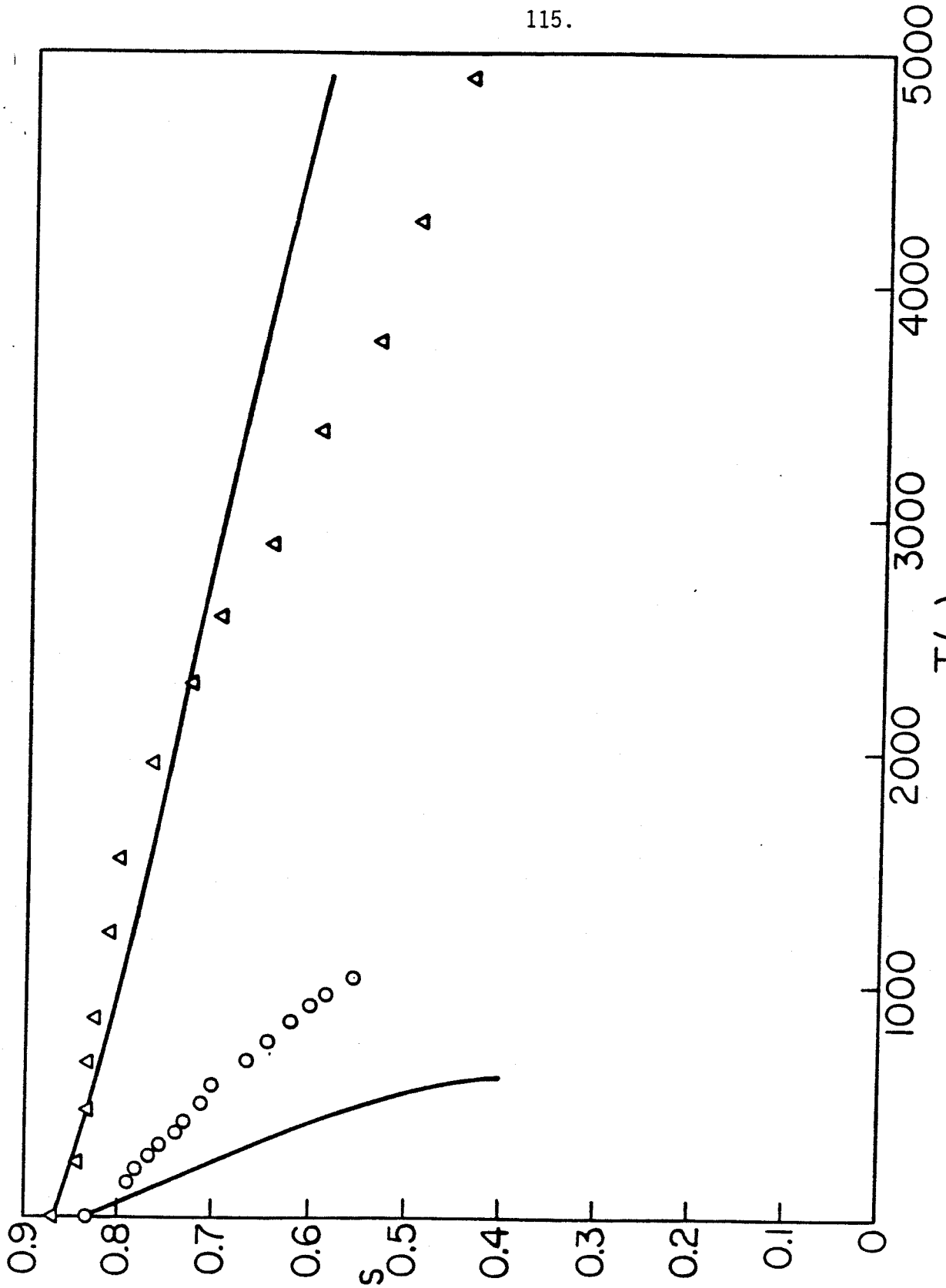

Figure 4d

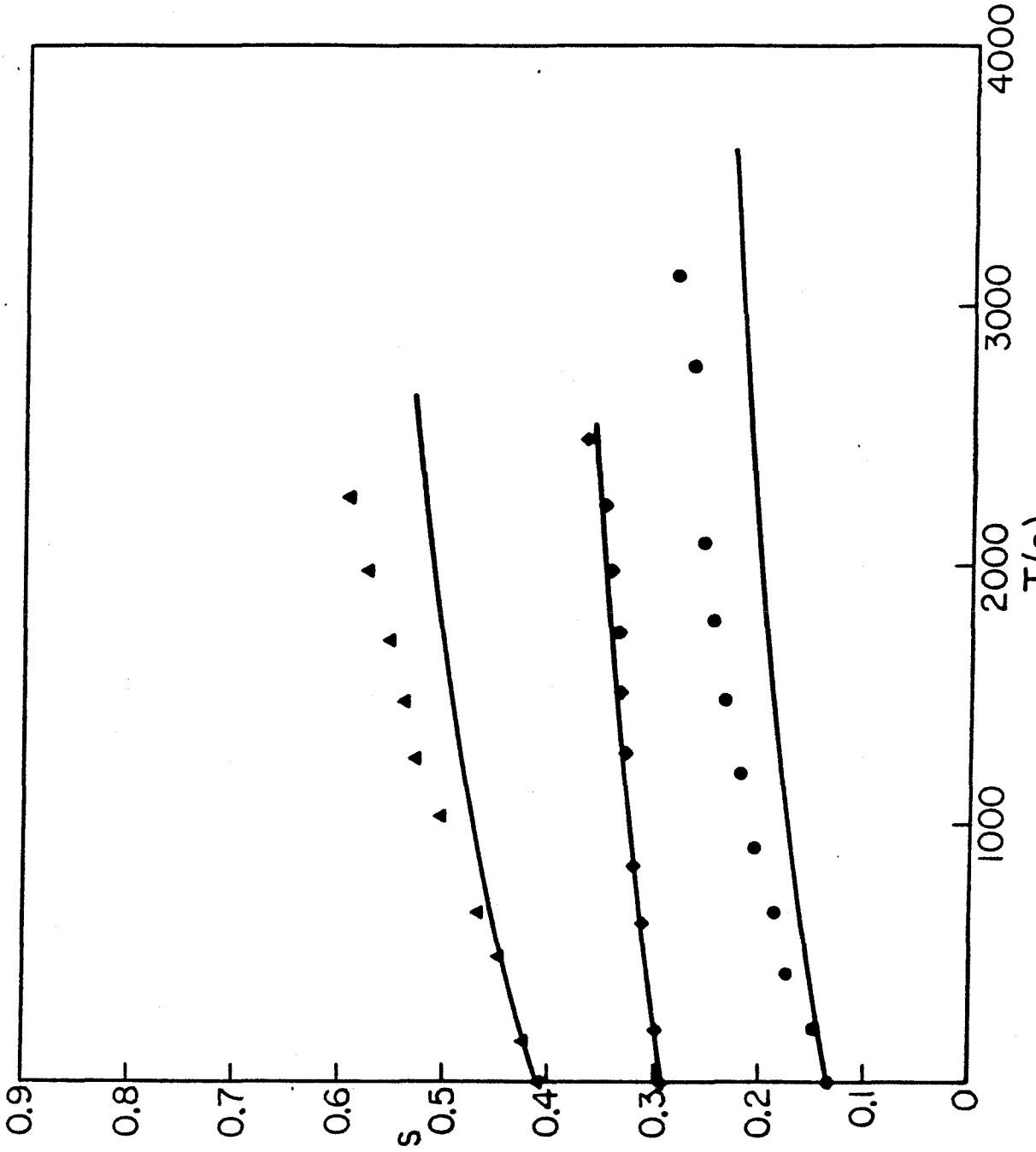

Figure 5a

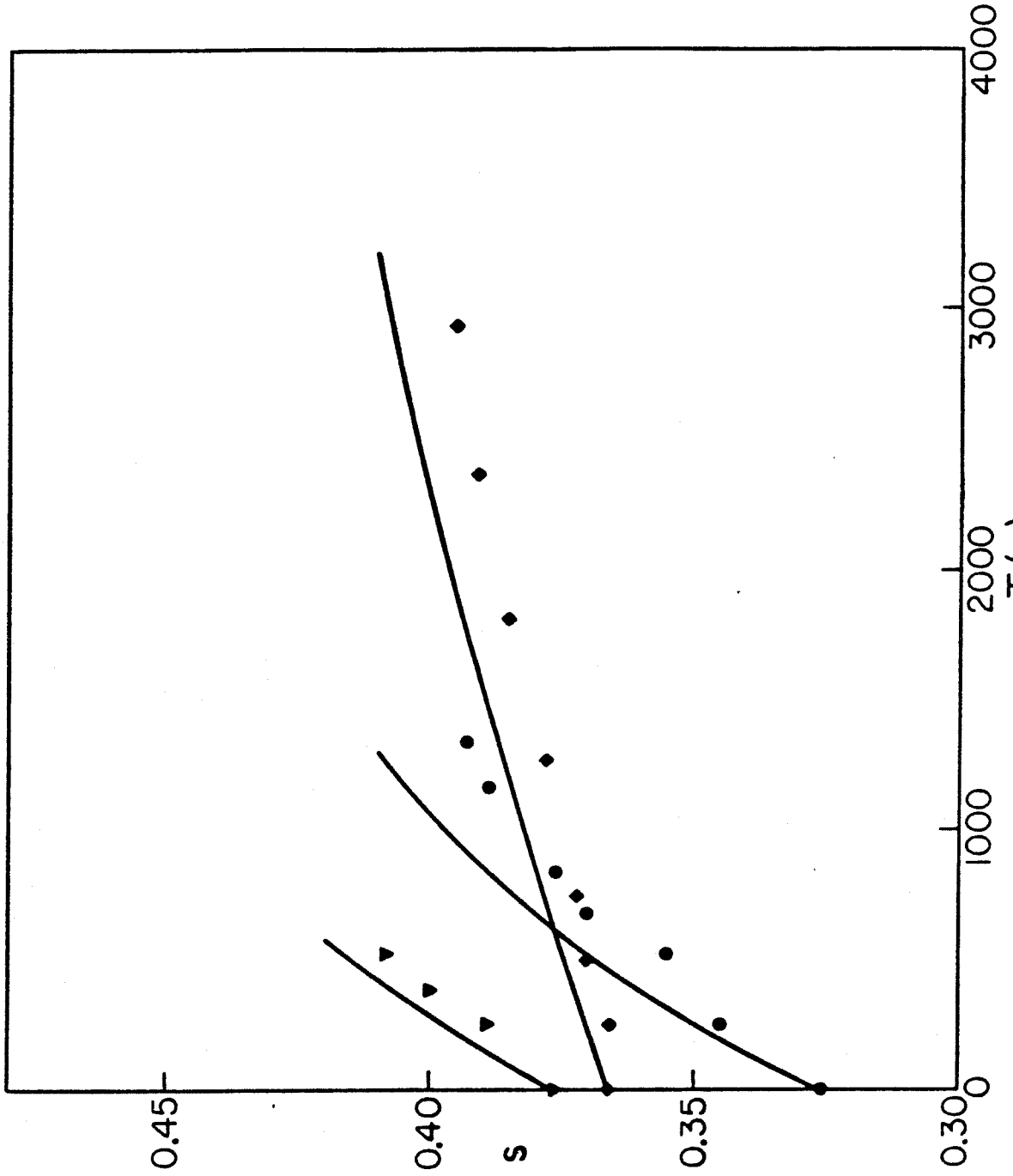

Figure 5b

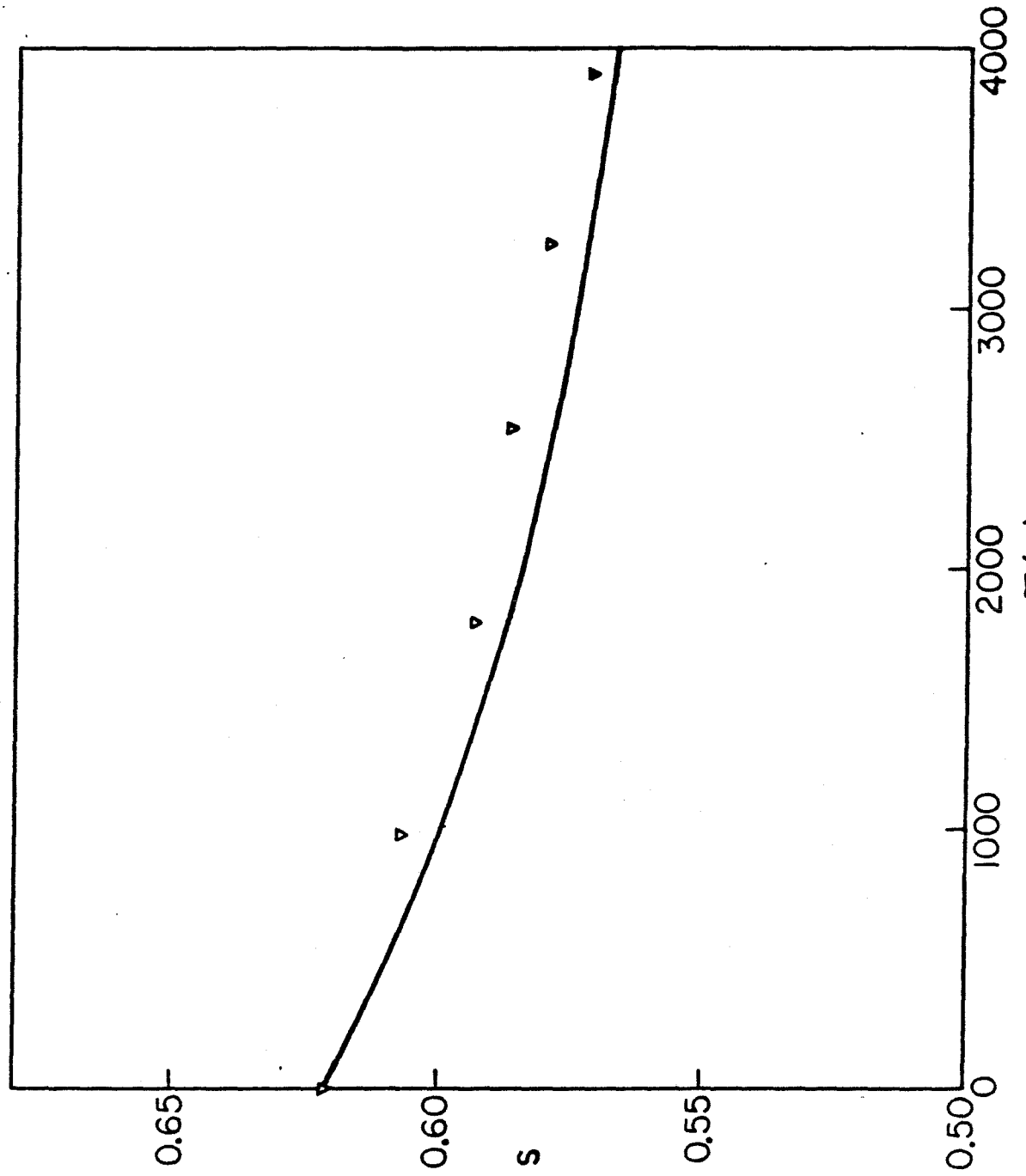

Figure 6a

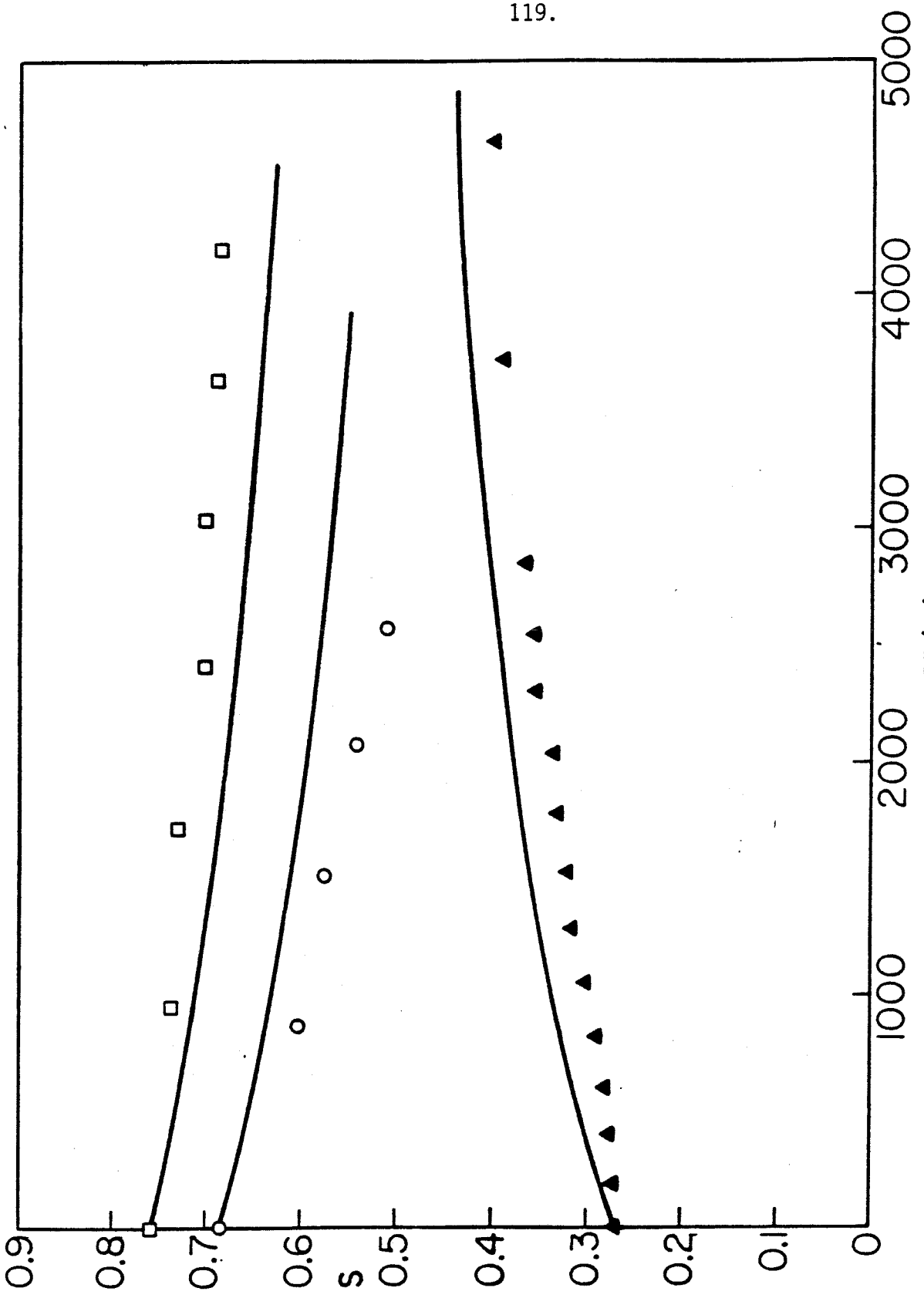

Figure 6b

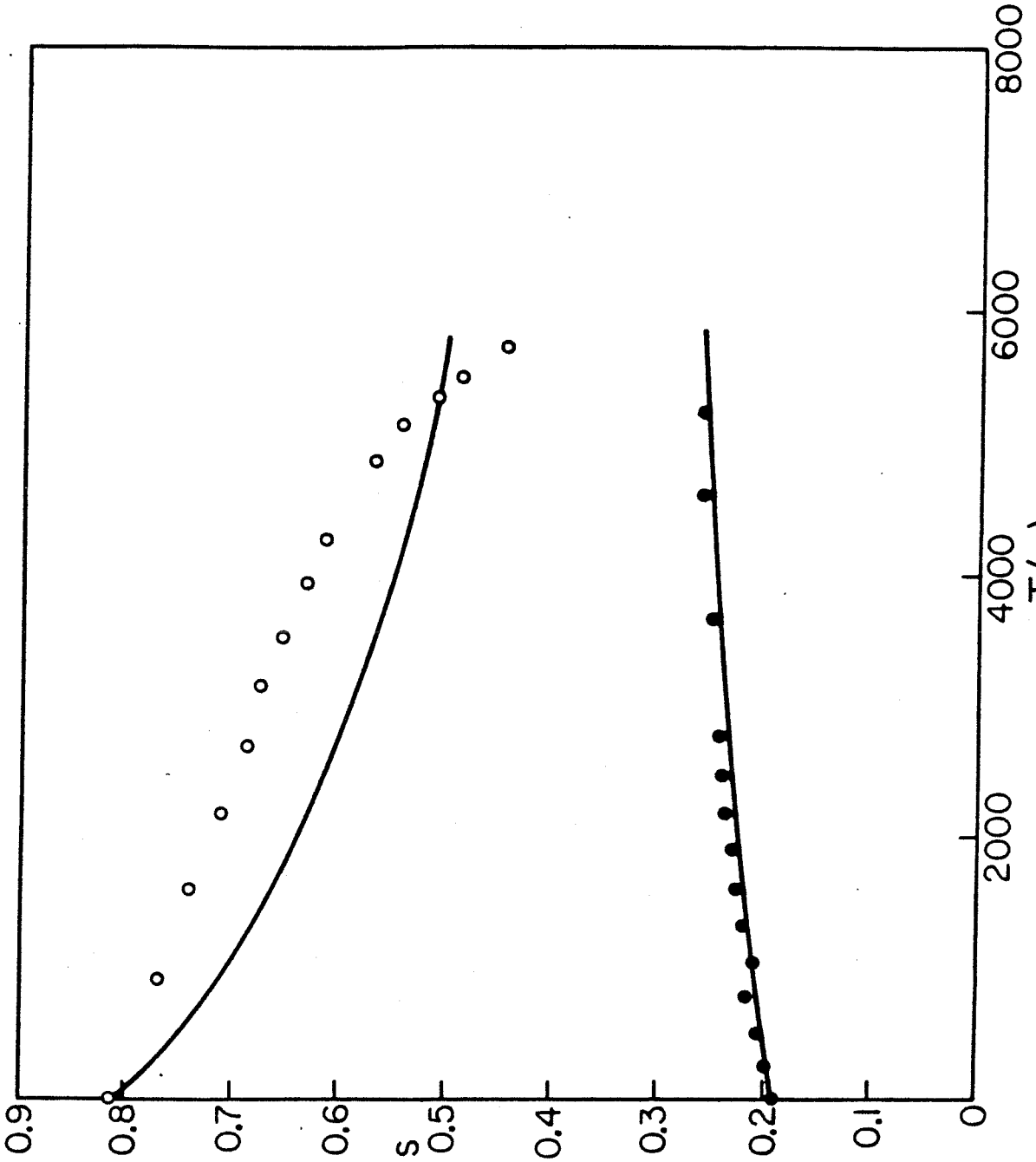

Figure 6c